TALEN-mediated site-directed mutagenesis of HLH proteins lyl1 and Id4 to reveal their role in haematopoietic and neural stem cell fate

TAMILVENDHAN DHANASEELAN

Thesis submitted to the University of Nottingham

for the degree of Doctor of Philosophy

October 2015

Abstract

Basic Helix-Loop-Helix proteins are transcriptional regulators crucial for many development processes. Using gain- and loss-of-function analysis in zebrafish, the functional role of two members of this protein family, lyl1 (Lymphoblastic leukaemia 1) and Id4 (Inhibitor of differentiation 4) in stem cell fate was determined. Ectopic overexpression of lyl1 resulted in the expansion of haematopoietic stem cell pool and its progeny promoting erythrocyte differentiation and suppressing myeloid differentiation. TALEN-mediated lyl1$^{-/-}$ embryos developed normally but displayed distinct marker gene expression during primitive and definitive haematopoiesis establishing a role for lyl1 in both waves of haematopoiesis. During primitive haematopoiesis expression of scl/tal1 and gata1 was unaltered but expression of pu.1 was increased suggesting that lyl1 antagonises myeloid differentiation. Lyl1-deficiency resulted in reduction of Gfi1aa expression during primitive and definitive haematopoiesis. In addition, a reduction in the expression of c-myb in the caudal hematopoietic tissue and rag1 in the thymus was observed indicating that lyl1 is required to maintain the definitive haematopoietic stem cell pool and to drive T lymphopoiesis. In adult zebrafish lyl1 regulates lineage choice driving lymphopoiesis and suppressing myelopoiesis. Morpholino-mediated knockdown of Id4 alone or in combination with p53 resulted in reduced cell proliferation, increased cell death and premature neuronal differentiation. Phenotypic analysis of TALEN-mediated Id4 mutants confirmed that Id4 plays a crucial role in the expansion of neural stem cells and timing of neuronal differentiation. Inhibition of p38MAPK in Id4 morphants as well as Id4$^{-/-}$ mutants resulted in a phenotypic rescue establishing that Id4 negatively regulates p38MAPK activity to ensure normal neurogenesis.

ACKNOWLEDGEMENTS

First of all I would like to thank my supervisor Prof. Fred Sablitzky for giving me the opportunity to work in his lab. I am very grateful to for his guidance and support throughout my time in the lab. I would like to thank Dr. Peter Jones for his support and discussions during lab meeting.

I also thank Dr. Martin Gering and team who always there whenever I ran out of reagents. I extend my thanks to the Fish facility (BNSU) staff for taking care of my mutant fish.

I am very thankful to Tao, Deniz, Maha, Chen, Maryam and Kerry for their continued support and help.

Finally, I thank my mom, sister and my friends back in India for their continuous support and prayers.

ABBERAVATIONS

%	Percent
AGM	Aorta gonad mesonephros
ALM	Anterior Lateral Mesoderm
bHLH	basic Helix-Loop-Helix.
bp	base pairs.
Cas	CRISPR associated
CHT	Caudal Haematopoietic Tissue
CNS	Central Nervous System.
CRISPR	Clustered regularly interspaced palindromic repeats
DAPM	N-[N-3,5-difluorophenacetyl]-L-alanyl-S-phenylglycine methyl ester
DIG	Digoxygenin
DMSO	Di Methyl Sulfoxide.
DNA	Deoxyribose Nucleic Acid.
DNase	Deoxyribonuclease
dUTP	2’-Deoxyuridine 5’-phosphate.
EDTA	Ethylenediaminetetraacetic acid
Elavl3/HuC	ELAV like neuron-specific RNA binding protein 3
Gata1	GATA binding protein 1a
Hpf	hours post fertilisation.
ICM	Intermediate Cell Mass
Id	Inhibitor of DNA binding/ Inhibitor of Differentiation.
Id4	Inhibitor of DNA binding 4/ Inhibitor of Differentiation 4.

Lyl1	Lymphoblastic Leukemia 1
MABT	Maleic Acid Buffer Tween
MOs	Morpholino Oligos.
mRNA	messenger Ribose Nucleic Acid.
$NaCH_3COONa$	Sodium Acetate.
Ngn1	Neurogenin 1
NPCs	Neural Precursor Cells.
NSCs	Neural Stem Cells.
PBI	Posterior Blood Island
PBS	Phosphate Buffered Saline.
PBST	Phosphate Buffered Saline Tween.
PCR	Polymerase Chain Reaction.
PFA	Paraformaldehyde.
PLM	Posterior Lateral Mesoderm
Pu.1/spib	Spi-1 proto-oncogene b
Rag1	Recombination activation genes
RVD	Repeat Variable Diresidue
Scl/tal1	Stem Cell Leukemia/T-cell Acute Lymphoblastic Leukemia1
SOX2	SRY (Sex Determining region Y)- box2
SSC	Saline sodium citrate
TALENs	Transcription Activator Like Effector Nucleases
T-ALL	T-cell Acute Lymphoblastic Leukemia
TBE	Tris Borate EDTA.
TdT	Terminal deoxynucleotidyl Transferase.

TUNEL	Terminal deoxynucleotidyl Transferse dUTP Nick End Labelling.
ZFN	Zinc Finger Nucleases

Contents

List of Figures

List of Tables

Chapter 1

Introduction

1.1 bHLH protein family

Helix-Loop-Helix (HLH) or basic (b) helix-loop-helix (bHLH) proteins have been shown to regulate many cellular processes during development and adulthood. More than 200 members of bHLH proteins have been identified in organisms from yeast to human. bHLH proteins have been found to play important role in cellular differentiation, gene expression, cell cycle control, lineage commitment and sex differentiation (Jan and Jan, 1993; Massari and Murre, 2000). Cell-type-specific bHLH proteins are involved in cell fate determination such as Id4 in neurogenesis and scl/tal1 in haematopoiesis while ubiquitously expressed Myc proteins regulate transcription initiation and when associated with Max proteins they function as transcription activators (Jones *et al.,* 2004; Bedford *et al.*, 2005; Gering *et al,*, 1998; Schmidt, 2004; Nair and Burley, 2003).

bHLH proteins possess two highly conserved and functionally different domains. The N-terminal end of the bHLH domain is the basic domain that binds DNA whereas the helix-loop-helix domain facilitates homo and hetero dimer formation (Fairman *et al.,* 1993). Based on tissue distribution, dimerisation abilities and DNA-binding specificity Murre *et al* (1994) divided the bHLH proteins into seven different classes. Class I consist of E proteins that are expressed in many different tissues. Expression of class II bHLH proteins including myoD, neurogenins, MASH1, scl/tal1 and lyl1 is restricted to certain tissues. Class II bHLH proteins are known to form heterodimers with Class I E proteins (Murre *et al.*, 1989; Massari and

Murre, 2000). Members of class II regulate myogenesis (MyoD and myogenic regulatory factors), neurogenesis (Ngn1, Math1) cardiogenesis (dHAND, eHAND) and haematopoiesis (scl/tal1, lyl1) (Weintraub, 1991; Jan and Jan, 1993; Srivastava and Olson, 1997; Porcher *et al.,* 1996).

The Myc family of transcription factors belongs to Class III that possesses a Leucine-Zipper domain adjacent to the HLH domain (Henthorn *et al.,* 1991; Zhao *et al.,* 1993) and Class IV HLH proteins such as Mad andMax form heterodimers with the Myc proteins (Blackwood and Eisenman, 1991). Myc/Mad/Max family transcription factors expressed widely in many different cell types and their main targets are genes involved in cell cycle control (Grandori *et al.,* 1997; Jones, 2004).

Id proteins (class V) also comprise a HLH domain but they are lacking the DNA-binding basic domain. Heterodimers of Id proteins and class I and class II bHLH proteins cannot bind DNA and as such Id proteins negatively regulate the activity of these bHLH proteins (Ellis *et al.,* 1990).

Class VI bHLH proteins (Hes family) have a proline in their basic region that alters the DNA-binding specificity (N-box instead of E box) and class VII members feature a bHLH-PAS domain (Figure 1.1; Klambt *et al.,* 1989; Crews, 1998; Rushlow *et al.,* 1989)

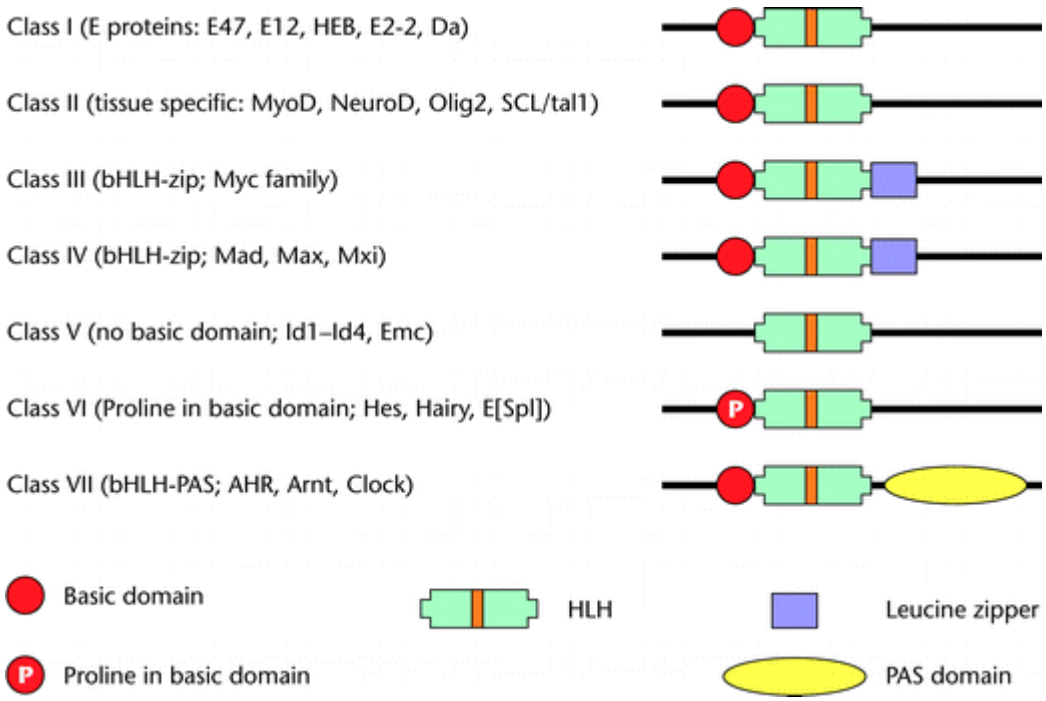

Figure 1.1 Subdivision of HLH protein families. HLH region which mediates homo or hetero dimerisation is made up of two amphipathic α helices, each 15-20 residues long, separated by a shorter intervening loop. Adjacent to the HLH domain is the basic domain (b), which binds DNA at E-box or N-box. Id family members lack the basic domain and negatively regulate other bHLH proteins. Some members of bHLH proteins possess an additional domain for dimerisation. Class III and IV HLH family have a leucine zipper domain whereas class VII have a bHLH-PAS domain (Sablitzky, 2005).

1.2 Id Proteins

Id (Inhibitor of differentiation) proteins (Id1 - Id4 in vertebrates and *extramacrochaetae* (*emc*) in drosophila) are dominant-negative HLH transcription factors that antagonise bHLH protein function (Benezra *et al.*, 1990; Norton *et al.*, 1998; Massari and Murre, 2000). Id proteins compete with bHLH proteins in dimer formation sequestering one of the bHLH proteins. As Id proteins lack the basic domain, Id/bHLH hetero dimers cannot bind DNA (Figure 1.2). The HLH domain is highly conserved between the Id proteins with each protein possessing some unique amino acids. Id4 has four such amino acids in the first helix and loop. Id1 has 3 such change whereas Id2 has 4 and ten in Id3.

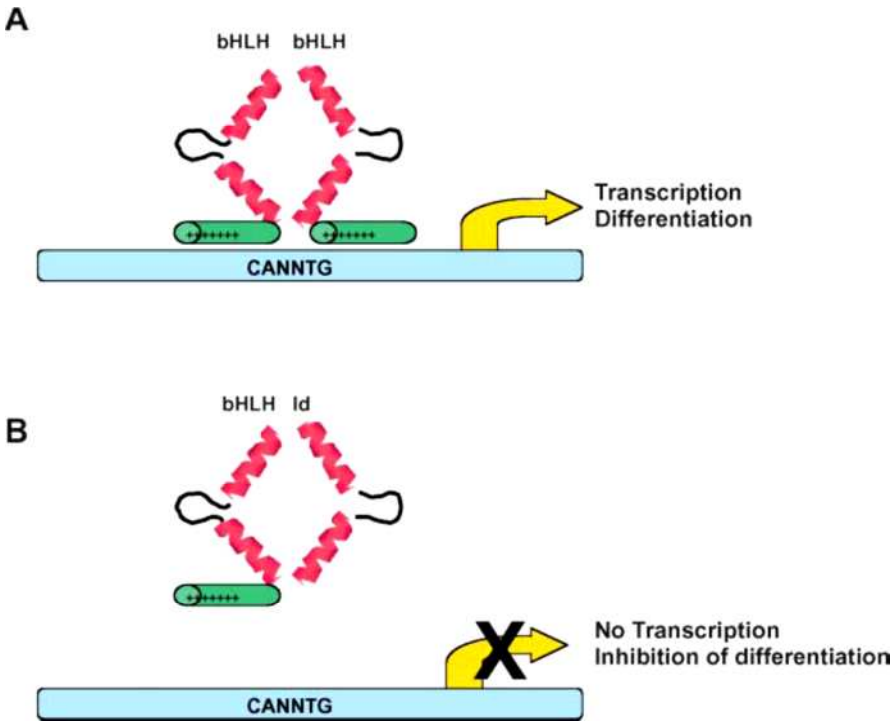

Figure 1.2 Mechanism of Id activity. A. A bHLH protein heterodimer binds to the E box sequence (CANNTG), which leads to transcription of downstream target genes resulting in cell differentiation. **B**. Id proteins form inactive heterodimers with bHLH protein that cannot bind DNA. Hence transcription of downstream target genes is blocked and cell differentiation is inhibited (Sikder *et al.*, 2003).

Id proteins play an important role in regulating early embryogenic processes, such as cell proliferation, differentiation and apoptosis (Benezra *et al.,* 1990). Biochemical and genetic data revealed that Id proteins are positive regulators of cell proliferation and negative regulators of differentiation (Benezra *et al.,* 1990; Norton *et al.,* 2000; Yokota, 2000; Lasorella *et al.,* 2001). Id proteins are highly expressed in undifferentiated, proliferating cells and the expression is subsequently down-regulated in differentiated cells. In mammalian cell culture systems, down-regulation of Id proteins resulted in cell differentiation whereas up-regulation blocked differentiation and increased cell proliferation (Lasorella *et al.,* 2001).

1.3 bHLH proteins function in neural stem cell proliferation and differentiation

The nervous system develops from neural stem cells in the neural epithelium that differentiate to mature and functional neuronal and/or glial cell types (Ross *et al.,* 2003; Guillemot *et al.,* 2005). Several transcription factors and signalling pathways control this process to ensure stem and progenitor cells proliferate sufficiently prior to differentiation, maintenance of progenitor population throughout development and timing of the differentiation at appropriate locations (del Corral and Storey 2001; Bertrand *et al.,* 2002; Ross *et al.,* 2003). Vertebrate nervous system development follows three sequential processes such as the proliferation of the neural stem cells, neurogenesis and gliogenesis. During early stages of neural development the neuroepithelial cells undergo a rapid proliferation to form neural plate. These neuroepithelial cells are actually neural stem cells that are mitotically active giving rise to progenitor cells. Neural stem cells are found throughout the brain during early development but the stem cell population declines over time (Rao, 1999; Temple, 2001; Fujita, 2003). Neuroepithelial cells become radial glia cells, which are also embryonic neural stem cells with some glial characteristics that undergo rapid cell division producing radial glial cells and neurons. Glial cells remain in the ventricular

zones whereas neurons migrate to the outer layer via radial fibres. After producing neurons radial glial cells switch to differentiate to glial cell types such as astrocytes and oligodendrocytes (Bayer and Altman 1991; Temple, 2001). Several bHLH proteins and signalling pathways control the differentiation of neural stem cells into the different cell types. Premature differentiation results in the production of early born neurons and in a disorganised brain architecture (Bertrand *et al.,* 2002; Ross *et al.,* 2003).

It is critical that neural stem cells expand sufficiently before they differentiate. Two different classes of bHLH proteins Id and Hes factors maintain neural stem cells in a proliferative state and regulate the timing of neural differentiation. Once the neuronal cell fate is specified which leads to the transition of proliferation to neurogenesis the expression of the repressor factors Id and Hes decreases while the expression of proneural bHLH proteins increases (Ross *et al.,* 2003; Kageyama *et al.,* 2005).

Both Id and Hes factors are expressed in the ventricular zones of the telencephalon (Jen *et al.,* 1997; Akazawa *et al.,* 1992). Loss of Hes family genes (Hes1 and Hes5) leads to premature neuronal differentiation both *in vivo* and *in vitro* (Nakamura *et al.,* 2000; Kabos *et al.,* 2002) and forced expression results in restricted neurogenesis with an increase in progenitor population (Ishibashi *et al.,* 1995). Knockdown of Id proteins also resulted in precocious differentiation of progenitors into neurons and oligodendrocytes (Lyden *et al.,* 1999; Wang *et al.,* 2001; Yun *et al.,* 2004; Bedford *et al.,* 2005). Overexpression of Id proteins blocked differentiation of neurons and oligodendrocytes (Kondo and Raff, 2000; Wang *et al.,* 2001). These factors repress the proneural genes by direct binding to proneural bHLH proteins (Hes factors) or binding to the E-proteins that are needed for the proneural activity (Id proteins) (Sasai *et al.,* 1992; Norton, 2000).

Proneural bHLH proteins (Neurogenins, Mash1 and Math) are expressed at low levels during development but once progenitors are specified to the neuronal fate their expression

increases resulting in neurogenesis. Proneural genes are expressed in the telencephalon, where neural stem cells start to differentiate and not in the cortical plate where mature neurons are located (Wilson and Rubenstein, 2000). In the absence of proneural factors the number of cortical neurons decreased, which is due to a failure in progenitor specification and also resulted in premature astrocyte differentiation (Fode *et al.,* 2000; Nieto *et al.,* 2001; Tomita *et al.,* 2000). Glial cell differentiation starts after the neurons have migrated to their target locations. Hes factors are known to promote astrocyte development. Ectopic expression of Hes proteins convert retinal progenitors to muller glia cells (Hojo *et al.,* 2000) and initiate astrocyte differentiation in the spinal cord (Wu *et al.,* 2003). It is known that the loss of proneural genes blocked neurogenesis and during later stages of development there is an increased differentiation of glial cells suggesting that the proneural genes inhibits glial cell and astrocyte formation in addition to their role in neuronal differentiation (Tomita *et al.,* 2000; Nieto *et al.,* 2001). While astrocyte differentiation occurs in the dorsal telencephalon the ventral telencephalon differentiates to form oligodendrocyte progenitors. Olig1 and Olig2 bHLH proteins are required for the oligodendrocyte fate and their disruption leads to complete loss of oligodendrocytes (Lu *et al.,* 2000; Zhou *et al.,* 2000; Zhou and Anderson *et al.,* 2002). Thus different members of bHLH proteins regulate each other to mediate stem cell fate and the timing of differentiation in the developing CNS. In addition, the expression of certain bHLH proteins at specific region within the developing brain determines the fate of neural stem cells to differentiate into neuronal and glial subtypes.

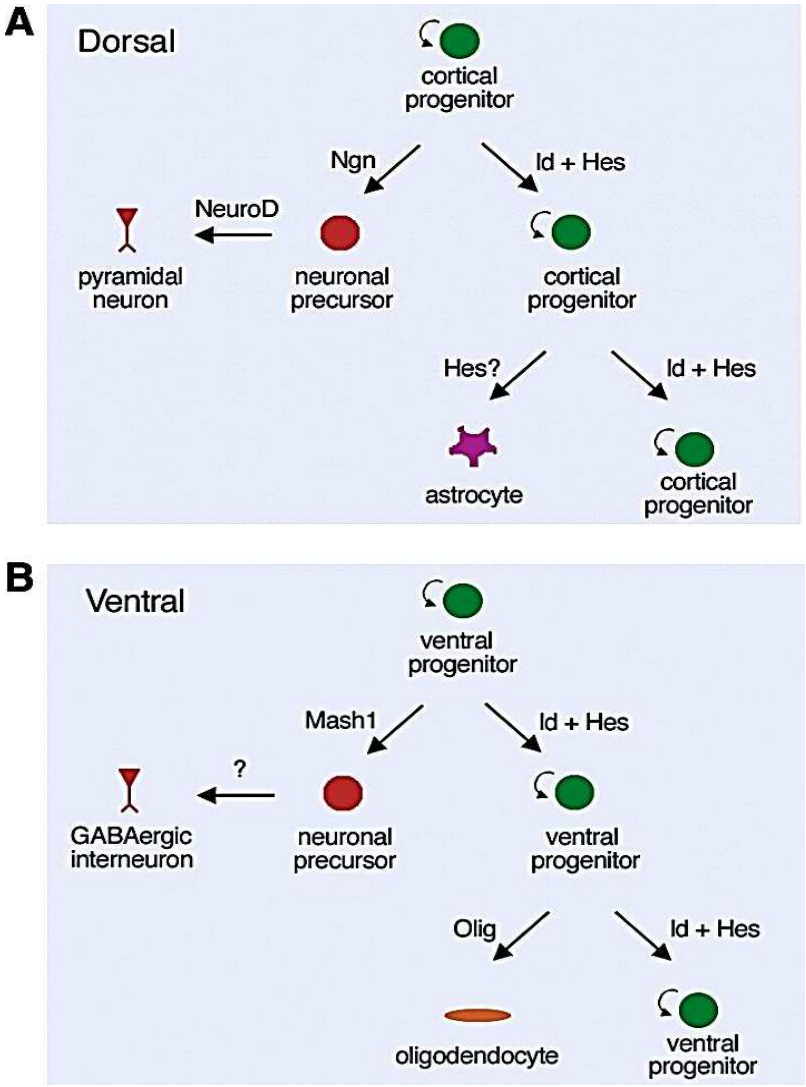

Figure 1.3: bHLH mediated progenitor specification and differentiation in telencephalon. Id and Hes proteins maintain cortical progenitors in the dorsal and ventral telencephalon. **A.** Ngn and neuroD promotes the formation of pyramidal neurons in the dorsal telencephalon and Hes is involved in astrocyte differentiation. **B.** On the ventral side Mash1 is required for GABAergic interneuron specification. Olig proteins specify ventral progenitors to differentiation into oligodendrocytes (Ross *et al.*, 2003).

1.4 Id4 function in neural stem cell proliferation and differentiation

During mouse development Id1, Id2 and Id3 exhibited overlapping expression in multiple tissues including the nervous system. In contrast, Id4 expression was more restricted and particularly seen throughout the development of nervous system (Duncan *et al.,* 1992; Evans and O'Brien 1993; Neuman *et al.,* 1993; Ellmeier *et al.,* 1995; Riechmann and Sablitzky 1995; Zhu *et al.,* 1995; Jen *et al.,* 1997).

At embryonic day 11.5, the expression of Id4 was observed throughout the telencephalic vesicles, later noticed in the spinal cord and in the presumptive motor neurons of the mesencephalon. During embryonic day 12.5 the expression of Id4 is seen in many areas of the brain including frontal and parietal cortex of the telencephalon, medulla, cerebellar peduncle, epithalamus, postoptic and preoptic areas. It is also expressed in the mantle and marginal layers of the thalamus and in the post-mitotic nuclei of the hind brain and mid brain (Riechmann and Sablitzky, 1995; Jen *et al.,* 1997). At embryonic day 17.5, Id4 expression was reduced in the telencephalon and mesencephalon (Riechmann and Sablitzky, 1995). Expression of Id4 is also noted in adult tissues such as brain, kidney, testis (Riechmann *et al.,* 1994), thyroid, pancreas, (Rigolet *et al.,* 1998), prostate (Sharma *et al.,* 2013) and mammary gland (Dong *et al.,* 2011).

1.4.1 Id4 regulates timing of neural differentiation

As outlined above, development of the nervous system is a complex process involving many external and internal factors that determine the fate of multipotent neural stem cells that in turn generate lineage restricted progenitors followed by cell-type restricted progenitor cells which finally differentiate into neurons and glial cells (Anderson, 2001; Gage, 2000; Frisen and Lendahl 2001; Vetter, 2001). *In situ* hybridization on mouse embryos showed that Id4 is specifically expressed in ventricular zones (Riechmann and Sablitzky, 1995).

Two Id4 null mouse model were developed (Fred Sablitzky's group and Mark Israel's group) that had a common phenotype, reduced forebrain. In the model established by Sablitzky's group the HLH domain and most of the regions in the C-terminal was replaced by lacz-neo cassette via homologous recombination and Mark Israel group replaced the first two exons with GFP-neo (Bedford *et al.,* 2005; Yun *et al.,* 2004).

Lack of Id4 resulted in reduction in forebrain size due to the reduction of proliferative cells in the ventricular zones by 20-30% suggesting the loss of neural progenitor cells. This proliferation defect was followed by 3-fold increase in the apoptosis in the neocortex. The mice also displayed precocious neuronal differentiation. In addition, the adult mice brain also displayed reduced astrocytes indicating the premature differentiation of the neural progenitor cells during early development has led to the loss of astrocytes in the adult (Bedford *et al.,* 2005, Sablitzky group Id4 model).

Israel group also reported that the loss of Id4 leads to reduction in the forebrain size especially the dorsomedial progenitor zones (ventricular zone) due to premature differentiation of the neural progenitor cells. They also reported that the reduced brain size is due to the defect in the G1-S transition of the neuroepithelial cells that resulted in reduced proliferation of the neuro epithelium, but increased in the region outside the ventricular zones. However they did not observe any abnormal apoptosis as observed in Bedford *et al.,* 2005 (Yun *et al.,* 2004).

1.4.2 Id4 is required for timing of oligodendrocyte differentiation

Ectopic expression of Id4 inhibits oligodendrocyte differentiation in cultured progenitor cells and the expression of Id4 declines once the progenitors start to differentiate both *in vitro* and *in vivo* (Kondo and Raff, 2000). Loss of Id4 in mice resulted in premature differentiation into oligodendrocytes determined by the expression of late oligodendrocyte

markers and mature CC1 oligodendrocytes in the sub-ventricular zones and white matter of neonatal Id4-deficient mice (Marin-Husstege *et al.,* 2006). Premature differentiation also resulted in decreased oligodendrocyte progenitors and increased apoptosis in adult mice (Marin-Husstege *et al.,* 2006). Enforced expression of Id4 blocks the activity of myelin basic protein promoter (Gokhan *et al.,* 2005). In the Id4 null neonatal mice the level of myelin gene transcripts for MBP and CGT were increased with PLP and MAG protein levels decreased. But the expression of myelin genes and myelination looked normal in the adult despite the smaller size of the brain (Marin-Husstege *et al.,* 2006).

1.5 Id4 function in the adult

1.5.1 Id4 is required for self-renewal of spermatogonial stem cells (SSC) and act as marker to distinguish A_s from other spermatogonia progenitors

Spermatogenesis is a process by which undifferentiated single spermatogonia (A_{single} or A_s) forms an A_{paired} that proliferates to form $A_{aligned}$ which eventually differentiates into spermatozoa. A_s cells have self-renewal ability to maintain the stem cell pool and A_{paired}, $A_{aligned}$ are progenitors. Within the spermatogonial populations Id4 selectively labels the A_{single} cells whereas the other Id proteins (Id1-3) are expressed in spermatocytes and sertoli cells (de Rooij and Russell 2000; Oatley and Brinster 2012). Disruption of Id4 resulted in impairment of quantitatively normal spermatogenesis as it loss resulted in premature differentiation of the SSC. The fertility defects are mainly due to reduced population of germ cells and not due to the altered endocrine system (Oatley *et al.,* 2011). Expression of Id4-GFP transgene is restricted to the rare subset of cells that possess regenerative capacity in the undifferentiated cells of spermatogonial population. This suggests that a subset of A_s cells are progenitors while the other functions to maintain the SSCs pool by self-renewing and the subsets were distinguished based on Id4 expression. Transplantation of Id4-GFP^+ cells

confirmed that these cells have regenerative capacity suggesting that Id4 represents SSC pool (Chan *et al.,* 2014).

1.5.2 Id4 regulates mammary gland development by suppressing p38 MAPK activity

Id4 is also expressed in mammary epithelial and basal cells (de Candia *et al.,* 2006). Expression of Id4 was observed in myoepithelial and in luminal cell population of adult mammary gland whereas it is expressed in terminal end buds cap cell layer and in myoepithelium of subtending ducts during puberty. A severe developmental defect in the mammary gland was observed in the Id4-deficient mice. It also required for ductal elongation, cap and luminal epithelial cell proliferation (Dong *et al.,* 2011). The developmental defects are followed by decreased proliferation and increased apoptosis as observed in Id4-deficient mouse (Bedford *et al.*, 2005). Id4 promotes proliferation of cell by suppressing p38MAPK, which is known to block cell cycle by activating cell cycle inhibitors and supressing cyclin D1. In Id4-deficient mouse mammary gland the activity of p38MAPK was elevated suggesting this increased activity of p38MAPK is responsible for reduced proliferation and increased apoptosis in the Id4 null mammary gland. One of the downstream targets of p38MAPK is known as BimEL that is involved in apoptosis. BimEL was found to be activated in the Id4-deficient mammary gland that caused the increased apoptosis of terminal end buds. Suppression of p38MAPK in the Id4 null mice reversed the defects caused by Id4 in mammary development. Id4 stimulates proliferation of mammary epithelium by suppressing the p38MAPK activity, which was increased in Id4-deficient mammary gland (Dong *et al.*, 2011).

1.6 Id4 functions as a tumour suppressor as well as oncogene depending on the cell type and context

Expression of Id proteins were observed in a variety of tumours and often resulted in loss of differentiation, enhanced malignancy and aggressive clinical behaviour of tumours (Lasorella *et al.,* 2001; Perk *et al.,* 2005; Fong *et al.,* 2004). Apart from proliferation and differentiation of normal and cancer cells, Id proteins are also involved in tumour progression (Park *el al.,* 2005; Fong *et al.,* 2004) such as the ability of tumour cells to invade neighbouring tissues, metastasise and promote the formation of new blood vessels, which allows expansion of the tumour mass (Fong *et al.,* 2004; Hanahan and Weinberg 2000). Id4 acts as tumour suppressor in many cancers including leukemia, pancreatic cancer, gastric cancer, lymphoma, glial neoplasia and lung cancers (Chan *et al.,* 2003; Yu *et al.,* 2005; Vincent *et al.,* 2011; Hagiwara *et al.,* 2007; Castro *et al.,* 2010). However, Id4 also act as an oncogene promoting glioblastoma and ovarian cancer (Kuzontkoski *et al.,* 2010).

In glioblastoma multiforme and its derived cell lines the expression of Id4 is elevated. Xenograft from the cell lines expressing high levels of Id4 had broad vasculature, increased expression of matrix GLA proteins (Kuzontkoski *et al.,* 2010), which is known to promote tumor angiogenesis (Chen *et al.,* 1990). The pro-angiogenic functions of Id4 are mediated by matrix GLA proteins (Kuzontkoski *et al.,* 2010). In another report it was found that Id4 suppresses the invasion of glioblastoma multiforme *in vitro*. Expression of MMP2 (Matrix metalloproteinases 2) which is known to digest the various components of brain extracellular matrix to mediate tumour invasion, was down-regulated in the glioma cell lines expressing high levels of Id4. This reduced expression of MMP2 was due to the direct interaction of Id4 with Twist1 another bHLH protein that is known to promote MMP2 expression (Rahme and Israel, 2014). Enforced expression of Id4 in Ink4a/Arf-deficient mouse astrocytes resulted in dedifferentiation of glioma cells to glioma stem-like cells. Neurospheres exhibited properties

of brain cancer stem cells such as self-renewal activity and increased expression of marker genes like sox2, nestin and CD133. This enforced expression of Id4 supports tumour formation by activating notch signalling and up-regulating cyclin E (Jeon *et al.,* 2008).

Glioma stem cells, a subpopulation of cancer cells in brain tumour, are responsible for tumour initiation, self-renewal, differentiation and progression of glioma (Singh *et al.,* 2003; Vescovi *et al.,* 2006). These stem cells are resistant to chemotherapy and irradiation (Dean *et al.,* 2005; Bao *et al.,* 2006). Id4 supresses microRNA-9* to enhance sox2 expression and sox2 directly regulates the ATP binding cassette transporters ABCC3 and ABCC6 which supports the chemoresistance of Glioma stem cells (Jeon *et al.,* 2011).

In normal breast epithelium and in carcinoma the expression of Id4 is limited to oestrogen receptor (ER) negative cells suggesting that Id4 is negatively regulated by ER. Id4 promoter was frequently hyper-methylated in breast cancer cell lines and tissues indicate the suppressor role of Id4 in breast cancer (Noetzel *et al.,* 2008; Umetani *et al.,* 2005). Id4 is also known to promote mammary and ovarian tumourigenesis by suppressing the expression of BRCA1 (Beger *et al.,* 2001; Roldán *et al.,* 2006). Id4 expression marks a subpopulation of basal cells that have the ability to produce multi-lineage mammary epithelial cells. As mentioned earlier, Id4 is required for normal mammary ductal morphogenesis and luminal differentiation (Dong *et al.,* 2011; Junankar *et al.,* 2015). Id4 is also expressed in basal like breast cancer (BLBC) and these BLBC are thought to be derived from luminal progenitors especially the one with a mutation in BRCA1 (Lim *et al.,* 2009; Molyneux *et al.,* 2010; Junankar *et al.,* 2015). BLBC expressing high levels of Id4 possess properties more similar to basal cell than to luminal cells and expressed mammary stem cell markers (Junankar *et al.,* 2015). Id4 is also highly expressed in the cancer stem cell population isolated from the 4T1 cell line, a mouse mammary cancer line and knockdown of Id4 in these cells resulted in reduced tumoursphere formation (Park *et al.,* 2011).

In prostate cancer, Id4 acts as tumour suppressor and its expression is downregulated in prostate cancer as well as in DU145 prostate cancer cell line due to hyper-methylation (Carey *et al.,* 2009). In the adult mice prostrate Id4 is highly expressed in the glandular epithelial cells in a way similar to human prostrate. Id4 loss in the mouse prostate resulted in reduced size of the genital tract, decreased size and number of tubules, and lack of differentiated epithelial cells (Sharma *et al.,* 2013). A similar phenotype was observed with the loss of androgen receptor (Simanainen *et al.,* 2007). Id4-deficient mice exhibited a ductal branching morphogenesis, epithelial hyperplasia and dysplasia that are also observed in Nkx3.1 deficient mice (Bhatia-Gaur *et al.,* 1999; Sharma *et al.,* 2013). Id4 loss further supported the formation of PIN (prostatic intraepithelial neoplasia) lesions, earliest stage of prostate cancer which was associated with increase in expression of Myc, sox9 and Id1. (Sharma *et al.,* 2013).

1.7 Id4 function in zebrafish development

17.1 Knockdown of Id4 during zebrafish development results in reduced brain size and lack of brain boundaries

Id4 is expressed in the central nervous system of zebrafish (Thisse *et al.,* 2001) and RT-PCR has shown that Id4 mRNA is present as early as 6 hpf in the developing zebrafish embryos (Bashir, 2010). Knockdown of Id4 using translation blocking morpholinos (MOs) resulted in various phenotypes in the developing embryo at 10.6 hpf and 24 hpf. The embryos displayed reduced brain size and lacked brain boundaries at 24 hpf. As some morpholinos have been shown to result in upregulation of the p53 pathway causing similar phenotypes as described above, p53 MOs were co-injected with Id4 MOs to eliminate these off-target effects. Double morphants still showed a similar phenotype in the developing embryos, albeit

less severe, suggesting the requirement of Id4 in normal brain development (Bashir, 2010; Dhanaseelan, 2011).

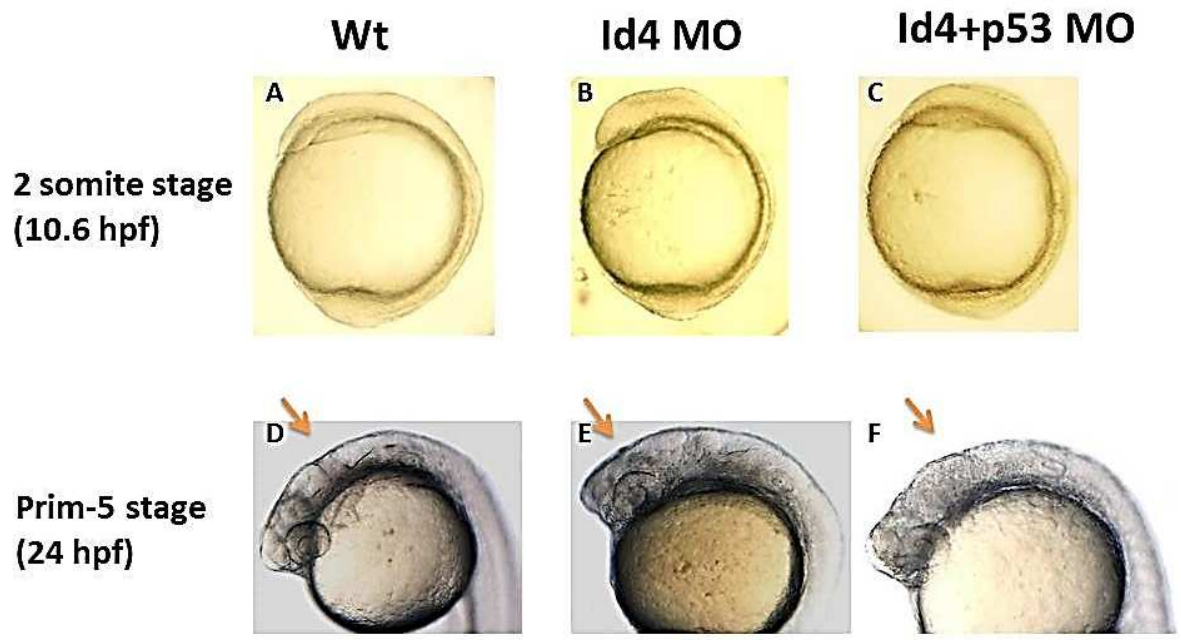

Figure 1.4: Morpholino mediated knockdown of Id4 resulted in a severe phenotype in the developing brain. Wild type embryos at 2 somites (A) and 24 hpf (D). Embryos injected with Id4 morpholinos (B, E) lack proper development of the brain. Co-injection of p53 morpholino (C, F) eliminated the p53 mediated off-target effects but the embryos still displayed reduced brain size, revealing the requirement of Id4 for normal brain development (Bashir, 2010; Dhanaseelan, 2011).

1.7.2 Id4 morphants exhibit decreased cell proliferation and increased apoptosis

Id proteins are highly expressed in the proliferating cells while the expression is reduced in the differentiating cells indicating that they are important for proliferation (Norton *et al.*. 1998; Lyden *et al.*, 1999). Loss of Id4 in mouse revealed that 20-30% of proliferative cells was lost in the neural region (Bedford *et al.*, 2005). Id4 and Id4/p53 morphant embryos also showed a reduction in the number of proliferative cells (Figure 1.4). Up to 50% of the cells were lost in Id4 morphants and in Id4/p53 morphants proliferating cells were reduced by 30-35% (Figure 1.4 H). In addition to this proliferation defect, the embryos also demonstrated an 8 fold increase in apoptotic cells (Figure 1.4 D-G, I). Reduced proliferation and increased apoptosis in the developing embryos is likely to impact on the expansion of neural epithelium resulting in a reduced brain size at later stages (24 hpf) of development (Dhanaseelan, 2011).

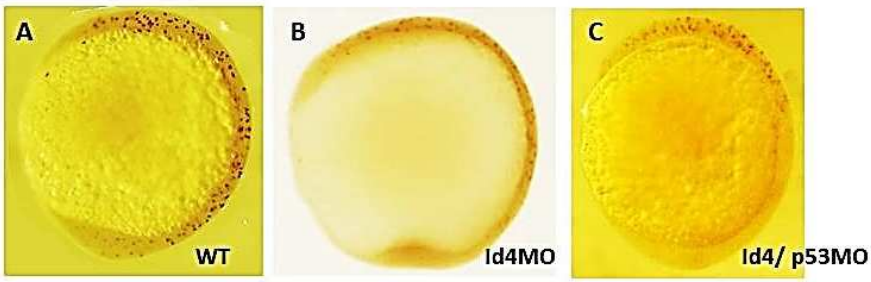
A
WT
B
Id4MO
C
Id4/ p53MO

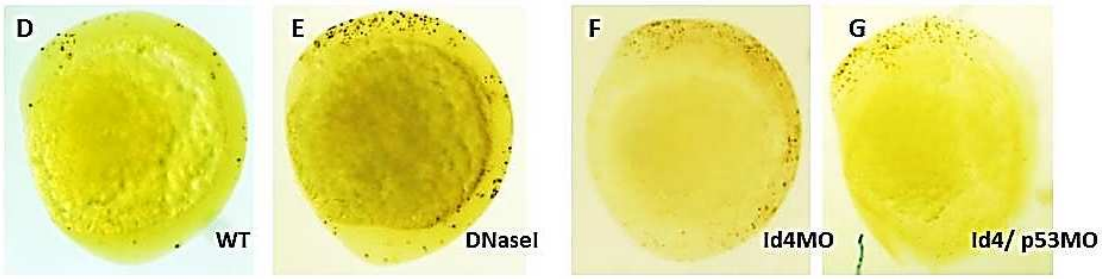
D
WT
E
DNaseI
F
Id4MO
G
Id4/ p53MO

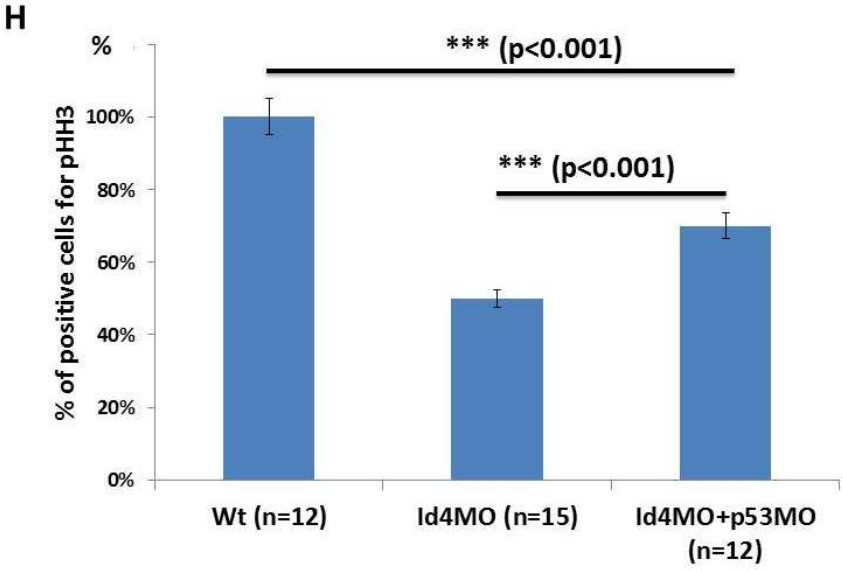
H
%
% of positive cells for pHH3
100%
80%
60%
40%
20%
0%
*** (p<0.001)
*** (p<0.001)
Wt (n=12)
Id4MO (n=15)
Id4MO+p53MO (n=12)

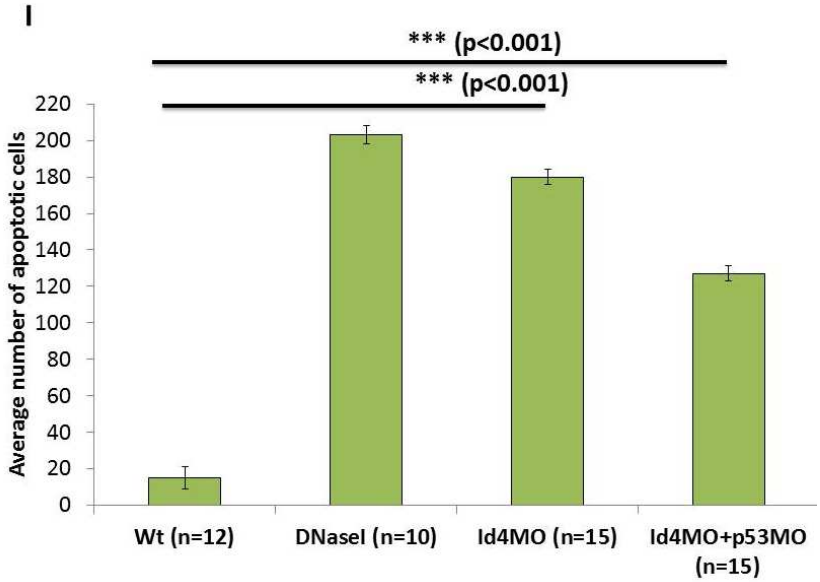

Figure 1.5: Knockdown of Id4 resulted in reduced cell proliferation and increased apoptosis. Phospho-histone H3 immunostaining revealed a reduction in proliferating cells in Id4 and Id4/p53 morphants (B and C) compared to the wild type (A). TUNEL staining of Id4 and Id4/p53 morphants (F and G) reveals that more cells are undergoing apoptosis in the morphants. (D) Wild type and (E) DNaseI treated wild type embryo, positive control. Quantification confirms that there is significant reduction in the number of proliferating cells (H) and an increase in the number of apoptotic cells (I) (Dhanaseelan, 2011).

1.8 Notch signalling and nervous system development

Notch signalling mediates various cell-cell interactions via lateral inhibition where cells adopting a fate inhibit its neighbour cells from embracing a similar fate (Bray, 1998; Artavanis-Tsakonas et al., 1999). Notch functions as receptor and forms a single-pass transmembrane heterodimer to its ligands Delta and Jagged gene families (Kopan and Illagan, 2009). Upton binding to its ligand, γ secretase cleaves the Notch transmembrane domain and releases the intracellular domain (NICD) from the plasma membrane. The NCID enters the cytoplasm and activates the Recombining binding protein suppressor of hairless (RBPJ) by recruiting co-activators like Mastermind. The activated RBPJ upregulates the expression of *Hes* and *Herp* genes that antagonise the proneural bHLH proteins (Wu *et al.,* 2001; Kopan and Illagan, 2009; Bertrand *et al.,* 2002). Thus notch signalling inhibits neuronal differentiation through lateral inhibition.

It has been reported that Mind bomb1 (Mib) an ubiquitin ligase, activity is essential for the endocytosis of notch ligand and they are known to regulate all of the notch ligands. In zebrafish and mouse *mib* mutants, notch signalling mediated lateral inhibition was reduced leading to premature differentiation of the neural progenitor cells (Itoh *et al.,* 2003; Koo *et al.,* 2005). Thus, Notch signalling is activated by Mib mediated ubiquitylation followed by the interaction of Notch with its ligands. Interaction of Notch with its ligands activates the proteolytic cleavage of the notch receptor resulting in a membrane-bound Notch fragments. The NCID fragment was released into the cytosol and activates RBPJ once the remaining receptor fragments are cleaved by γ secretase (Itoh *et al.,* 2003; Lai, 2004; Brou *et al.,* 2000).

In zebrafish, Notch pathway can be disrupted by three different ways. Deletion of *mib1* will prevent the binding of the notch with its ligands. Zebrafish naturally occurring mind bomb mutant has a defective *mib* activity. Secondly, γ secretase mediated cleavage can

be inhibited using chemical inhibitors such as DAPM (N-[N-3,5-difluorophenacetyl]-L-alanyl-S-phenylglycine methyl ester). This will result in the NCID fragment bound to the membrane thus inhibiting the activity of RBPJ complex (de Strooper and Annaert, 2010). Activation of Hes proteins by RBPJ is critical for notch-mediated lateral inhibition. Targeting RBPJ using morpholinos (or genome editing) will block the interaction of RBPJ with the Notch intercellular domain. This restrict the activity of notch target genes (*Hes*) (Sieger *et al.*, 2003).

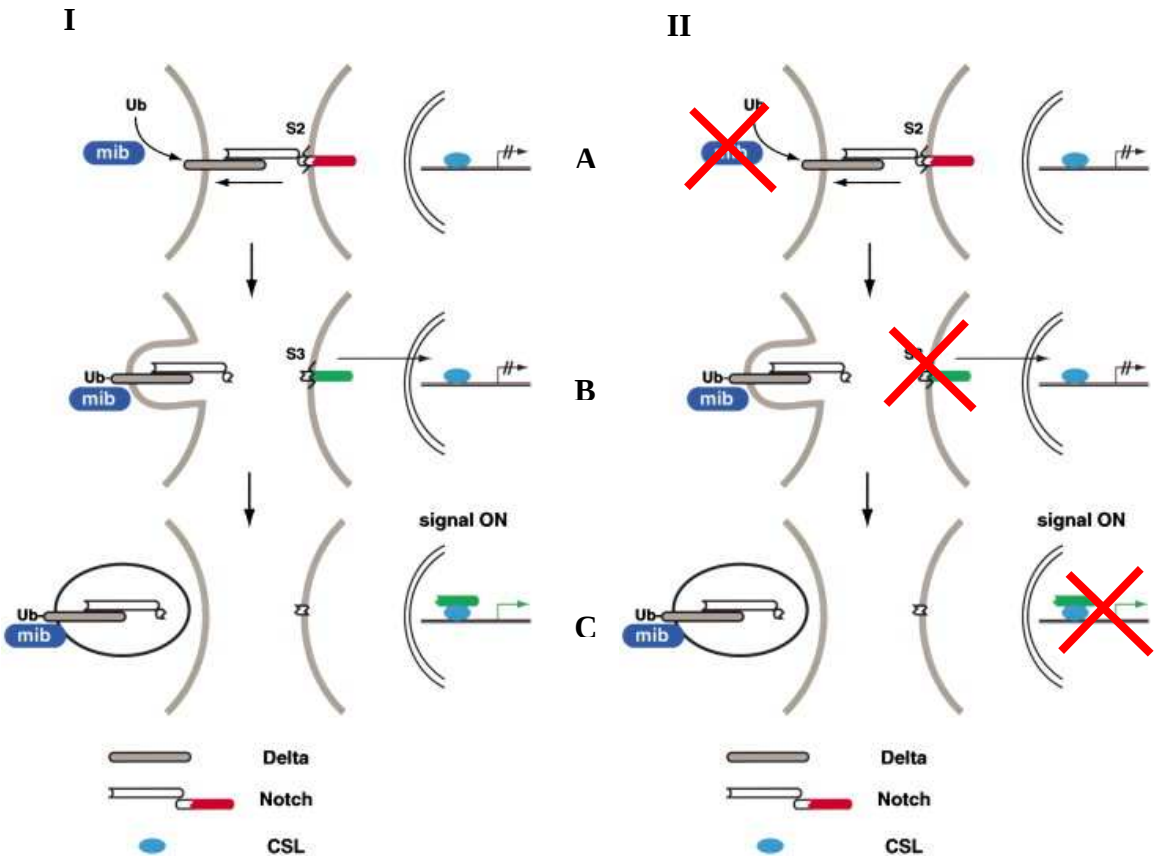

Figure 1.6: Hypothetical model of Notch signalling based on Delta endocytosis and ways to block Notch signalling. I. Notch signalling is initiated once Mib interacts with Delta which promotes its ubiquitylation and endocytosis. This endocytosis then assists the S2 proteolytic cleavage which releases the Notch extracellular domain. The remaining NICD is then cleaved by γ secretase releasing the NICD into nucleus which activates target genes. **II.** Notch signalling can be blocked by different ways to inhibit notch activity **A.** Mutation in *mib* can block the interaction of Notch with its receptors thereby preventing the entire process. **B.** Inhibition of γ secretase by DAPM can prevent the release of NICD from the extracellular domain. **C.** Morpholinos (Su(H)/RPBJ) that can prevent the formation of transcription activator complex. This blocks the activation of notch target genes. (Itoh *et al.*, 2003)

1.9 bHLH proteins in haematopoiesis

Haematopoiesis is a process, through which multipotent haematopoietic stem cells differentiate into lineages restricted progenitors and to functionally different unipotent blood cells types such as erythrocytes, monocytes/macrophages, neutrophils, basophils, eosinophils, platelets and lymphocytes (Orkin and Zon, 2008). Haematopoiesis is controlled through a network of signalling pathways and transcription factors (Huang and Zon, 2008). Haematopoietic stem cells have the ability to self-renew in the way in which one or two of the daughter cells have the characteristics of the mother cell to maintain the HSC pool at the constant level (He *et al.,* 2006). During murine development, haematopoiesis first occurs as cell cluster in yolk sac blood islands and later in the aorta-gonad-mesonephros (AGM), placenta, fetal liver and finally in the bone marrow. Zebrafish haematopoiesis is initiated in the Anterior Lateral Mesoderm (ALM) and Posterior Lateral Mesoderm (PLM) then in intermediate cell mass (ICM) and subsequently in the AGM, the caudal haematopoietic tissue before the cells colonise in kidney marrow (Orkin and Zon, 2008; Dzierzak *et al.,* 2008).

1.9.1 Haematopoietic stem cells (HSCs)

Haematopoietic stem cells are cells that have the capacity to regenerate the entire blood system of an adult (Orkin and Zon, 2008). Transplantation of HSC from bone marrow to lethally irradiated mice resulted in complete, long-term engraftment of all blood lineages by donor-derived stem cells (Till and McCulloch *et al.,* 1961; Müller *et al.,* 1994; Moore *et al.,* 1970). HSC isolated from the recipient using monoclonal antibodies that are specific for various cell-surface proteins like c-kit and stem-cell antigen 1 (SCA 1) demonstrated the HSC containing cell population and in this population one in 5 cells showed the property of long-term engraftment (Yilmaz *et al.,* 2006). Thus HSCs are pluripotent, which is

characterised by their potential to generate eight major haematopoietic lineages such as the erythrocytes, megakaryocyte/platelets, basophils, eosinophils, neutrophils, monocytes, B and T cells (Jordan *et al.,* 1990; Szilvassy *et al.,* 1990). HSCs maintain high proliferation potential and are self-renewal (Morrison *et al.,* 1994; Osawa *et al.,* 1996). HSCs possess multipotency as well as self-renewal ability and give rise to multipotent progenitors (MPPs) that possess limited self-renewal ability but can maintain full-lineage differentiation potential (Morrison and Weissman, 1994; Christensen and Weissman, 2001). MPPs differentiate into lymphoid-primed multipotent progenitor cells (LMPPs). LMPPs can be differentiated into common lymphoid progenitors (CLPs) that give rise to lymphocytes and NK cells. LMPPs have reduced ability to differentiate into megakaryocytes and erythrocytes. Hence these cells must develop through common myeloid progenitors (CMPs) that differentiate into megakaryocyte-erythrocyte progenitors (MEPs) that develop into erythrocytes/platelets and granulocyte-monocyte progenitors (GMPs) which further differentiates into granulocytes/macrophages/dendritic cells (Serwold *et al.,* 2009; Kondo *et al.,* 1997; Adolfsson *et al.,* 2005; Zandi *et al.,* 2010).

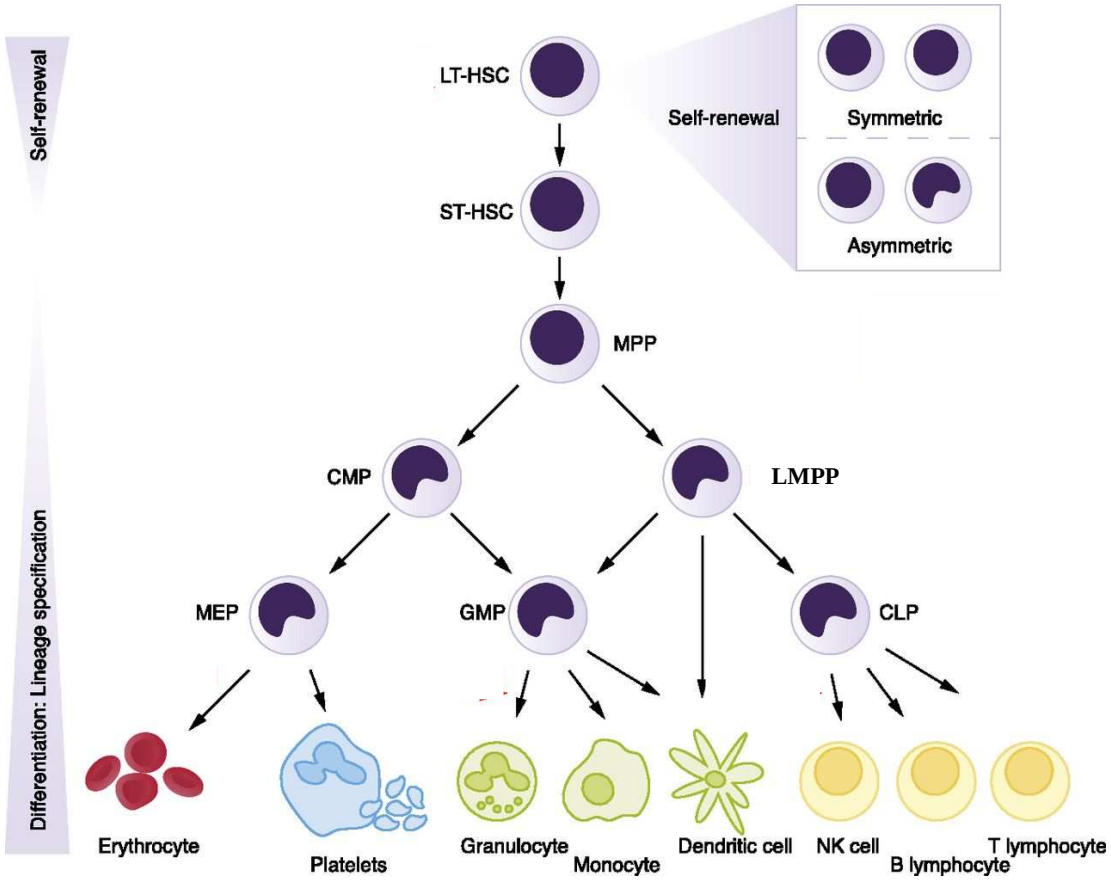

Figure 1.7: Haematopoietic hierarchy. Haematopoietic system is maintained by HSCs that have the self-renewal ability, giving rise to various progenitor cells which proliferate progressively and generates mature blood cells. These progenitor cells have only limited self-renewal ability, hence they were replaced continuously. Abbreviations: LT-HSC, long-term haematopoietic stem cells; ST-HSC short-term haematopoietic stem cells; MPP, multipotent progenitor; CMP, common myeloid progenitor; LMPP, lymphoid-primed multipotent progenitor; CLP, common lymphoid progenitors; MEP, megakaryocyte/erythroid progenitors; GMP, granulocyte/ macrophage progenitor. (Blank and Karlsson, 2015).

1.9.2 Waves of haematopoiesis

Vertebrates display two waves of haematopoiesis known as the embryonic or primitive haematopoiesis and adult or definitive haematopoiesis. Primitive haematopoiesis results in the production of red blood cells and macrophages, which provides the rapidly developing embryo with tissue oxygen and innate immunity respectively. This primitive wave is transient and is replaced by definitive or adult haematopoiesis. The primitive haematopoiesis was seen extra-embryonically in the yolk sac while the adult one is noted intra-embryonically in the ventral wall of the dorsal aorta known as the aorta-gonad-mesonephros (AGM), where HSC arise (Taoudi et al, 2007). *In vitro* studies using mouse have shown the presence of majority of the multipotent haematopoietic precursors in these regions (Godin et al, 1999; de Bruijn et al, 2000). Apart from AGM haematopoietic activity was also observed in umbilical arteries and in allantois where co-localisation of haematopoietic and endothelial cells occurs (Inman and Downs, 2007). Umbilical veins lack the haematopoietic potential but HSC were observed in mouse placenta (Gekas *et al.,* 2005; Ottersbach and Dzierzak, 2005). In mammals, definitive haematopoiesis involves colonisation of the fetal liver, thymus, spleen and ultimately bone marrow. It is believed none of these sites generated HSC de novo and that populations of HSCs have been migrated there from the AGM (Orkin and Zon, 2008).

1.9.3 Zebrafish haematopoiesis

Like the vertebrates, Zebrafish also display two waves of haematopoiesis: primitive or the embryonic and definitive or the adult wave. Primitive wave is initiated in the ventral lateral mesoderm at 10 hpf giving rise to haemangioblast which express markers for both haematopoietic (*scl/tal1, lmo2*) and endothelial markers (*flk1*) (Galloway and Zon, 2003; Dooley *et al.,* 2005; Paik and Zon, 2010). Ectopic expression of *scl/tal1* resulted in the

expansion of both blood and endothelial precursors indicating its importance in haemangioblast specification (Gering *et al.,* 1998). Primitive haematopoiesis give rise to a transition population of erythrocytes and primitive myeloid cells (Ciau-Uitz *et al.,* 2014). Primitive haematopoiesis occurs in anterior lateral mesoderm (ALM) and posterior lateral mesoderm (PLM) (Davidson *et al.,* 2003; Detrich *et al.,* 1995). ALM expresses the myeloid marker *pu.1* at 12hpf which migrates rostrally and then laterally across the yolk sac. These myeloid progenitors later mature into different myeloid populations expressing myeloid-specific *l-plastin* and granulocytic specific myeloperoxidase (Lieschke *et al.,* 2002; Bennet *et al.,* 2001).

At 4 somites stage in the PLM the expression of gata1 in a subset of scl/tal1^{+} cells which marks the erythrocyte precursors (Davidson *et al.,* 2003; Detrich *et al.,* 1995). PLM cells migrate medially to fuse to the midline forming intermediate cell mass (ICM) at 14 somite stage. Primitive erythropoiesis occurs in the ICM which produces the primitive Red Blood Cells (prRBC) (Sood and Liu, 2012). These scl/tal1^{+}/ gata1^{+} cells give rise to the first circulating blood cells (Lieschke *et al.,* 2002). These primitive erythrocytes are morphologically different from the adult zebrafish erythrocytes, which have less cytoplasm and a long nucleus. Transfusion experiments using rhodamine labelled circulating erythrocytes have demonstrated that these primitive erythrocytes are the only circulating erythroid cell during the first 4 dpf (Weinstein *et al.,* 1996). *Gata1* and *pu.1* antagonise each other to promote erythroid and myeloid differentiation, respectively. Loss of *gata1* resulted in the transformation of erythroid precursors into myeloid and knockdown of *pu.1* increases the erythroid production at the expense of myeloid cells (Galloway *et al.,* 2005; Berman *et al.,* 2005).

Definitive haematopoiesis in zebrafish occurs in two waves; a transient pro-defintive wave in the posterior blood island (PBI) at 24 hpf which produces erythro-myeloid progenitors (EMP) and second definitive wave that produces HSCs (Ciau-Uitz *et al.,* 2014). EMPs are observed before HSC and have the potential to give rise to both erythroid and myeloid colonies in culture but they were not observed in kidney marrow or thymus *in vivo* (Bertrand *et al.,* 2007). Zebrafish definitive haematopoiesis that give rise to HSC occurs at around 30 hpf from the heamogenic endothelium on the ventral wall of dorsal aorta (Burns *et al.,* 2002; Bertrand *et al.,* 2010). From 48 hpf the HSC that are *c-myb* and *runx1* positive, migrate to caudal haematopoietic tissue (CHT). CHT acts an intermediate niche for HSC expansion and differentiation to erythroid and myeloid cells. Definitive erythropoiesis occurs approximately from 3.5 dpf and gradually replaces the primitive erythrocytes whereas the myelopoiesis starts from 3dpf (Murayama *et al.,* 2006; Jin *et al.,* 2009; Monteiro *et al.,* 2011). HSC starts to seed the thymus and from 4 dpf thymus express the lymphoid differentiation marker *rag1* (Kissa *et al.,* 2008; Le Guyader *et al.,* 2008). HSCs also start to seed the developing kidney marrow from 4dpf which acts as primary site of haematopoiesis (Bertrand *et al.,* 2010).

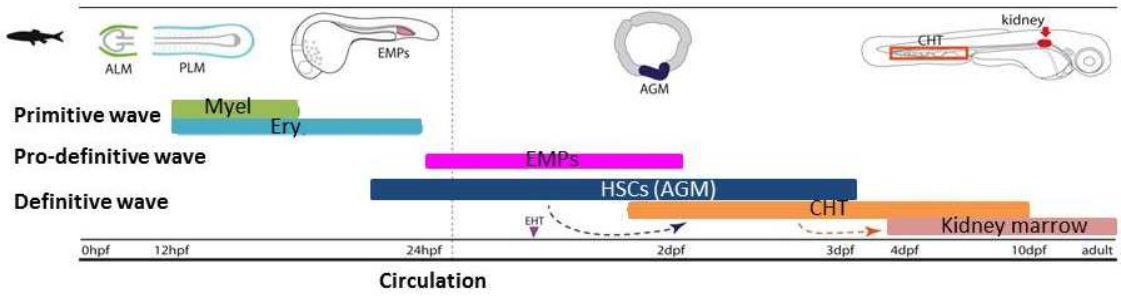

Figure 1.8. Zebrafish haematopoiesis. Haematopoiesis in zebrafish occurs in two waves primitive and definitive wave.Primitive waves occurs at 2 somites in two regions known as the ALM and PLM which produces myeloid (Green) and erythrocytes (Blue) respectively. Before the wave switch to definitive there was transient phase (pro-definitive wave, 22-24 hpf) that produces EMPs (Pink) arise from PBI. Definitive wave occurs in the ventral wall of dorsal aorta where HSCs are generated. Unlike, other vertebrate EHT does not occurs in the lumen of the DA but occurs in the space between the DA and posterior cardinal vein. The HSC then seed the CHT where they differentiate into erythroid and myeloid progenitors. HSC finally seed the kidney marrow at around 4dpf. Lymphoid differentiation occurs in thymus. HSC-Haematopoietic stem cells; ALM- anterior lateral mesoderm; PLM- posterior lateral mesoderm; EMP- erythroid myeloid progenitor; PBI- posterior blood island; DA-dorsal aorta; CHT- caudal haematopoietic tissue (Ciau-Uitz *et al.*, 2014),

1.10 Lymphoblastic leukemia 1 (lyl1) function in haematopoiesis

Lyl1 (lymphoblastic leukemia 1) is a member of class II bHLH protein and closely related to scl/tal1 (Stem cell leukemia) (Mellentin *et al.,* 1989; Visvader *et al.,* 1991). Lyl1 was first discovered at chromosomal translocation sites in T-cell acute lymphoblastic leukemia (Mellentin *et al.,* 1989). Both lyl1 and scl/tal1 displayed more than 90% amino acid identity in the bHLH region and interact with the leukemia oncogene proteins LMO1/LMO2 (lim-only-domains) suggesting that they share some biological functions (Mellentin *et al.,* 1989; Wadman *et al.,* 1994; Porcher *et al.,* 1996; Schlaeger *et al.,* 2004). However, the domains other than bHLH domain are quite diverged indicating distinct roles for these bHLH proteins (Visvader *et al.,* 1991; Kallianpur *et al.,* 1994). Indeed, lyl1 and scl/tal1 display overlapping but not identical expression patterns in the mouse (Visvader *et al.,* 1991; Chapman *et al.,* 2003; Giroux *et al.,* 2007) and analysis of knockout mice have demonstrated both redundant functions as well as distinct roles for both proteins in haematopoiesis (Souroullas *et al.,* 2009).

1.10.1 Comparison of scl/tal1 and lyl1 expression in mouse haematopoietic system and other tissues of mouse

At 7 dpc (days post-coitum) expression of scl/tal 1 was observed both at mRNA (Silver and Palis, 1997) and protein (Kallianpur *et al.,* 1994) level in the extra-embryonic mesoderm. The mouse reporter line also showed β-gal activity in extra-embryonic mesoderm at 7 dpc (Elefanty *et al.,* 1998). Expression of lyl1 mRNA had a similar pattern to that of scl/tal1 at this stage but the reporter mouse (whose C-terminal end was replaced by a *lacZ* reporter gene) didn't show any β-gal activity (Giroux *et al.,* 2007). In the yolk sac blood islands both lyl1 and scl/tal1 mRNAs were detected but still β-gal activity was undetectable

(Silver and Palis, 1997; Giroux *et al.,* 2007). At 7.75 dpc the first β-gal activity for lyl1 was observed in the intra-embryonic mesoderm in the pre-cardiac plate. During the later stages of cardiac development the expression of lyl1 and scl/tal1 mRNAs as well as the β-gal activity was restricted to the endocardium (Giroux *et al.,* 2007).

By 10.5 dpc HSC production in the AGM reaches its maximum level and β-gal activity in lyl1^{lacZ} embryos was detected in the ventro-lateral part of the dorsal aorta known as the haematopoietic intra-aortic clusters (HIAC) where the HSC are cytologically identifiable (Garcia Porrero *et al.,* 1995; Bertrand *et al.,* 2005). Yolk sac derived circulating haematopoietic cells colonise the fetal liver and later AGM derived HSCs move to the fetal liver marking it as a major haematopoietic organ of the embryo. The presence of X-gal positive haematopoietic cells in the fetal liver as soon as it is morphologically traceable suggests the presence of lyl1/ β-gal protein in some of the yolk sac derived cells. The X-gal positive haematopoietic fetal liver cells had a different morphology indicating that lyl1 is expressed by multiple haematopoietic cell types. β-gal activity was also seen in the developing spleen from 13 dpc and in the circulating cells between 9-10 dpc; but absent in thymus of the lyl1^{lacZ} embryos suggesting that T cells do not express lyl1 (Godin *et al.,* 1999; Visvader *et al.,* 1991; Giroux *et al.,* 2007).

Besides the endothelial and the haematopoietic system, scl/tal1 is expressed in the central and peripheral nervous system (Kallianpur *et al.,* 1994; Elefanty *et al.,* 1999; van Eekelen *et al.,* 2003). Also scl/tal1 is expressed in dermis, epidermis, nasal epithelium, adrenal medulla, ribs and jaws (Kallianpur *et al.,* 1994). Neither lyl1 mRNA nor the β-gal activity was observed in the nervous system and some other areas where scl/tal1 expression was noted. Thus, lyl1 is specifically expressed in the endothelial, endocardial and haematopoietic cells during the development of mouse (Giroux *et al.,* 2007).

1.10.2 Adult haematopoietic stem and progenitors require lyl1 for survival

The importance of scl/tal1 for haematopoietic development was demonstrated early on when scl/tal1-deficiency in mice resulted in the absence of haematopoietic progenitors as well as vascular defects and lethality (Robb *et al.,* 1995; Shivdasani *et al.,* 1995). However, transplantation analysis indicated that loss of scl/tal1 impairs short term repopulation ability of HSCs but long term self-renewal ability of the HSCs was normal (Curtis *et al.,* 2004) indicating that scl/tal1 is required for the formation but not for maintenance of adult HSCs (Mikkola *et al.,* 2003). In contrast to scl/tal1, lyl1-deficient mice did not show any embryonic lethality but had a reduced number of B cells (Capron *et al.,* 2006). Although the common lymphocyte precursor was normal, the immature B cell compartment was reduced. The number of multipotent progenitor spleen colony forming units was also reduced and lyl1-deficient mice exhibited decreased erythropoiesis with partial arrest in differentiation and enhanced apoptosis (Capron *et al.,* 2006, Capron *et al.,* 2011). Transplantation experiments revealed however, that fetal liver as well as bone marrow-derived HSCs lacking lyl1 were severely impaired in their reconstitution ability, especially in respect of B and T cells (Capron *et al.,* 2006).

4 Scl/tal1 loss leads to absence of haematopoietic progenitors and to vascular defects suggesting normal development of blood and blood vessels require scl/tal1 (Robb *et al.,* 1995; Shivdasani *et al.,* 1995). However scl/tal1 is not required for the maintenance of HSCs after development as a conditional knockout of scl/tal1 in adults has no impact on long-term HSC repopulation (Curtis *et al.,* 2004; Mikkola *et al.,* 2003; Hall *et al.,* 2005). Double knockout mice revealed that lyl1 is critical for normal maintenance of adult HSC function in the absence of scl/tal1 (Souroullas *et al.,* 2009). A single allele of lyl1 in scl/tal1 null HSCs could maintain normal haematopoiesis whereas rapid apoptosis was observed when both lyl1 and scl/tal1 were deleted (Souroullas *et al.,* 2009). This functional alteration of scl/tal1 and

lyl1 in adult HSCs was unexpected as lyl1 was not able to rescue the scl/tal1 during early haematopoiesis (Chan *et al.,* 2006; Porcher *et al.,* 1999). As both proteins possess an essentially identical bHLH domain, they have been shown to dimerise with the same set of proteins such as E-proteins, Lmo1/2 and other factors required for normal haematopoiesis and lineage commitment (Miyamoto *et al.*, 1996; Wadman *et al.,* 1994). When both lyl1 and scl/tal1 are deleted, HSCs undergo rapid cell death, which is due to the disruption of multiple transcriptional networks. However, some molecular features of lyl1 must be different to scl1/tal1 to be able promote adult HSC survival and maintenance in the absence of scl1/tal1 (Souroullas, *et al.,* 2009). Similarly, during development both proteins appear to have different functions that might be mediated through domains other than the bHLH domains (Porcher *et al.*, 1999).

1.10.3. Lyl1-deficiency induces stress erythropoiesis

Lyl1-deficiency leads to reduced reconstitution capacity of the erythroid lineage from bone marrow although their progenitors appeared normal. This decrease in differentiation of bone marrow erythroblast followed by increase in apoptotic cells with a decrease the Bcl-$_{XL}$ which is known to prevent apoptosis during erythropoiesis (Capron *et al.,* 2011). Although accompanied by reduced differentiation in the bone marrow, spleen erythropoiesis looked normal and the spleen derived mature erythroblast in the lyl1-deficient mice showed an increase expression in gata1 and scl/tal1. This suggests that this transcription factor might compensate lyl1 loss in the spleen (Capron *et al.,* 2011). Lyl1-deficient phenotype is much more similar to the gata1^{low} erythropoiesis than scl/tal1$^{-/-}$ erythropoiesis. Both in lyl1$^{-/-}$ and gata1^{low} didn't seems to affect the erythroid progenitors in the bone marrow but altered erythroid maturation (Vannucchi *et al.,* 2001; Kuo *et al.,* 2007; Gregory *et al.,* 1999). The difference observed in the spleen and bone marrow in the lyl1-deficient mice might be due to

the compensatory mechanism related to the altered erythropoiesis which leads to stress erythropoiesis or its different role in bone marrow and spleen. Although different in bone marrow and spleen lyl1 has a role in erythropoiesis and its function is required to maintain bone marrow erythropoiesis while it negatively regulates spleen erythropoiesis (Capron *et al.,* 2011).

1.10.4 Role of lyl1 in the maturation of adult blood vessels:

Overlapping expression of lyl1 and scl/tal1 is also seen in the developing vasculature and endocardium (Girox *et al.,* 2007). Scl/tal1 was undetectable in the adult quiescent endothelium but is active in the newly formed blood vessels (Kallianpur *et al.,* 1994; Pulford *et al.,* 1995) including the vascular proliferation and tumour lymphatic vessels (Chetty *et al.,* 1997; Tang *et al.,* 2006). In contrast to scl/tal1, lyl1 is expressed in both angiogenic and mature adult endothelium. Loss-of-function analysis showed that lyl1 is not required for the initiation of angiogenesis but required for postnatal remodelling to promote the maturation of newly formed blood vessels (Pirot *et al.,* 2010). In lyl1-deficient mice tumour growth was accelerated and the tumour blood vessel exhibited poor coverage, increased vascular leakage, and lumen enlargement. Bone marrow and fetal liver transplantations exhibited higher tumour rate and reduced vessel coverage were not due to haematopoietic defects of the lyl1-deficient mice and the same was observed in the caveolin-l-deficient mice (Lin *et al.,* 2007). Lyl1 acts as a stabilising signal for developing vessels and its expression occurs both in angiogenic and mature vessels suggesting lyl1 involved in the maintenance of quiescent vessels (Pirot *et al.,* 2010).

1.10.5 Overexpression of lyl1 expands T cells and haematopoietic progenitors and supports leukemia formation

Lyl1 overexpression resulted in significant increase in T cells and haematopoietic progenitor population by driving proliferation and suppressing apoptosis. Scl/tal1 and lyl1 have overlapping expression and scl/tal1 targets transcription factors and members of MAPK pathways to facilitate proliferation and lyl1 might target these genes as well to stimulate stem and progenitor cell proliferation. Overexpression of lyl1 resulted in T cell lymphoproliferative effect and also stimulates the expansion of the leukemia cells with stem / progenitor cell like phenotype (Lukov *et al.,* 2011). Aberrant expression of lyl1 in the mouse resulted in shorten tails and loss of hair follicles and it was also found to be lethal when expressed at high levels (Zhong *et al.,* 2007). A similar phenotype was observed in scl/tal1 transgenic mice (Aplan *et al.,* 1997). Ectopic expression of lyl1 was oncogenic which induced highly malignant lymphoma with respect to both the B and T cells. Lyl1 inhibits the function of E2A by competitively binding to it and loss of E2A resulted in high degree T-cell lymphoma (Bain *et al.,* 1997; Yan *et al.,* 1997). Scl/tal1 inhibits E2A–HEB and thus scl/tal1 induces leukemia by repressing E2A-HEB complex by recruiting mSin3A/HIDAC to its target genes (Aplan *et al.,* 1997; Chervinsky *et al.,* 1999; O'Neil *et al.,* 2004). Lyl1 also inhibited E2A-HEB activity and some of its target genes (CD5, RAG1/2) were down-regulated in the thymus of lyl1 transgenic mice (Zhong *et al.,* 2007).

1.11 Zebrafish as a model organism

Mammalian models systems are always challenging to use as they develop internally in the female and genetic studies often require detailed analysis of the embryo, hence a new system with feasible access was needed. Zebrafish is considered to be an ideal alternative as it develops externally with a short generation time. During early embryonic development the embryos remain transparent making it easy for microscopic observations. A single breeding pair can yield large number of embryos and due to their small size are easy to maintain with relatively low cost (Chakrabarti *et al.,* 1983; Walker and Streisinger 1983; Streisinger *et al.,* 1986; Lin 2000). As the development of Zebrafish occurs outside the female in a transparent form it is easy to manipulate the embryos. Large-scale genetic screens in zebrafish led to the identification of new pathways and genes related to vertebrate development (Driever *et al.,* 1996; Haffter *et al.,* 1996). As many of the zebrafish mutant phenotypes have similarities with human diseases, zebrafish have also been used as disease models (Dooley and Zon 2000; Amsterdam and Hopkins 2006). The recent techniques such as anti-sense morpholinos, artificial endonucleases, RNA guided nucleases and Tol2 system have been successfully used in zebrafish to manipulate the gene of interest where the genome editing in the past had only limited success (Sun *et al.,* 1995; Doyon *et al.,* 2008; Meng *et al.,* 2008; Sander *et al.,* 2011; Auer *et al.,* 2014).

1.11.1 Reverse genetics in zebrafish

Earlier geneticists depended on forward genetic tools to uncover the genes involved in a biological pathway or processes. This is an unbiased approach which involves generation of heritable mutagenic lesion using agents like irradiation, murine leukaemia virus and N-ethyl-N-nitrosourea and observing the phenotype of carrier embryos followed by mapping of the allele within the genome (Chakrabarti *et al.,* 1983; Walker and Streisinger, 1983; Mullins *et*

al., 1994). The forward genetic screens have identified novel genes and pathways in vertebrate development including those required for gastrulation / mesoderm induction, cilia formation, cardiovascular development, organogenesis (Driever *et al.,* 1996; Haffter *et al.,* 1996; Zhang *et al.,* 1998; Sun *et al.,* 2004; Bakkers, 2011) Due to the functional redundancy between genes it is impossible to identify the function of all developmental genes using forward genetics. Further, whole-genome sequencing and expression analysis have identified possible genes that are likely responsible for the certain developmental processes (Vogel, 2000; Thisse and Thisse, 2008; Flicek *et al.,* 2011). The recent advancement in various reverse genetics tools has made it possible to identify a gene from the genomic sequence to make specific mutation of that gene and analyse the resulting phenotype.

1.11.1.1 Morpholino mediated gene knockdown in zebrafish

Antisense morpholinos has been widely used reverse genetic tool in zebrafish to knockdown gene of interest (Heasman *et al.,* 2000). Morpholinos are modified oligonucleotide sequence of 25 monomers, that are resistant to nucleases (Nasevicius and Ekker, 2000; Bill *et al.,* 2009). Morpholinos may be splice morpholinos targeting the intron exon junctions to block the pre-mRNA splicing and cause exon skipping (Draper *et al.,* 2001) or translation blocking morpholinos targeting the start codon to prevent the mRNA translation (Summerton *et al.,* 1999). Injecting morpholinos into early zebrafish embryos have global effect on the protein expression and activity is limited to the dorsal forerunner cells when the timing of the injection was delayed (Amack and Yost, 2004). Conditional gene knockout in certain tissues was achieved with caged morpholino, which can be activated or repressed under UV (Shestopalov *et al.,* 2012) and with fluorescein labelled morpholinos the cell population of the targeted genes can be observed (Hyde *et al.,* 2012).

Morpholinos have helped us to understand the role of genes during early development including primordial germ cell migration, haematopoietic stem cell development, left-right asymmetry (Doitsidou *et al.,* 2002; North *et al.,* 2009; Neugebauer *et al.,* 2009). The degree of knockdown in the embryos is variable and since the morpholino amount declines over time, their efficacy is limited to 5 days (Nasevicius and Ekker, 2000; Bill *et al.,* 2009; Eisen and Smith, 2008). Another problem with using morpholinos is the possible upregulation of p53 pathway resulting in neuronal apoptosis. This can be prevented by co-injecting p53 morpholinos (Robu *et al.,* 2007). Hence it is important to perform rescue and control experiments to conclude the observed phenotypes were actually due to the knockdown of the gene of interest (Eisen and Smith, 2008)

1.11.1.2 Zinc finger nucleases

Zinc finger nucleases (ZFNs) are the first reverse genetic tool to be used to introduce targeted mutations into the zebrafish genome. ZFNs have a modular structure containing two domains; a DNA-binding Zinc finger protein domain fused to *FokI* endonuclease cleavage domain (Kim *et al.,* 1996). The *FokI* domain is very crucial for ZFNs targeted genome editing and it requires dimerisation to cleave DNA. Due to its dimeric requirement two adjacent ZFNs with a spacer of 5-7 bp are required to generate a lesion in the genome and the dimerisation doubles the length of recognition sites, which substantially increases the specificity (Urnov *et al.,* 2010). ZFNs consist of tandem arrays of Cys_2His_2 zinc fingers that determine the sequence specificity of the ZFNs and a single zinc finger recognizes 3-bp DNA sequence. Usually 3-6 zinc fingers form a single ZFN subunit which can bind approximately 9 to 18 bp. Zinc finger array is responsible for site specific DNA binding and cleavage activity is provided by the endonuclease. This cleavage leads to a double stranded break in the genome, which is repaired by non-homologous end joining (NHEJ) leading to indel

mutations (Urnov *et al.,* 2010; Bibikova *et al.,* 2002; Handel *et al.,* 2009). Mutations generated by ZFNs in zebrafish have provided the new understanding of the developmental processes including the chemokine signalling in vasculature patterning (Siekmann *et al.,* 2009; Bussmann *et al.,* 2011). Although Zinc fingers were successfully applied to modify the genome of different organisms and *in vitro* cells the efficiency of zinc finger nuclease to cause mutations is rather low. Generation of ZFNs with high specificity and efficiency is complex, time consuming and very expensive. ZFNs are known to cause off-target effects leading to developmental defects and also have a limited targeting range; one potential target to every 500 bp making it difficult to target certain genes (Foley *et al.,* 2005).

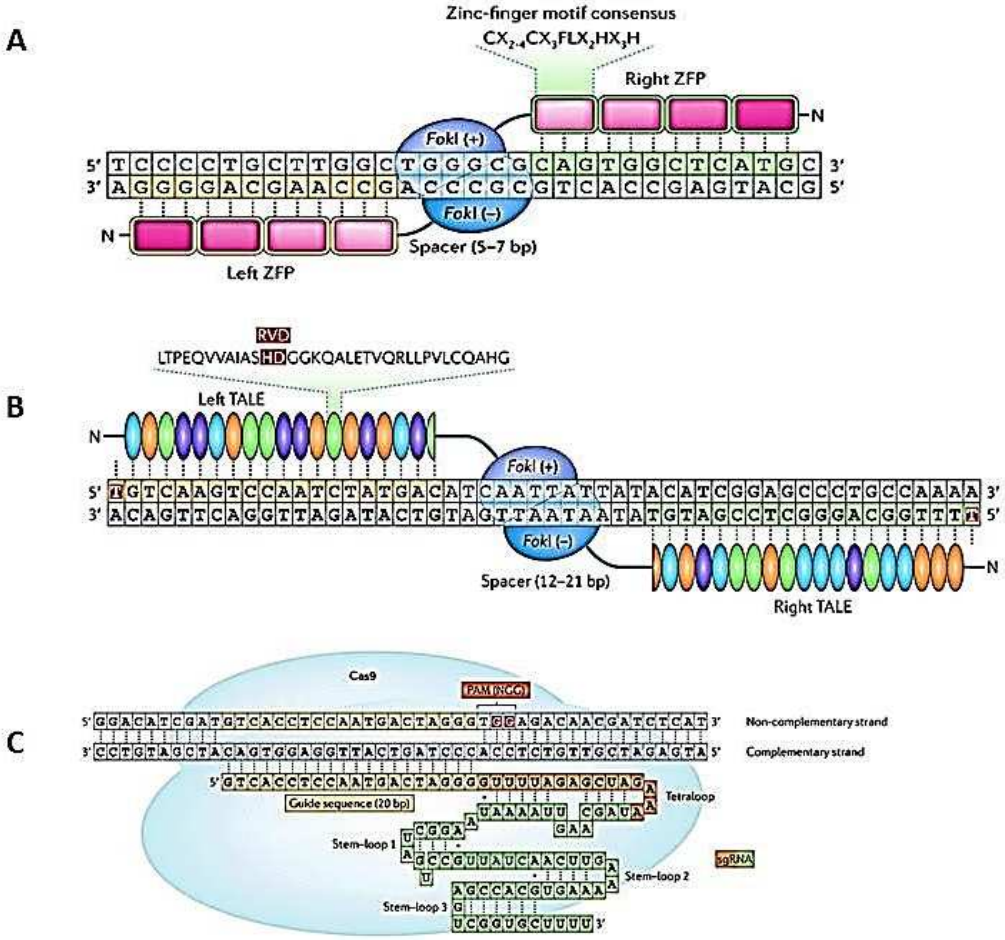

Figure 1.9: Schematic representation of ZFN, TALENS and RGN. A. ZFNs contain a ZFP that mediate DNA recognition while the double stranded break is generated by *FokI* dimerisation. **B.** TALEN has a DNA binding TALE domain made up of several tandem repeats, which is fused to *FokI*. Each repeat in the TALE domain has 33-35 amino acids, the position of the RVD 12 and 13 amino acids recognise a specific nucleotide. **C.** RNA-guided engineered nuclease contains CRISPR cas9 and guide RNA (sgRNA) which has 20 bp complementary to the target (Kim and Kim, 2014).

1.11.1.3 Transcription Activator Like Effector Nucleases (TALENS)

TALEs are bacterial proteins secreted by the plant pathogen Xanthomonas species to infect plant cells (Bogdanove *et al.,* 2010; Scholze and Boch, 2011). TALE proteins consist of N-terminal nuclear translocation domain, C-terminal transcription activation domain and a central DNA binding domain. Once injected into the cell by the bacteria these factors promote pathogen multiplication and spreading. The DNA binding domain that is responsible for sequence recognition has 15.5-19.5 single repeats and each repeat has 34 highly conserved amino acid residues except for the last residue which has only 20 amino acids hence it is half repeat (Boch *et al.,* 2009). The position of amino acid at 12 and 13 of each repeats known as the repeat-variable di-residues determines the DNA binding specificity for a single nucleotide. Thus any sequence of interest can be targeted by modular assembly of multiple repeats, which was not at possible with zinc finger nucleases (Boch and Bonas, 2010; Cermak *et al.,* 2011). TALENS were made by fusing the DNA binding TALE domain with the cleavage domain, *FokI* endonuclease (Miller *et al.,* 2011; Christian *et al.,* 2010). As the *FokI* functions only as dimer a pair of TALENS was required (Bitinaite *et al.,* 1998). Once the TALENS are bound to their specific target site *FokI* dimerisation results in a double stranded break in the genome that can be repaired by either NHEJ pathway leading to indel mutations or through homologous recombination (Lombardo *et al.,* 2007). TALENS were considered as an alternative to ZFN mainly due to their high mutation rate (Moore *et al.,* 2012). Further they offer high targeting range with high specificity and low off-target effects (Reyon *et al.,* 2012). TALEN-mediated targeted genome editing has been successfully used in yeast, zebrafish, mouse, rat, drosophila, frog and human somatic and pluripotent stem cells (Li *et al.,* 2011; Huang *et al.,* 2012; Lei *et al.,* 2012; Tesson *et al.,* 2011; Hockemeyer *et al.,* 2011). In addition, the cleavage domain of TALEN can be replaced by a transcription

activator domain or repressor to activate or knockdown endogenous gene expression (Miller *et al.,* 2011; Zhang *et al.,* 2013).

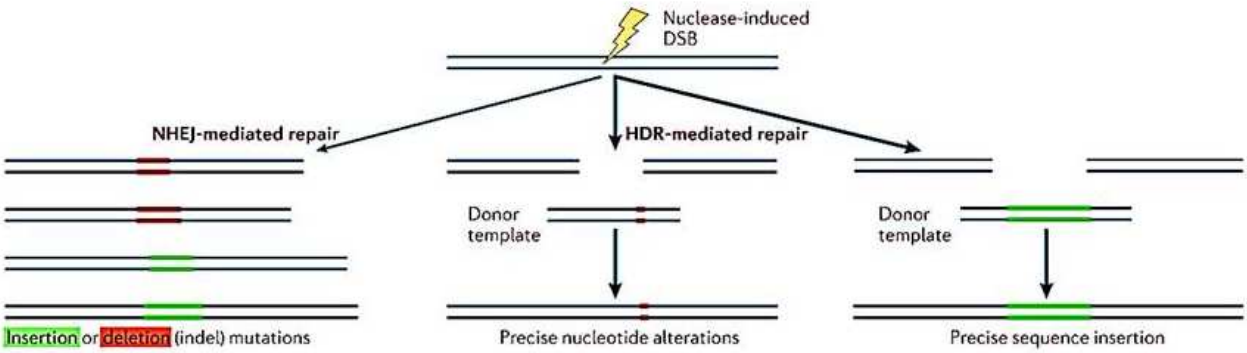

Figure 1.10: Nucleases based genome editing. Use of nuclease creates DSB at the target locus that can be repaired by either NHEJ mediated leading to indel mutation (insertion/ deletion) or homology-directed precise insertions. (Joung and Sander, 2013)

1.11.1.4 CRISPR-cas9

Clustered regularly interspaced palindromic repeats / CRISPR associated (CRISPR/Cas) are part of bacterial adaptive immune system that defend them against the foreign nucleic acids of invading viruses (Marraffini and Sontheimer, 2008; Bhaya *et al.,* 2011). Type II CRISPR-Cas system depends on the CRISPR locus to uptakes the foreign DNA and transcribe it in the form of small CRISPR RNAs (crRNAs), which then anneal to trans-activating crRNA (tracrRNA) that guides the Cas protein to the site leading to site specific cleavage of the foreign nucleic acids (Barrangou *et al.,* 2007; Brouns *et al.,* 2008; Jinek *et al.,* 2012). For genome editing a single guide RNA (sgRNA) consisting of both the crRNA and tracrRNA has successfully directed the Cas9 to cleave the target site *in vitro* (Jinek *et al.,* 2012). sgRNA has complementary sequence to the target site in its 5' and tracrRNA derived cas9-interaction interface in its 3' end. RNA guided nucleases (RGN) requires a 20 nucleotide complementary sequence of the target site in the sgRNA, which will bind to the genomic locus and lead to Cas9-mediated cleavage at the site. In addition to the 20 nucleotides the widely used cas9 from *Streptococcus pyogenes* need a protospacer adjacent motif (PAM) sequence (NGG) to the 3' end of the target site (Hsu *et al.,* 2013; Jinek *et al.,* 2012). Cleavage of the target site by cas9 leads to DSB in the genome and was repaired in a way similar to other nucleases that is through NHEJ or HR (Jinek *et al.,* 2012; Hwang *et al.,* 2013). RGN has been successfully employed in cultured mammalian cells and also in various animal models such as zebrafish, Drosophila, mouse, medaka and *C. elegans* (Chang *et al.,* 2013; Hwang *et al.,* 2013; Dicarlo *et al.,* 2013; Basset *et al.,* 2013; Ansai and Kinoshita, 2014). Multiplex gene editing was highly effective with CRISPR/cas9 as in mouse stem cells it simultaneously deleted five genes and 8 alleles (Wang *et al.,* 2013). CRISPR/cas9 stand out from other gene editing techniques as they are relatively cheap, quick and does not require assembling of fingers (as in zinc fingers) or modular assembly (in case

of TALENs). Genome editing with RGN often leads to some off target effects. Although 12bp match including the PAM site does not targeted in mice (Wang *et al.,* 2013), *C. elegans* (Friedland *et al.,* 2013) and *Drosophila* (Bassett *et al.,* 2013; Gratz *et al.,* 2013) a mismatch of five nucleotide off-target cleavage was observed in zebrafish and cultured human cells (Jao *et al.,* 2013; Hsu *et al.,* 2013; Chao *et al.,* 2014). To reduce the off-target effect two sgRNA complementary to opposite strand of the target site was cleaved with mutated cas9 that can only nick a single strand and the two individual nicks resulted in a site-specific DSB repaired by NHEJ (Ran *et al.,* 2013). Truncating the sgRNA from 20 to 17 nucleotides also reduced the off-target cleavage (Fu *et al.,* 2014).

1.12 Objectives

The main objective was to study the functional role of Id4 in neurogenesis and lyl1 in haematopoiesis using TALEN-mediated mutagenesis. Primary studies using mopholino-mediated knockdown of Id4 has suggested its role in neural progenitor proliferation. However we also observed an upregulation of p53 that caused neuronal apoptosis. The Id4 mutant will eliminate this disadvantage and can also be used to study the relation between Id4 and p53. Lyl1-deficient mice highlighted the importance of lyl1 in HSC function and clearly demonstrated its distinct role from scl/tal1. However, it did not address the question whether lyl1 is required for primitive haematopoiesis neither did they reveal the position of lyl1 in the gene regulatory network regulating HSC fate. This lack of knowledge is in part due to the rather complex experimental approaches required when using mice as a model system. To overcome such limitations we want to utilise zebrafish and determine lyl1 function in primitive haematopiesis and extend the current knowledge of lyl1 function in adult HSCs.

.

- To this end, ectopic overexpression (gain-of-function) and morpholino-mediated knockdown as well as TALEN-mediated mutagenesis (loss-of-function) was employed.
- Phenotypic analysis utilising marker gene expression and Flow cytometry was performed to establish potential mechanisms underlying the function of Id4 and lyl1.
- Cell proliferation using pHH3 and TUNEL (apoptosis) in the presence/absence of chemical inhibitors was performed to dissect the role of Id4 and p38MAPK in neural progenitor proliferation

In the first part of this thesis we will be using TALEN to generate target disruption of the lyl1 and id4 locus and subsequent establishment of the homozygous lines. Next, spatial and temporal expression of the lyl1 will be analysed. Gain-of-function analysis by injecting Lyl1 RNA into zebrafish embryos to study its possible role in primitive and haematopoietic waves using various lineage markers at different time points. Then the embryos from the lyl1 mutant and $lyl1^{-/-}$ adult kidney were studied to further determine its role using markers and FACS.

In the final part, we will study the expression pattern of Id4 during development and in embryos in which the notch pathway is blocked to check whether Id4 is regulated by notch signalling. Next, we will inhibit p38MAPK in the Id4 and id4/p53 morphants to study its connection with impaired proliferation and increased apoptosis. To validate the morphant phenotype we will analyse the $id4^{-/-}$ embryos with expression markers for neurogenesis. Finally, cell proliferation and apoptosis of the Id4 mutant embryos with and without the p38MAPK inhibitor will be analysed.

Chapter 2

Materials and Methods

2.1 Materials

2.1.1 Zebrafish Maintenance

Zebrafish were maintained at 28.5^{o}C in system water on a 12 hour light / 12 hour dark cycle. Fertilisation of the eggs is almost synchronous and embryos were collected after natural spawning and raised at 28.5^{o}C in a water containing methylene blue, a fungicide. Staging of the fish was done according to the standard criteria shown by Kimmel *et al.*, (1995).

2.1.2 Maintaining mutant lines

All mutant lines are maintained as described in section 2.1.1. Id4 mutant line were maintained as heterozygous carrier and crossed with each other to obtain homozygous mutant. Lyl1 mutant lines were maintained both as heterozygous carrier and homozygous mutants. All the zebrafish experiments were performed under the Home office project licence authority (40/3457) and personal licence (IE8CAOD7A)

2.1.3 Technical laboratory equipment

Name	Source
Pipettes (2 µl, 20 µl, 200 µl and 1000 µl)	Gibson
Heating block DRI-BLOCK DB3	Jencons Techne
Electrophoresis power supply EPS300	Pharmacia Biotech
Centrikon T-42K centrifuge	Kontron instrument
Minispin plus centrifuge	Eppendorf
Water bath	Jencons
Dual-intensity UV transilluminator	UVP, LLC

2.1.4 Microinjection apparatus, Microscope used during microinjection and Image visualisation

Name	Source
Fine forceps	World Precision instruments
Incubator	LEEC
Microloader tips (2µl and 20µl)	Eppendorf
Glass capillary 1mm/0.58 mm	Harward apparatus
Needle puller	Sutter instrument CO
Morpholino	Gene tool
Camera DS-5MC	Nikon
Cold light source KL 1500 LCD	Zeiss
Stereomicroscope stemi SV 6	Zeiss
Digital Sight DS-U1	Nikon

2.1.5 Buffers and solutions

Gel electrophoresis	
6X loading buffer	New England Biolabs
1kB DNA ladder	New England Biolabs
1X TBE (Tris Borate EDTA buffer)	45mM Tris Borate; 1mM EDTA
Microbiological media	
Antibiotics	Ampicillin Stocks 100mg/ml in distilled water, working concentration 100µg/ml
LB (Luria-Bertani) Medium	10g bactotryptone; 5g yeast extract; 5g NaCl; adjusted to pH 7 with 1M NaOH and made up to 1 litre with Distilled water
LB agar	LB agar used for plates solidified with 1.5% bacto- agar
Whole Mount *in situ* Hybridization	
BCL Buffer III	0.1M Tris-HCL pH 9.5; 0.1M NaCl; 50mM $MgCl_2$;

	0.1% Tween20
BM purple	Roche
DIG block	2% Blocking reagent (Roche) dissolved in MABT
Hybridization Buffer ($Hybe^+$)	50% deionised formamide; 5X SSC; 0.5mg/ml yeast tRNA; 50mg/ml Heparin; 9.2 mM citric acid; 0.1 % Tween 20
Maleic acid buffer (MAB)	0.1M Maleic acid; 0.15M NaCl; pH 7.5
MABT	0.1% Tween 20 in MAB
Phosphate Buffered Saline (PBS)	1.7mM KH_2PO_4; 5.2mM Na_2HPO_4; 150 mM NaCl
PBST	0.1% Tween 20 in PBS
Paraformaldehyde (PFA)	4% PFA in 1X PBS
20X SSC (Saline Sodium Citrate)	Promega
tRNA from Baker's yeast	Roche
Immunostaining	
Anti-Phospho Histone H3	Cell signalling (Cat no: 9701s)
Swine Anti-Rabbit IgG	Dako (Cat no: P0217)
DAB (3,3′-Diaminobenzidine tetrahydrochloride)	Sigma Aldrich
PBSBT (Phosphate Buffered Saline+ BSA and Triton X-100)	0.2% BSA; 0.1% Triton X-100 in PBS
TUNEL Assay	
ApopTag Peroxidase *In Situ* Apoptosis detection kit	Millipore (S7100)

2.1.6 Primers

Primers	Sequence (5'-3')
Lyl1 FP	TTCGGGATCTTCAGTAACGC
Lyl1RP	AGTATGGGCTCCCTGCTGTG
Lyl1 full length FP	ATGAGCAGTGATGATGGAGAAG
Lyl1 full length RP	CCAGTATGGGCTGGGCTGG
Id4 FP	TGCGTTCACACTCAGAGAGG
Id4 RP	GGAACGGATTCTCTCCAA
Lyl1 TALEN screening FP	CTGTTCCAGGATAAATG
Lyl1 TALEN screening RP	CACACCTCACTGCTACAAATCACTG
Id4 TALEN screening FP	GTCAAAGCTCGAGCGGAT
Id4 TALEN screening RP	TTTCGGGTCCTGCTTACGT

2.1.7 TALEN plasmid

Plasmid	Target sequence
Lyl1 Left (TAL3111)	TCATACGAGCGTTACTGA
Lyl1 Right (TAL3110)	TCTTTCCTCATGCCGCCG
Id4 Left (TAL3294)	TTTATTACAATGAAGGCC
Id4 right (TAL3295)	TAGAAGGAAGCTTATGAG

2.2 Methods

2.2.1 DNA preparation

2.2.1.1 Transformation of Competent cells

DH5α (Invitrogen) and NEB5α (New England Biolabs) competent cells were used to amplify plasmids. 50µl of the cells were thawed on ice and 10-100ng of the plasmid DNA was added, mixed gently, incubated on ice for 30 minutes, heat-shocked at 42^{o}C for 45 seconds and immediately chilled on ice for 2 minutes. Pre-warmed SOC medium (250µl) was then added to this suspension and the bacteria was allowed to grow for an hour in 37^{o}C shaking incubator. Half of the culture was spread out into LB agar containing 100mg/ml ampicillin or 30mg/ml kanamycin and incubated at 37^{o}C overnight. The following day the LB plates were observed and colonies were picked and incubated overnight in LB broth containing appropriate antibiotics at 37^{o}C with agitation at 220rpm.

2.2.1.2 Plasmid DNA preparation

Plasmid DNA was extracted using sigma mini prep DNA kit. The overnight grown bacterial culture was transferred to a 1.5 ml eppendorf tube and was centrifuged in a microfuge at room temperature at 10,000 rpm for 5 minutes. The supernatant was discarded and pellet was resuspended in 200 µl of resuspension buffer P1. Then 200 µl of lysis buffer P2 was added and mixed by inverting for 4-6 times to lyse the bacterial cells. Finally 300 µl of the neutralization buffer N3 was added and mixed by inverting the tubes. After this, the suspension was centrifuged at 13,000 rpm for ten minutes and the lysed cells were pelleted. The sigma spin column was prepared by applying 500µl of column preparation buffer and centrifuged at 13,000 rom for a minute. The buffer was discarded and the resulting supernatant from the suspension was applied to the spin column either by decanting or pipetting. The column was centrifuged at 13,000 rpm for a minute and it was washed with 500 µl wash buffer centrifuged for a minute. The flow through was discarded. The column

was again washed with 700 µl of PE buffer and centrifuged for one minute. The flow through was discarded and further spun for a minute to remove any residual buffer. Plasmid DNA was eluted by adding 50 µl of elution buffer to the centre of the column and centrifuged for a minute.

2.2.1.3 Quantification of DNA

The concentration of DNA was determined by using a Nanodrop 3300 spectrophotometer with a UV absorbance at 260 nm. The Nanodrop peddle was cleaned with 70% ethanol and blank reading was made using nuclease free water. Then 1.5 µl of the sample was loaded and the concentration was measured. The purity was assessed by 260nm/280nm and 260nm/230nm ratios.

2.2.1.4 Restriction enzyme digestion

Restriction enzymes and their buffers were obtained from New England Biolabs (NEB). To obtain a desired fragment from the plasmid construct about 1 µg of DNA/ 1 unit of enzyme is required. Hence a reaction is set with 1 µg DNA, 2 µl of 10X digestion buffer, 10 units of each restriction enzyme, and nuclease-free water was added to make up the mixture to 20 µl. The tubes were placed in 37^{o}C incubator for 2 hours. DNA digestion was confirmed by running the sample on 1% agarose gel along with undigested DNA and 1kb DNA ladder.

2.2.1.5 Agarose gel electrophoresis

Agarose gel electrophoresis was performed to separate the DNA fragments by their size. DNA is negatively charged at neutral pH and it will move towards the positive pole once an electrical potential is applied. The DNA is allowed to pass through agarose gel, smaller molecules passes through the gel easily while the larger molecules are slowed down. Thus a mixture of large and small DNA molecules in a mixture is separated. Usually 1-1.5%

agarose was melted in 1x TBE buffer and once cooled nucleic acid stain SafeView was added (1µl SafeView to 10ml). Agarose gel is solidified in a gel casting tray and 5X loading dye was added to the nucleic acid samples to give a 1X final concentration. The sample and DNA molecular weight ladder (1Kb) which is used to determine the size were added to the gel one by one and allowed to run for an hour at 120V. Then, the gel was taken to the gel doc system and bands were visualised by using dual intensity UV trans-illuminator.

2.2.1.4 Gel extraction

Gel extraction was performed using Macherry-Nagel gel and PCR Purification kit (Cat no: 28704). DNA fragment were purified by gel extraction using NucleoSpin Gel and PCR clean-up kit. After electrophoresis the desired fragment is excised from the gel under low intensity UV. The gel size is weighed and for every 100mg of the gel slice 200µl of NTI buffer was added. The gel with the buffer was incubated at 50^{o}C for 10 minutes with occasional vortex and once the gel is dissolved completely it is bind to the spin column by centrifuging at 13,000 rpm for a minute. Flow through is discarded, column is washed by adding buffer NT3 and spun a minute to completely remove the buffer. Purified DNA was then eluted from the column with 30µl buffer NE.

2.2.1.5 Ligation

DNA ligation involves the joining of two DNA molecule ends by creating a phosphor diester bond between the 3' hydroxyl of one and the 5' phosphate of another catalysed by T4 DNA ligase. For cohesive end 50ng of vector was mixed with a 3-5 fold molar excess of insert, 1µl 10x ligation buffer and 1µl of T4 DNA ligase (NEB). The volume was adjusted to 10µl with dH2O. The reaction was left overnight at 16^{O}C and 2-5ul was transformed in competent *E.coli* cells. For blunt-ended fragments, 100ng of vector with the vector insert molar ratio of 1: 5-10 was used.

2.2.1.6 Phenol chloroform extraction

Equal volume of phenol: chloroform: isoamylalcohol (25:24:1) was added to the DNA sample, mixed, centrifuged at 13,000 rpm for 5 minutes. The upper aqueous phase was carefully transferred to a fresh tube and extracted with equal volume of chloroform. DNA was precipitated by Sodium acetate (pH 5.2) to a final concentration of 0.3M and 2.5 volumes of ice-cold ethanol. The sample was mixed by inverting the tubes and allowed to precipitate at -20^{o}C for 30 minutes and they were centrifuged at 13,000 rpm for 30 minutes at 4^{o}C. The supernatant was discarded and the pellet was washed with 70% ethanol, air dried and resuspended in 15µl of nuclease free water.

2.2.1.7 Polymerase chain reaction

A 50µl reaction was step up using 2µl of extracted DNA, 1X Q5 reaction buffer, 200µM dNTPs, 0.5µM of each primer and 0.1 units of Q5 hot start high-fidelity DNA polymerase. For high GC-rich sequence 1x Q5 GC enhancer was added to improve the reaction. The reaction conditions are initial denaturation at 98^{o}C for 2 minutes followed by 30 cycles of 98^{o}C for 30 seconds, 45-60^{o}C for 30 seconds, 72^{o}C for 45 seconds and a final extension for 2 minutes at 72^{o}C and maintained at4^{o}C until use. The amplified products were verified by analysing the samples in 1.5% agarose gel.

2.2.1.8 Preparation of pBUT-HA + Lyl-1Plasmid

pBUT-HA and pSC-B-lyl1 plasmids are double digested with XbaI and XhoI. Digestion of the plasmid pSC-B-lyl1 releases the lyl1 fragment which was then purified by gel extraction. Lyl1 fragment is then ligated to pBUT-HA and mailed to source bioscience for sequencing and the analysis of the sequence confirmed that HA was in-frame to lyl1.

2.2.2 RNA manipulation

2.2.2.1 *In vitro* transcription of RNA for embryo injection

Injection of capped RNA into zebrafish have been routinely used to study the function of genes by overexpress and gene editing tools like TALEN, ZFN, CRISPR-cas9 are injected as capped mRNA. mRNA's are synthesized using mMessage mMachine Transcription kits (ambion). A transcription reaction containing 1µg of linearized plasmid, 10µl of NTP mix, 2µl T7 buffer and 2µl T7 enzyme was set, mixed and incubated at 37^{o}C. After two hours the DNA was digested with 1µl turbo DNase at 37^{o}C for 15 minutes. TALEN mRNA was processed for an additional polyA tailing reaction for 45 minutes at 37^{o}C by adding a mix containing 1x E-PAP buffer 1mM ATP, 2.5mM MnCl2 and 8U E-PAP. The reaction is stopped by adding 10µl of ammonium acetate solution. mRNA is extracted by equal volume of phenol: chloroform: isoamylalcohol (25:24:1) and then by chloroform. The upper aqueous phase is transferred to a fresh tube and RNA was precipitated by chilling the mix with isopropanol for 30 minutes. Centrifugation at high speed for 15 minutes yielded the pellet which was washed, resuspended in DEPC water and stored at -80^{o}C.

2.2.2.2 *In vitro* transcription of mRNA for whole mount *in situ* hybridization

To make RNA probes for *in situ* hybridization the plasmid DNA was linearized using desired restriction enzyme, extracted by phenol/ chloroform and transcribed using T7, T3 or SP6 RNA polymerase (Promega). A 20 µl reaction was set with 2.5 µg of linearized and purified DNA template, 4 µl of 5X transcription buffer (Promega), 2 µl of 10X DIG labelling mix/ 10X fluorescein labelling mix (Roche,) 2µl of 100mM DTT, 0.5 µl RNasin (Promega) and 2 µl of RNA polymerase (T7, T3 or SP6; Promega). The reaction was incubated for 2 hours at 37^{o}C. The residual plasmid was removed by digesting with 1 µl of DNase I (RNase free; Roche) at 37^{o}C for 15 minutes. This reaction was stopped by adding 1 µl of 0.5M

EDTA and 9 µl of nuclease free water. Further, the volume was raised to 100 µl with nuclease free water. The RNA was precipitated for 20 minutes at -20^{o}C by adding 10/3 volume 10M ammonium acetate and 2.5 volume ice cold 100% ethanol. It was centrifuged at 13,000 rpm for 15 minutes at 4^{o}C, washed with 70% ethanol, air dried and resuspended in 50 µl of DEPC water. The presence of the RNA was visualised by running on a 1.5% Agarose gel and stored at -70^{O}C. For *in situ* hybridization a typical dilution of 1µl of probe to 200µl of hybridization mix was used.

2.2.3 RNA extraction and cDNA synthesis

2.2.3.1 RNA extraction

Zebrafish embryos at different stages were collected and their RNA was isolated using Trizol. Embryos were washed briefly with PBS and 100µl of Trizol was added. Then it was homogenized with a pestle and further 900µl of Trizol was added. This mixture was incubated for 5 minutes at room temperature. 200µl of chloroform was added, mixed and incubated for two minutes at room temperature. The suspension was centrifuged at 13,000 rpm for 10 minutes and the upper phase containing the RNA was carefully transferred to a new tube. 0.7 volume of isopropanol was added, incubated at room temperature for 20 mins and centrifuged at 13,000 rpm for 10 minutes at 4^{o}C. The supernatant was removed and the pellet was washed with 75% ethanol, air dried and resuspended in 50 µl of RNase free water and stored at -80^{o}C.

2.2.3.2 Assessment of total RNA quality and quantification

The quality of the RNA was assessed by running the RNA on a 1.5% RNase free agarose gel after denaturing the RNA at 65^{O}C. The presence of sharp, clear 18s and 28s rRNA bands used to indicate that the RNA was not degraded. A Nanodrop was used to quantify the extracted RNA. The optimal ratio of absorbance at 260nm/280 nm 2.0 and 260nm/230nm 2.0-2.4 indicated that the RNA samples were pure.

2.2.3.3 Reverse transcription

First strand cDNA was synthesised using Superscript II Reverse Transcriptase (RT). 1µg RNA was denatured with random hexamer primer at 65^{O}C for five minutes and cooled on ice. A mixture containing 200 units of Superscript RT, 40 units of RNaseOUT, 4µl of First-strand buffer, 0.1M DTT was added to the denatured RNA. Complementary DNA was synthesised by incubating at 25^{O}C for 10 minutes and further 50 minutes at 42^{O}C. The reaction was terminated by denaturing the enzyme at 70^{O}C for 15 minutes and the cDNA was stored at -20^{O}C.

2.2.4 Manipulation of zebrafish embryos

2.2.4.1 Microinjection

Microinjection allowed rapid and efficient introduction of foreign substance such as morpholino, RNA and DNA into zebrafish embryos. The setup has needle loaded with injection sample connected to a micro-manipulator and the micro-manipulator controls were adjusted in a manner to obtain required injection volume.

2.2.4.2 Preparation and loading of needles for microinjection

Injection needles were prepared by pulling the glass capillaries in a micropipette puller with the settings P=500, Heat=295, pull=200, velocity=115, and time=115. The needled is then loaded with morpholino or mRNA and fixed into the micropipette holder which was connected with picopump to allow injection with pressure. Using a fine forceps the tip of the needle was broken under the microscope at highest magnification (5X). The injection volume was calibrated to 500pL or 1nL by injecting the sample into mineral oil on a micrometre and adjusting the pressure. Embryos are aligned along the edge of the slide which is placed on a petri-dish lid. So to allow the needle to pass through the yolk and into the cell, the embryos animal pole was faced on the edge of the slide.

2.2.4.3 Morpholino and mRNA Injection

Translation blocking morpholinos were designed and synthesised (Gene tools). Stocks were prepared at 50ng/nl concentration in non DEPC treated nuclease free water and stored at -20^{o}C. Before injection morpholino was heated at 65^{o}C for five minutes and cooled for few seconds. Finally they were centrifuged at 13,000 rpm for a minute. Working concentration was prepared from the stocks and the morpholino were injected into the blastomere of the animal pole of the 2 to 8 cell staged embryos as their small size allows efficient diffusion. Capped full-length mRNA stock were thawed on ice and diluted to required concentration in DEPC water. The diluted working solution was loaded into the injection needle and calibrated. Embryos at 2 cell stage were collected, aligned, injected into the animal pole and incubated at 28.5^{o}C. Injected embryos were collected in a petridish containing fish water with methylene blue or in the E3 medium. Wild type embryos were collected separately. Both the injected and wild type embryos were incubated at 28.5^{o}C. The development of the embryos were checked periodically and once they reach the desired stage they were taken out for phenotypic analysis and imaging.

2.2.4.5 Microinjection of TALEN mRNA

Equal amount of left and right TALEN mRNAs were injected into one cell stage zebrafish embryos. On the following day the embryos were observed under the microscope and the dead/deformed embryos were removed. The embryos which looked normal were analysed to check the efficiency of the TALENs.

2.2.4.6 Detection of somatic mutations

Presence of mutation in the embryos was determined by extracting genomic DNA from at least 10 individual embryos followed by PCR and restriction digestion. A single embryo was placed in microfuge tube and boiled for 30 minutes at 95^{o}C in 50µl 1X base solution. The tube is cooled to room temperature and neutralised with 50µl neutralisation

solution. The reaction was spun at 3000 rpm for 5 minutes, stored at 4^{o}C and 2µl was used for a 50µl PCR reaction with appropriate primers. PCR products was further analysed for the presence of indel mutations by restriction digestion. A 20µl reaction was set using 10µl of the amplified PCR product, 1x cut smart buffer and 10units enzyme. The reaction was incubated at 37^{o}C for 90 minutes and run in 1.5% agarose gel. Presence of un-cleaved bands indicated the presence of indel mutations. To detect the efficiency the PCR product was cloned by using StrataClone blunt end PCR cloning kit. At least 20 colonies were analysed by PCR and restriction digestion screening. Further the positive screens were purified and sequenced.

2.2.4.7 Detection of heritable mutation

Injected F0 fish were allowed to reach adulthood and out-crossed with wild type fish to asses heritable mutation. From each cross atleast genomic DNA was extracted from atleast 20 individual embryos and screened by PCR-restriction digestion assay. Positive screens were cloned and sequenced. F1 progeny of the founder screen was raised to adulthood and heterogeneous carriers were identified by fin-clipping and screened by extracting DNA followed by PCR-restriction digestion screening. Two heterogeneous carrier were crossed which each other to get a homogenous mutant.

2.2.4.8 Fin-clipping

Fish were anaesthetised by placing them in 0.012% MS-222. Once the gill movement is slowed the fish is removed into a paper towel and a small piece of the tail fin is clipped using scissors. The fish was immediately transferred to an isolated tank and allowed to recover. The fin-clip is placed in an eppendorf tube and processed for screening. Fish was observed for the next seven days for any signs infection.

2.2.4.9 Treatment of embryos with p38MAPK inhibitor SB 239063

A 10mM stock of the inhibitor SB239063 was prepared using DMSO. Once embryo reaches shield stage the fish water is replaced with 15µM inhibitor prepared with fish water

and allowed to develop to desired stage. After that they were fixed in 4% PFA and immunostaining was performed.

2.2.4.10 Fixation and storage of embryos for *In Situ* hybridization and immunostaining

Embryos at desired stage were fixed overnight at 4^{o}C in 4% PFA. Embryos older than 22 hpf were dechorionated before fixing. Next day, PFA was removed and the embryos were rinsed three times with PBSTw for 5 minutes each. Embryos that development pigments were treated with 3% H_2O_2/ 0.5%KOH at room temperature until the pigmentation disappeared and washed in PBSTw for 5 minutes. They were dehydrated through a series of washes in 25%, 50%, 75% and 100% methanol, each 5 minutes. Then they were stored at -20^{o}C in 100% methanol for at least overnight after which they were used either for *in situ* hybridization or immunostaining.

2.2.4.11 Whole-mount *In Situ* Hybridization

All the steps were performed in 1.5ml microfuge tube and the washes are done in 500µl volume. Embryos in 100% methanol were rehydrated through 75%, 50% and 25% methanol in PBSTw, five minutes each. Then the embryos were washed for four times in PBSTw for five minutes. Embryos were then permeabilized with Proteinase K (10µg/ml in PBSTw) at room temperature for 1minute for embryos younger than 15hpf, 10 minutes for embryos between 15-24 hpf and 30 minutes for embryos older than 24hpf. The proteinase K digestion was stopped by fixing embryos in 4% PFA for 20 minutes. To remove the PFA residues embryos were washed in PBSTw for four times, five minutes each. Embryos were then hybridised for 3 hours at 68^{O}C in 100% pre-hybridization solution. The pre-hybridization solution was removed and replaced by fresh hybridization mix containing a 1:200 dilution of labelled, antisense RNA probes. This hybridization reaction was allowed overnight at 68^{o}C.

Next day, the probes were removed and stored at -20^{o}C as they can be reused up to five times. Excess probe was removed from the embryos by series of washes at 68^{O}C for 5 minutes in prewarmed 66% hybridization mix/33% 2xSSC, 33% hybridization mix/ 66% 2xSSC, and 2x SSC (Hybridization mix does not contain heparin and tRNA). To prevent the non-specific hybridization of the probes high-stringency washes at 68^{O}C with pre-warm 0.2X SSCTw and twice in 0.1X SSCTw, 20 minutes each. Embryos were washed at room temperature for five minutes each with 66% 0.2X SSC/ 33% MABTw, 66% 0.2X SSC/ 33% and 100% MABTw. To saturate the non-specific binding sites for the antibody embryos were blocked 2% blocking reagent for 2 hours at room temperature with shaking. The block was removed and replaced with anti-digoxygenin/anti- fluorescein antibody fragments conjugated to alkaline phosphatase (Roche) solution diluted in 1/5000 with blocking reagent for either three hours at room temperature. The antibody solution was removed and the embryos were washed in MABTw for 6 times, 10 minutes each to remove any excess antibody. To avoid background the embryos were further allowed for an overnight wash with MABTw at 4^{O}C. The next day embryos were equilibrated by washing with freshly prepared BCL buffer III for three times, 5 minute each. Then, the embryos were stained in a solution containing 1:1 ratio of BM purple (Roche) and BCL buffer III. This reaction was protected from light and monitored regularly under the microscope. Once desired staining has reached staining in stopped by washing in PBSTw containing 20mM EDTA for 3 times, 10 minutes each and fixed with 4%PFA to stop the reaction permanently. Embryos were washed with PBSTw, mounted in 80% glycerol and stored at 4^{O}C.

2.2.4.12 Whole mount Phospho histone H3 immunostaining

Phospho histone H3 (PHH3) immunostaining was performed to determine the number of cells undergoing mitosis. Histone H3 phosphorylation may be initiated at different phases of cell division in different organisms, but metaphase chromosomes are always found to be heavily phosphorylated, which can be detected using anti-PHH3 antibody.

The dehydrated embryos were rehydrated through 75%, 50% and 25% methanol in PBS, five minutes each. Then they were washed twice in PBS for 1 hour each. Later, the embryos were bleached for 30 minutes in 1% H_2O_2, 5% formamide and 0.5X SSC. They were rinsed with PBS, PBSBT and blocked for an hour in 10% FBS in PBSBT. Embryos were then incubated in anti-phospho histone H3 antibody (1/ 1000 dilution) overnight at 4^oC.

Next day, the antibody was removed, washed in 10% FBS in PBSBT and then washed for four times in PBSBT one hour each. Then they were incubated in swine anti-rabbit IgG (1/2000) overnight at 4^oC. On the final day, swine anti-rabbit IgG antibody was removed and a brief wash was given with 10% FBS in PBSBT. Then the embryos were washed four times in PBSTB, each for an hour. They were then stained using DAB enhanced liquid substrate system for 10-60 minutes. The embryos were washed with water and then with PBS and finally stored in 90% glycerol at 4^oC.

2.2.4.13 Apoptosis assay (TUNEL staining by *In situ*)

Apoptosis is a process of programmed cell death which is controlled by multiple signals and pathways. Apoptosis in the embryos can be detected by TUNEL (Terminal deoxynucleotidyl Transferase dUTP Nick End Labelling) assay. The principle behind TUNEL is that the nick in DNA was detected by the enzyme TdT (Terminal deoxynucleotidyl Transferases) and this also catalyses the addition of nucleotide which is digoxigenin conjugated to the DNA. This incorporated digoxigenin conjugated nucleotide was then identified by using an anti- digoxigenin antibody. TUNEL assay can also detect

DNA that is severely damaged. TUNEL assay was done using the Apoptag Peroxidase *In Situ* Apoptosis detection kit from Millipore (Cat no: S7100).

The dehydrated embryos were rehydrated by washing with 75% methanol and 25% PBSTw, 50% methanol and 50% PBSTw, 25% methanol and 75% PBSTw, each wash for five minutes. Then, the embryos were washed for four times in PBSTw for five minutes and they were bleached for 30 minutes in 1%H2O2, 5% formamide, 0.5 X SSC to block the endogenous peroxidase activity. They were washed in PBSTw for five minutes, three times. Half of the wild type embryos were separated and used as positive control. Proteinase K (10µg/ml in PBSTw) was added to the remaining wild type and the morpholino treated embryos for one minute (This time period depends on the development stages of the embryos). The proteinase K reaction was stopped by fixing the embryos in 4% PFA for 20 minutes. After this the embryos were washed 3 times in PBS for 5 minutes. The removed wild type embryos were treated with DNase I (1µl DNase I (Roche, 04716728001)/ 50 µl equilibration buffer (From apoptag peroxidase *In situ* kit, Millipore, S7100)) at room temperature for 10 min then the embryos were washed 3 times with PBS for 5min each. Then, the embryos were incubated in the equilibration buffer. The equilibration buffer was replaced with the reaction buffer containing the TdT enzyme. The reaction was kept at 37^{o}C in a humid chamber usually in the water bath for an hour. Then, the reaction was stopped by adding the stop buffer. The embryos were washed with PBSTw twice for 5 minute each. Then, it was incubated in anti- digoxigenin antibody for 30 minutes and washed with PBSTw thrice for 5 minutes each. They were then stained using DAB enhanced liquid substrate system for 10-60 minutes. The embryos were washed with water and then with PBS and finally stored in 90% glycerol at 4^{o}C.

2.2.4.14 Imaging of Zebrafish embryos

Visualisation of live, *in situ* hybridised or immunostained embryos was carried out under a Nikon SMZ1500 microscope and the images were captured with Nikon-DS-5M camera, a Nikon DS-1 control unit and Nikon ACT-2U 1.40 software. Images were edited by cropping; brightness and contrast were adjusted in Adobe Photoshop.

Chapter 3

3.1 TALEN-mediated targeted mutagenesis

Loss-of-function studies in zebrafish largely relied on antisense morpholinos. Morpholinos offered an efficient knockdown of target genes by targeting the translational start site (Nasevicius and Ekker, 2000) or splice-site junctions (Draper *et al.,* 2001). Although morpholinos led to the understanding of gene function in early development it had various limitations such as transient knockdown, the degree of knockdown is variable, activity of the morpholino is limited to the first few days of development (Bill et al., 2009; Nasevicius and Ekker, 2000; Smart et al., 2004), off-target effects and p53-mediated neuronal apoptosis (Robu *et al.,* 2007). To overcome these limitations and to further study gene function during later stages of development, generation of germline mutations was critical. Zinc-finger nucleases (ZFNs) and Transcription Activator Like Effector Nucleases (TALENS) are site-specific nucleases that emerged as a powerful tools and have been successfully employed in zebrafish for gene disruption (Bogdanove and Voytas 2011; Carroll, 2011; Doyon *et al.,* 2008; Bedell *et al.,* 2012). ZFNs, a chimeric molecule that consist of a DNA-binding zinc-finger domain and *Fok*I cleavage domain allowed targeted germline gene inactivation in zebrafish (Doyon et al., 2008; Meng et al., 2008). As the cleavage is activated by dimerisation it is important to generate two zinc-fingers. Assembling engineered zinc fingers with high efficiency were always challenging and often the targeting range was limited making it difficult to target some genes (Sander *et al.,* 2011). TALENs offered an alternative option that uses the same principle as ZFNs. As the 12 and 13 position in each repeat determines the base specificity it allowed to customise the effector domain to target any sequence in the genome (Cermak et al. 2011; Reyon et al. 2012; Sanjana et al. 2012). Here,

we show that injection of TALEN RNA targeting zebrafish lyl1 and Id4 resulted in a site-specific genome modification creating null alleles.

3.2 Design and construction of TALENS targeting zebrafish lyl1/ Id4 locus

Lyl1 and Id4 are (b)HLH proteins that function by forming heterodimers mediated via their HLH domains. Therefore, TALEN target site were selected that would result in premature stop codons and possible truncated proteins that lacked the (b)HLH domain. Zebrafish lyl1 gene (Gene: ENSDARG00000091603) has five exons and encodes 320 amino acids. The bHLH domain of lyl1 is located in exon 5 and therefore TALEN pairs targeting exon 4 were selected. Left TALEN binding sequence (5'TCTTTCCTCATGCCGCCG3') and right TALEN binding sequence (5'TCATACGAGCGTTACTGA3') have both 17.5 TAL effector repeats for sequence specific binding which are separated by 16bp spacer containing the unique restriction site for HinfI (5'GCAG*GATTC*GGGATCT3'). The HLH region of Id4 is encoded in the first exon of the Id4 gene (Gene: ENSDARG00000045131); so TALEN pairs targeting sequences upstream of this region were selected. Left (5'TTTATTACAATGAAGGCC3') and right (5'TAGAAGGAAGCTTATGAG3') Id4 TALEN pairs were selected again with 17.5 repeats separated by a 16bp spacer that in this case contained a HpaII restriction site (5'AGCGTG*CCGG*TTCGCC3'). TALEN pairs were made by Keith Joung research group and purchased from addgene (addgene.org). All TALENs were synthesised by golden gate assembly on a JDS71 plasmid background (For plasmid maps refer to appendix I).

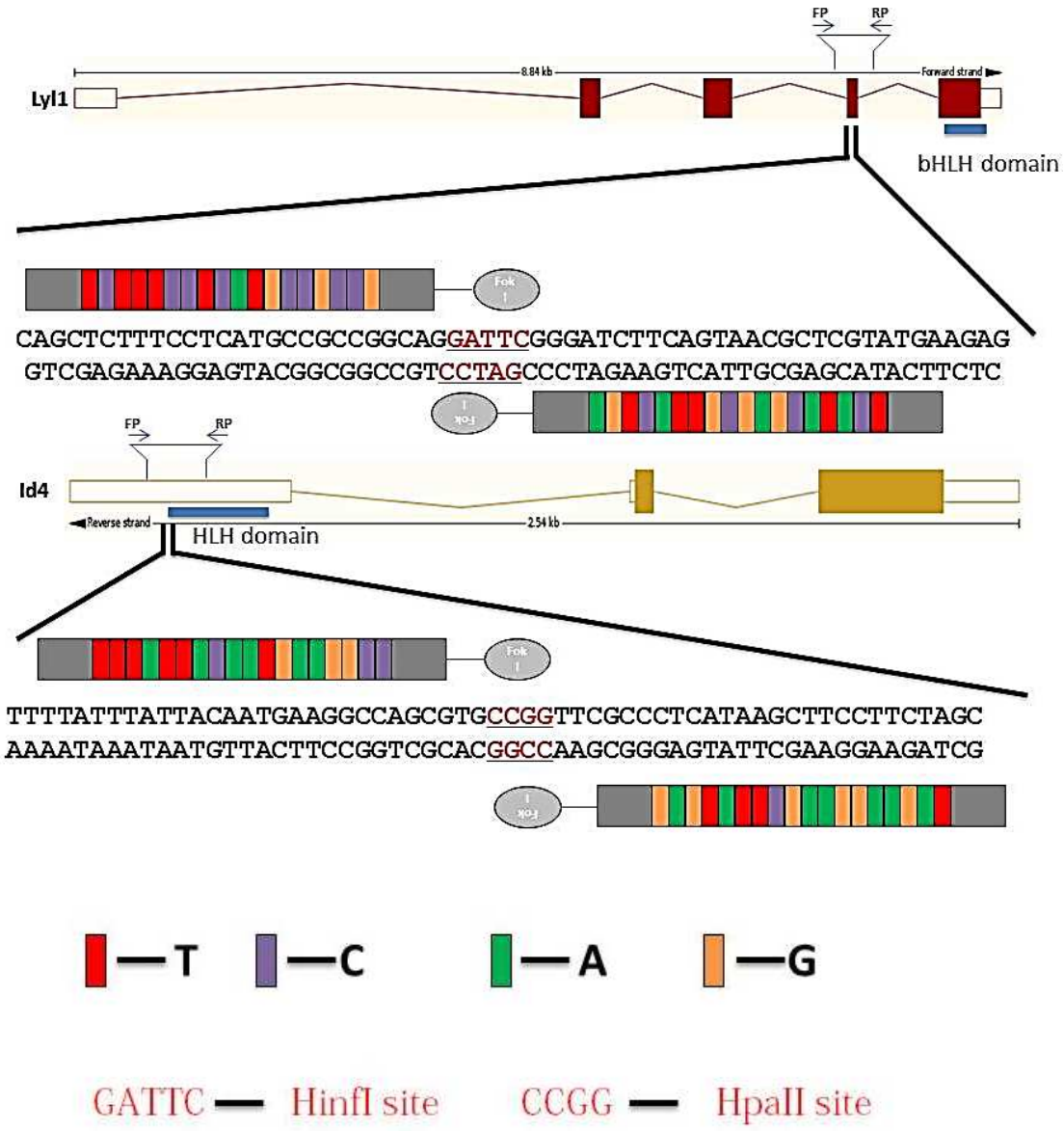

Figure 3.1: Disruption of zebrafish Lyl1 and Id4. Genomic structure of zebrafish lyl1 and Id4 genes, showing the primers for detecting the mutations. Lyl1 TALENs targets the 4th exon while the first exon of Id4 is targeted. Lyl1 spacer has a HinfI site and Id4 has a HpaII site for analysing the mutation. FP - Forward primer, RP - Reverse primer.

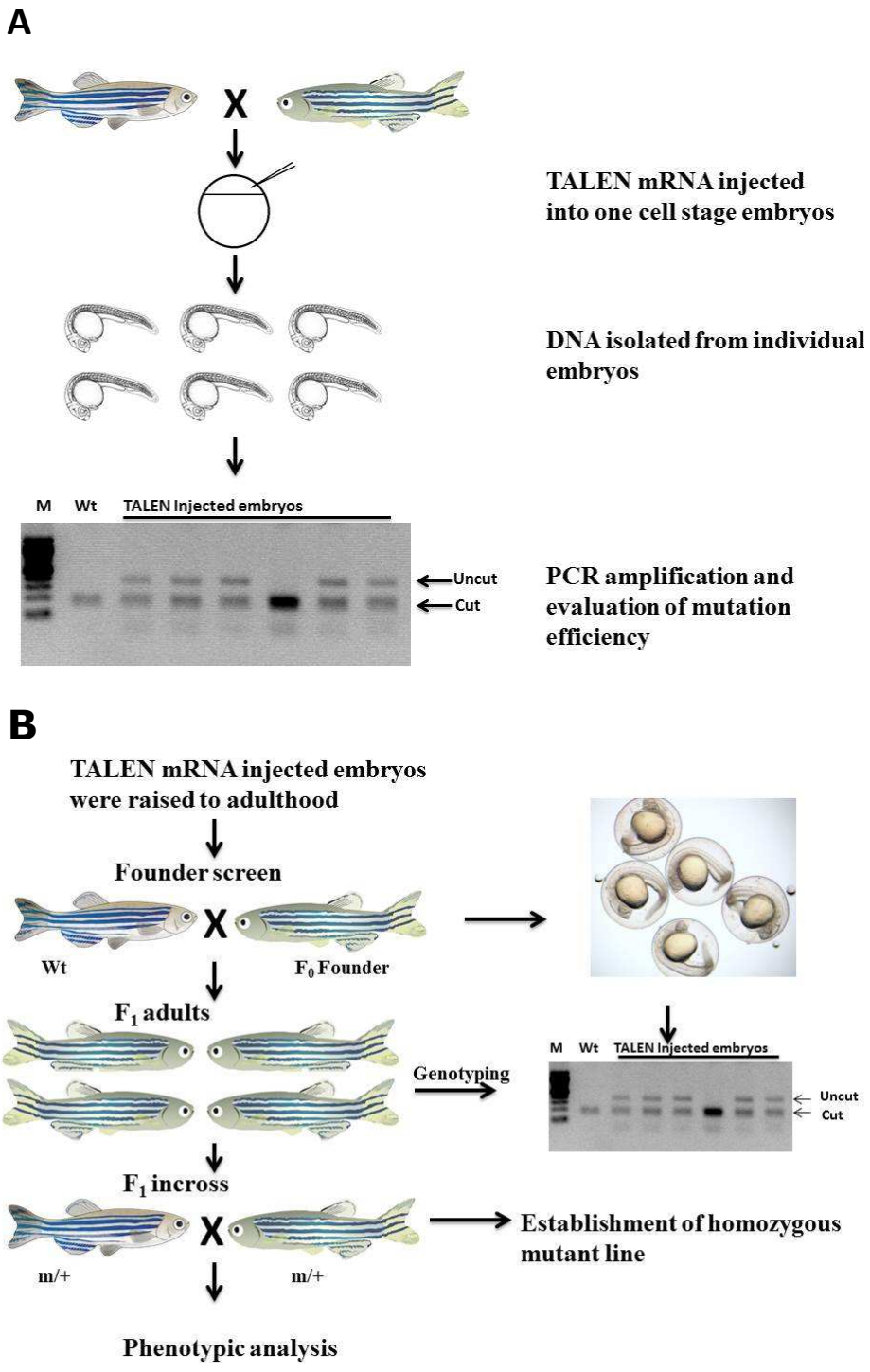
A
TALEN mRNA injected into one cell stage embryos
DNA isolated from individual embryos
M
Wt
TALEN Injected embryos
Uncut
Cut
PCR amplification and evaluation of mutation efficiency
B
TALEN mRNA injected embryos were raised to adulthood
Founder screen
Wt
F0 Founder
F1 adults
Genotyping
M
Wt
TALEN Injected embryos
Uncut
Cut
F1 incross
m/+
m/+
Establishment of homozygous mutant line
Phenotypic analysis

Figure 3.2: Overview of TALEN-mediated genome editing in zebrafish. A. Toxicity, mutation efficiency and the amount of RNA required for successful genome editing was calculated by injecting different concentration of TALEN RNAs. **B.** Then TALEN injected embryos were raised to adulthood and screened for heritable mutation. Embryos from positive founders were raised and fin clip genotyping was used to identify the carriers. Two heterozygous F1 fish were crossed and the embryos were used for phenotypic analysis. A null biallelic mutant was generated by growing the embryos from a carrier in cross.

3.3 Lyl1 and Id4 TALEN-induced site-directed mutagenesis in zebrafish

To determine the efficiency of TALENs, RNA was synthesized *in vitro* and injected into zebrafish 1 to 2 cell stage embryos at different concentration (50 pg - 500 pg). Genomic DNA was extracted from individual embryos (1-4 dpf) that apparently developed normally. PCR amplicons including the TALEN target site were made using *lyl1* TALEN screening primers or *id4* TALEN screening primers (see section 3.2). The PCR amplicons were then digested with either HinfI for lyl1 or HpaII for Id4.

A 400 bp DNA fragment was amplified covering the *lyl1* target site from either injected or control embryos and digested with HinfI. PCR amplicons from wild type control and low amount of TALEN RNA (125 pg) injected embryos were completely digested (220 bp and 180 bp fragments) indicating lack of mutations (Figure 3.3 A**).** In contrast, digestion of PCR amplicons isolated from embryos injected with 500 pg of *lyl1* TALEN RNA resulted in undigested fragment (400 bp) in addition to the two digested fragments (Figure 3.3 B) indicating the presence of mutations that had destroyed the recognition site for HinfI on either one allele in all cells or both alleles in some cells. To confirm the presence of mutations, PCR amplicons were cloned and the nucleotide sequences determined (Figure 3.3 C). Comparison to the wild type sequence indicated the deletion of 7 (2x independently), 11 and 102 nucleotides (Figure 3.2 C).

Genomic DNA from either wild type control or TALEN-injected RNA targeting Id4 was amplified and the PCR amplicons (580 bp) digested with HpaII (Figure 3.3 D). Digestion of wild type PCR amplicons gave rise to the expected sizes of 335 bp and 275 bp (Figure 3.3 D). In contrast, almost all amplicons derived from embryos injected with *Id4* TALENs (either 50 pg or 125 pg RNA) had genome modifications as indicated by the presence of undigested DNA fragments (580 bp; Figure 3.3 D&E). Nucleotide sequence analysis revealed deletions of 6, 7, 9 and 16 nucleotides (Figure 3.3 F).

3.4 Efficiency of TALEN-mediated mutagenesis appears to be target-site dependent

As described above, TALEN-mediated mutagenesis resulted in a variety of deletions ranging from 6 bp to 102 bp some of which resulting in a frameshift disrupting the open reading frame. The efficiency of TALEN-mediated mutagenesis was variable however. While in both cases the mutation efficiency increased with increasing amounts of RNA injected, a relatively high amount of TALEN RNA (500 pg) was required to target the *lyl1* locus (~13% of injected embryos), but much less TALEN RNA (50 pg) was needed in the case of Id4 (~55% of injected embryos) (Figure 3.4 A). Injection of 125 pg *id4* TALEN RNA resulted in over 95% of embryos with targeted mutations (Figure 3.4 A).

Injection of TALEN RNA was accompanied with phenotypic anomalies as well as embryonic death. Only ~40% of embryos injected with 50 pg *id4* TALEN RNA developed normally when analysed at 5 dpf and even injection of 125 pg of *lyl1* TALEN RNA, that did not give rise to targeted mutants, resulted in phenotypic abnormalities and embryonic death **(**Figure 3.4 B**).**

A

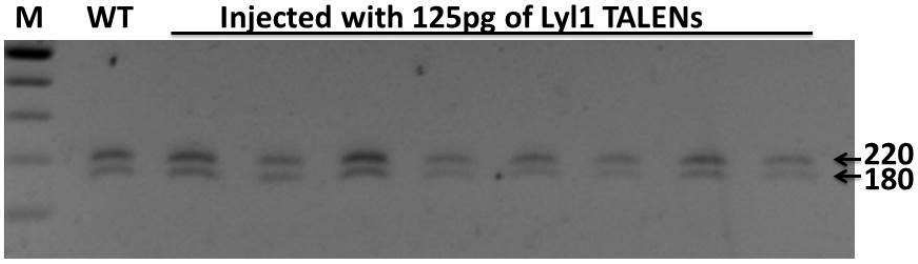

B

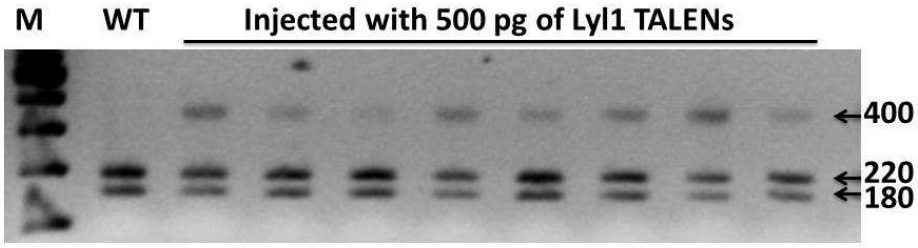

C

```
CTCTTTCCTCATGCCGCCGGCAGGATTCGGGATCTTCAGTAACGCTCGTATGAA WT
CTCTTTCCTCATGCCGCCGG-----------ATCTTCAGTAACGCTCGTATGAA Δ 11
CTCTTTCCTCATGCCGCCGGCAGG-------ATCTTCAGTAACGCTCGTATGAA Δ 7
CTCTTTCCTCATGCCGCCGGCA-------GGATCTTCAGTAACGCTCGTATGAA Δ 7
----------------------------------------------GTATGAA Δ 102
```

D

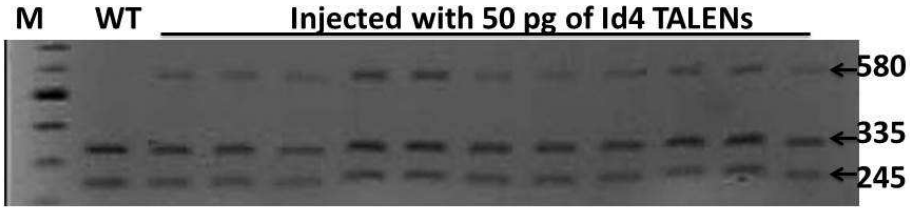

E

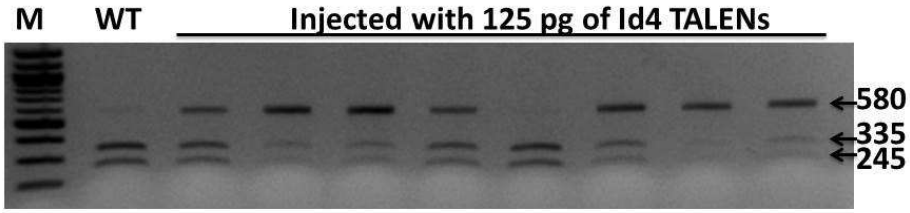

F

```
TTTATTACAATGAAGGCCAGCGTGCCGGTTCGCCCTCATAAGCTTCCTTCTA WT
TTTATTACAATGAAGGCCAGCGT-------CGCCCTCATAAGCTTCCTTCTA Δ7
TTTATTACAATGAAGGCC----------------CTCATAAGCTTCCTTCTA Δ16
TTTATTACAATGAAGGCCAGCGTGCC---------TCATAAGCTTCCTTCTA Δ9
TTTATTACAATGAAGGCCAGCGTG------CGCCCTCATAAGCTTCCTTCTA Δ6
```

Figure 3.3: Induction of somatic mutations using TALENs. PCR and restriction enzyme analysis of embryos injected with *lyl1* or *id4* TALEN RNA. **A, B.** HinfI digested PCR products from 125 pg and 500 pg *lyl1* TALEN RNA injected embryos respectively. Digestion of PCR amplicons from wild-type embryos yields two fragments. Amplicons from 125 pg *lyl1* TALEN RNA injected embryos also digested into two fragments by HinfI (A), while 500 pg *lyl1* TALEN injected embryos shows an undigested fragment. **C.** Sub-cloned sequences from 500 pg *lyl1* TALEN injected embryos. **D, E.** HpaII digested PCR product from *id4* TALEN injected embryos. Wild-type PCR products were digested into two fragments of size 335 and 275. Amplicons from 50 and 125 pg *id4* TALEN injected embryo an undigested fragment. **F.** Sub-cloned sequences from the injected confirm gene disruption. TALEN binding sites were highlighted in yellow and number on the right indicates deleted base pairs. WT, wild-type; M, Marker

A

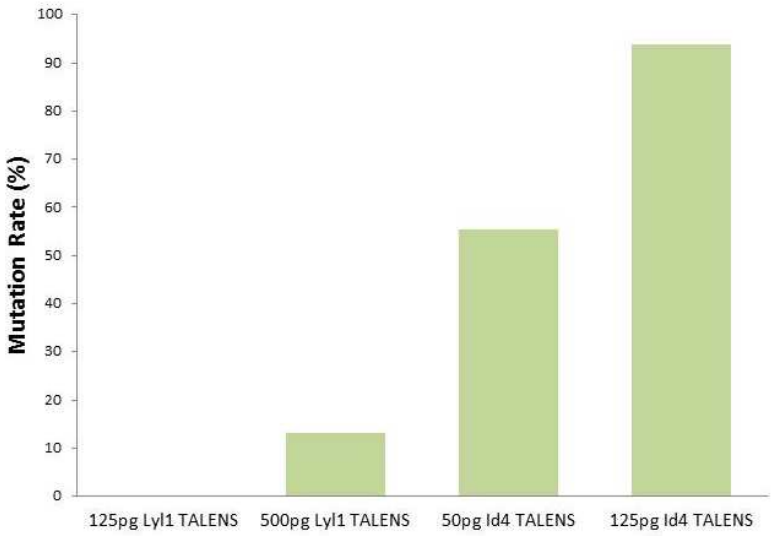
Mutation Rate (%)
100
90
80
70
60
50
40
30
20
10
0
125pg Lyl1 TALENS
500pg Lyl1 TALENS
50pg Id4 TALENS
125pg Id4 TALENS

B

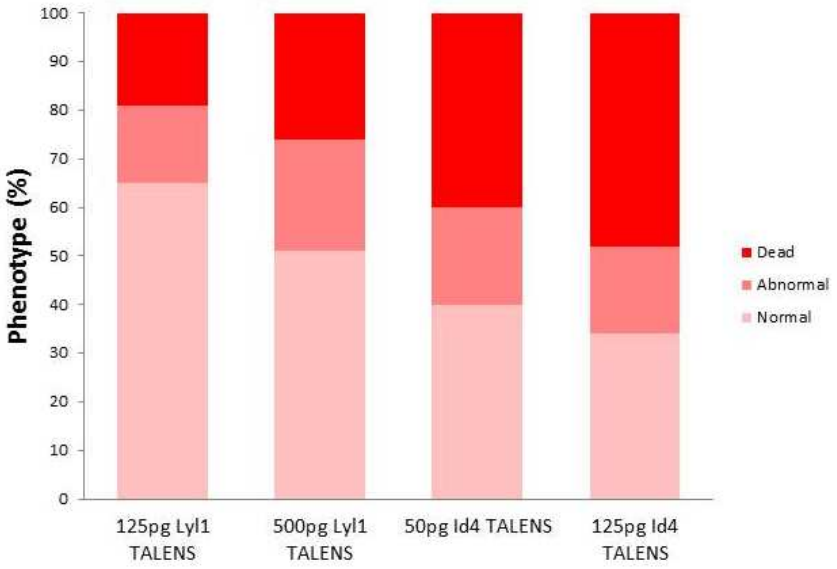
Phenotype (%)
100
90
80
70
60
50
40
30
20
10
0
125pg Lyl1 TALENS
500pg Lyl1 TALENS
50pg Id4 TALENS
125pg Id4 TALENS
Dead
Abnormal
Normal

Figure 3.4: Efficiency of targeted mutagenesis and off-target effects in embryos injected with either lyl1 or Id4 TALEN RNA. A. Mutation rate of lyl1 (0% for 125pg and 13% for 500 pg) and Id4 (55% for 50 pg and 95% for 125 pg) TALENS in somatic zebrafish cells. Mutation rate was calculated by dividing the number of positive clones (with indels) with total number of clones analysed. **B.** Percentage of dead, deformed and normal embryos (5 dpf) when injected with varying amounts of TALEN RNAs as indicated.

3.5 Efficient germ-line transmission of TALEN-induced mutations

Having established that injection of both, *lyl1* and *id4* TALEN RNA give rise to targeted mutations with sufficient efficiency, one cell stage embryos were again injected to identify founder (F0) zebrafish carrying the mutation. As outlined in Figure 3.2 B, embryos injected with TALEN RNA were allowed to develop to adulthood and subsequently crossed with wild type zebrafish. The offspring was screened for mutations to identify parent founders carrying the mutation. As before, genomic DNA from embryos was amplified and the amplicons subjected to restriction enzyme digests. Sequence analysis of potential mutant genomic DNA was performed to select founders that carried frameshift mutations. Initially F1 embryos were genotyped in groups and once the F0 founder was identified the embryos were genotyped individually.F0 founder fish was again crossed with wild type fish to establish mutant lines. Genomic DNA isolated from fin clips of adult offspring (F1) was subjected to the same analysis as before (Figure 3.7 to identify mutant F1 fish (Figure 3.4 B). F1 heterozygous fish (m/+) were in-crossed and the offspring (F2) genotypically and phenotypically analysed. Adult F2 fish were screened for homozygous mutants and these were in-crossed to establish homozygous lines.

Out of 100 embryos injected with 500 pg of lyl1 TALEN RNA, 55 developed normally (at 5dpf) and 30 reached adulthood. Ten of these were crossed with wild type fish and their offspring genotypically analysed revealing that two of out of the ten had successfully transmitted the mutation to their off-spring. The germ line transmission rate of both F_0 founders was 13% (3 out of 23) and 15% (3 out of 20), respectively (**Table 3.1**). Analysis of the sequences showed two types of mutation in Lyl1 F1 embryos Founder 1 had a 7bp deletion whereas founder 2 had a 10bp deletion and 26bp deletion (Figure 3.5, Table 3.2).

In the case of Id4, 46 embryos out of 126 injected with 125 pg of Id4 TALEN RNA hatched with only 17 reaching adulthood. Twelve F_0 fish were crossed with wild type fish and genotypic analysis of their offspring revealed that 8 of them had transmitted the mutation. Transmission rate ranged from 40% to 60%. Twelve different mutation patterns were observed as listed in Table 3.2 and shown in Figure 3.5. Both Id4 and lyl1 F1 embryos developed normally without any phenotype.

Table 3.1: Survival and germline transmission of TALEN injected animals

Concentration of targeting nucleases	**Number of Embryos injected**	**Number survived at 5 dpf**	**Number reached adulthood**	**Number of F0 animals screened**	**No. of animals with heritable transmission**
Lyl1(500 pg)	100	55	30	10	2
Id4 (125 pg)	126	46	17	12	8

Lyl1

Founder number	Embryos screened	Embryos with mutation	Transmission rate	Mutations
1	23	3	13%	-7bp
2	20	3	15%	-10/+26

Id4

Founder number	Embryos screened	Embryos with mutation	Transmission rate	Mutations
1	22	12	54%	-18bp
2	18	10	55%	-12bp
3	20	8	40%	-6bp, -9bp
4	18	9	50%	-8bp, -6bp
5	20	12	60%	-12bp, -10bp
6	24	12	40%	-12bp
7	20	11	55%	-9bp, -12bp
8	23	14	52%	-6bp

Table 3.2: Heritable mutation was observed in TALEN injected fish. TALEN injected embryos were raised and crossed with wild type fish for founder screening. Embryos from each cross were genotyped by PCR / restriction enzyme digestion. Both lyl1 and Id4 TALENS induced heritable mutation with frequency ranging from 13-60%.

Figure 3.5: Sequences of TALEN induced heritable mutations. Two *lyl1* TALEN RNA injected and 8 *id4* TALEN injected induced heritable mutation. Sub-cloning and sequencing of the PCR amplicons from F1 embryo confirmed the disruption of the genes. Red dashes indicate deletion and red letters indicates insertions. Out of frame deletions that are anticipated for frameshift are highlighted in bold. Yellow box on wild type (WT) sequence indicates TALEN binding sites.

3.6 Establishment of Lyl1 and Id4 mutant lines

As shown in Table 3.2 and Figure 3.5, both lyl1 mutations that were transmitted caused a frameshift and therefore both F0 founders 1 & 2 were again crossed with wild type fish and the offspring (F1) raised to adulthood. From 100 embryos only 40 reached adulthood and genotypic analysis of 21 of these using genomic DNA isolated from fin clips revealed that four F1 fish carried the same mutation in one allele (10 bp deletion and 26 bp addition) (Table 3.3, Figure 3.6). This mutation is predicted to result in a truncated lyl1 protein lacking the bHLH domain (Figure 3.7). The lyl1 mutant line will be referred to as **qmc801**. All the analysed F1 adult fish from founder 1(11 fish) turned out to be wild-type, hence the allele qmc801 was chosen. In-crossing of heterozygous lyl1 fish produced off-spring in mendelian fashion (Figure 3.8). Both heterozygous and homozygous lyl1 fish developed normally without any abnormality..

In the case of Id4, only F_0 founders 4 and 5 exhibited frameshift mutations (in addition to in-frame deletions; Table 3.2), so they were crossed with wild type fish and raised to adulthood. From initially 125 embryos (75 founder 4 and 50 founder 5), 55 reached adulthood (35 founder 4 and 20 founder5). Genomic DNA from 43 fish (28 founder 4 and 15 founder 5) were genotyped revealing that twenty fish (13 founder 4 and 7 founder 5) were heterozygous for Id4 mutations but only 5(4 founder 4 and 1 founder 5) carried frameshift deletion (Table 3.3, Figure 3.6). Four of them had an 8 bp deletion and the other one had a 10 bp deletion. 8 bp deletion would essentially retain six original amino acid while the 10bp deletion retains 4 original amino acid and also 36 amino acids that are encoded by a different reading frame. Both these deletion are predicted to truncate the HLH domain of Id4. (Figure3.7).

The Id4 mutant fish line will be referred to as **qmc803** (8bp deletion) and **qmc804** (10bp deletion). In-crossing of heterozygous Id4 fish (qmc803) produced off-spring in mendelian fashion (Figure 3.8) and homozygous Id4 fish (qmc803) are viable.

Qmc801 and qmc803 were picked to study their role in zebrafish development as they were available in pairs.

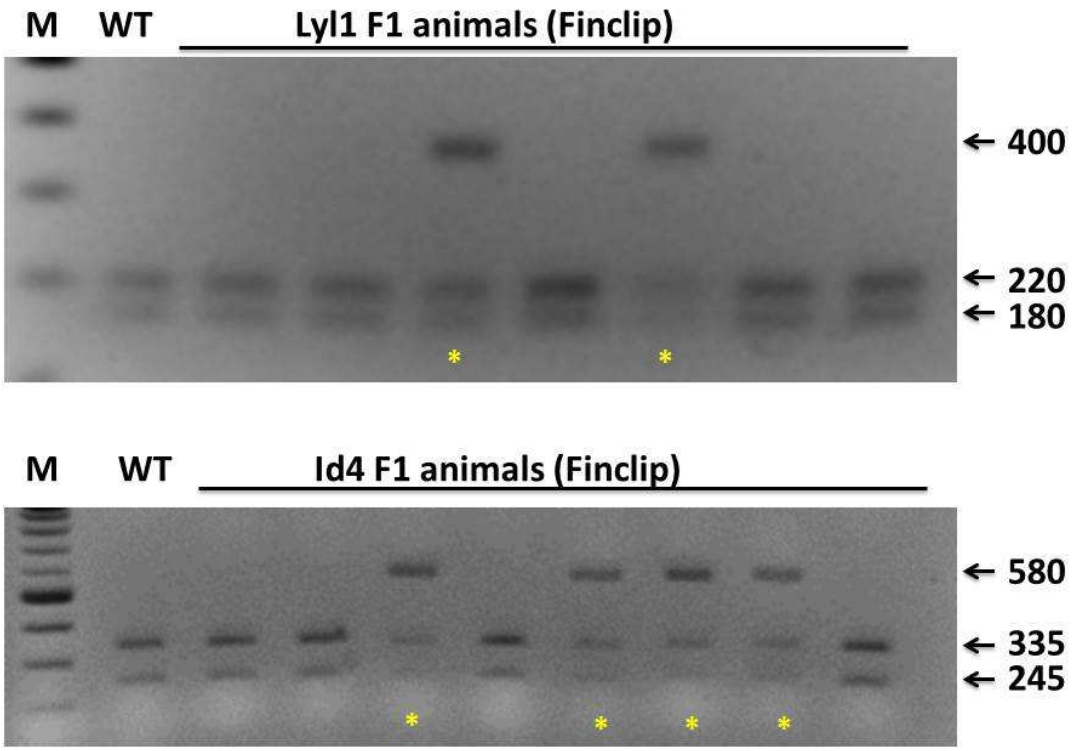

Figure 3.6: Establishment of mutant Lyl1 and Id4 lines. Off-spring from founders that carried frame shift mutations were raised and the adult fish genotyped by PCR / restriction enzyme digestion using genomic DNA isolated from fin clips. F1 heterozygous carriers are labelled: ***.**

Targeting nucleases	**Number of F1 animals screened by**	**Mutations observed**
Lyl1	21	4 (10 bp deletion / 26 bp addition)
Id4	43	6 (12 bp in-frame deletion, Founder 5) 9 (6 bp in-frame deletion, Founder 4) 1 (10 bp deletion, Founder 5) 4 (8 bp deletion, Founder 5)

Table 3.3 Distribution of mutation in F1 adults


A
Lyl1
TCTTTCCTCATGCCGCCGGCAGGATTCGGGATCTTCAGTAACGCTCGTATGA WT
TCTTTCCTCATGCCGC----------atgaggatcttcagtgaggatcatga
GGATCTTCAGTAACGCTCGTATGA (Δ10bp/+26bp)qmc801
B
60
WT MSSDDGEALLMEEQHPPRSSPASPSVLQPDPPAHACSTPPDHAEPRAQDTQEPGATGAET
qmc801 MSSDDGEALLMEEQHPPRSSPASPSVLQPDPPAHACSTPPDHAEPRAQDTQEPGATGAET
120
WT DSRRSSSRSPHCTTTDSRRGSSSASLPAHIPVISLAHSKPPLPPLPLLAALHPAPPPPHG
qmc801 DSRRSSSRSPHCTTTDSRRGSSSASLPAHIPVISLAHSKPPLPPLPLLAALHPAPPPPHG
180
WT PAELRLAQLSCLTGSSPAAALLPPAFLQTHPFISSSFLMPPAGFGIFSNARMKRRPSTHF
qmc801 PAELRLAQLSCLTGSSPAAALLPPAFLQTHPFISSSFLMPHEDLQ*----------
240
WT EVEIRSDGPPQKLARRVFTNSRERWRQQNVNGAFSELRKLIPTHPPDRKLSKNEILRLAM
qmc801 ----------
bHLH domain
300
WT KYIDFLEQLLNDQSQPEETGQRAHAHTPSTHSLLLLTASSGSSCYGDTDSEESTGPRACS
qmc801 ----------
WT TDPKHSREPILALTVSGGQR* 320 aa
qmc801 ---------- 195 aa


C
Id4
TTTATTACAATGAAGGCCAGCGTGCCGGTTCGCCCTCATAAGCTTCCTTCTA WT
TTTATTACAATGAAGGCCAGCGT--------GCCCTCATAAGCTTCCTTCTA Δ8 qmc803
TTTATTACAATGAAGGCCAGC----------GCCCTCATAAGCTTCCTTCTA Δ10 qmc804
D
60
WT MKASVPVRPHKLPSSCSQLSLRYLSESSRCKMEDEDLFCLQYDMNDCYSRLKRLVPTIPQ
qmc803 MKASVPS*----------
qmc804 MKASALISFLLAAVSSPCVICRRAADAKWKMRIFSVCSTT*----------
bHLH domain
120
WT DKKVSKVEILQHVIDYILDLQLALETHPALLKQTSPPASTRTPLTQINTEQRTTGVNKED
qmc803 ----------
qmc804 ----------
WT SLFLCR* 126 aa
qmc803 ------ 7 aa
qmc804 ------ 40 aa

Figure 3.7. DNA and predicted amino acid sequences of lyl1 and Id4 mutant fish lines. Nucleotide sequences from wt and qmc801 (lyl1 mutant) allele (A); WT and qmc803, qmc804 (Id4 mutant) alleles (C). TALEN binding sites are highlighted in yellow and red dashes indicate deletions. B. Alignment of amino acid sequences of WT and truncated lyl1 protein which lost the HLH domain. D. Alignment of amino acid sequences of WT and truncated Id4 protein.

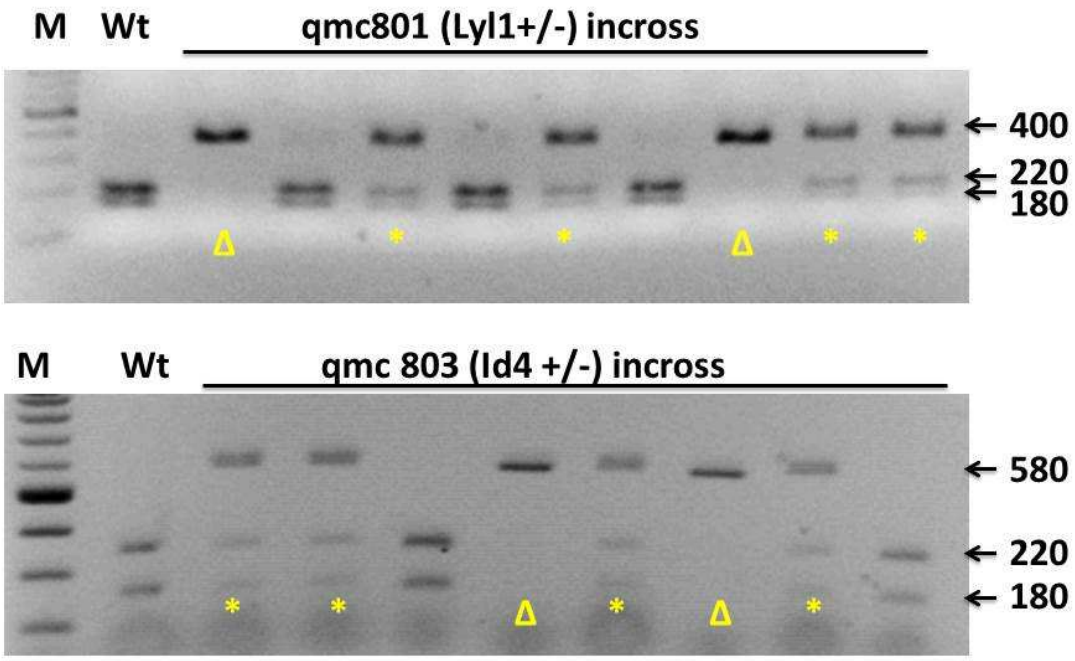

Figure 3.8: Mutant alleles are inherited in a mendelian fashion. A. Qmc801 ($lyl1^{+/-}$) was in-crossed and the embryos were screened by PCR / restriction enzyme digestion. We found 7/30 were homozygous (Δ), 14/30 heterozygous (*) and the 9/30 wild type. B. Embryos screened from qmc 803 ($Id4^{+/-}$) in-cross were also distributed in a similar way (WT 6/30; homozygous 9/30; heterozygous 15/30).

3.7 Summary

- Injection of lyl1 or Id4 TALENS resulted in targeted deletion in somatic zebrafish cells.

- Mutations induced were successfully transmitted to the germline (11-23% for lyl1 and 40-60% for Id4).

- TALEN-mediated targeted deletions resulted in in-frame mutations predicting production of truncated lyl1 and Id4 proteins lacking the (b)HLH domain.

- Lyl1 (qmc801) and Id4 (qmc803) mutant lines were established to study their role in haematopoietic and neural stem cell fate, respectively.

Chapter 4

4.1 Introduction

Like in other vertebrates such as the mouse and human, haematopoiesis in zebrafish occurs in two waves: primitive or the embryonic wave and definitive or the adult wave (Galloway and Zoon, 2003). But unlike mammals in which the site of primitive haematopoiesis are the extra-embryonic yolk sac blood islands, in zebrafish it is the intra-embryonic intermediate cell mass (Al-Adhami and Kunz, 1977; Detrich *et al.,* 1995). During definitive haematopoiesis in zebrafish, all major blood cell types are derived from haematopoietic stem cells that are initially formed from the ventral wall of dorsal aorta and later migrate and reside in the kidney marrow (Thompson *et al.,* 1998; Burns *et al.,* 2002; Kalev-Zylinska *et al.,* 2002; Murayama *et al.,* 2006; Jin *et al.,* 2007).

In addition, many transcription factors that controls haematopoiesis are highly conserved in vertebrates including zebrafish (Chen and Zon, 2009). Two such transcription factors, the class II bHLH proteins lymphoblastic leukemia 1 (Lyl1) and stem cell leukemia/ T-cell acute lymphocytic leukemia (Scl/tal1), have both been implicated in the regulation of haematopoiesis in the mouse (Robb *et al.,* 1996; Porcher *et al.,* 1999; Capron *et al.,* 2006). They share an almost identical bHLH domain (Mellentin *et al.,* 1989; Porcher *et al.,* 1999; Schlaeher *et al.,* 2004) and they both are known to interact with lim-only-domain leukemia oncogenes (Wadman *et al.,* 1991). Although, the expression patter of these two related transcription factors overlap in mouse haematopoietic and endothelial cells, Scl/tal1 expression is noted much earlier than Lyl1 (Giroux *et al.,* 2007) and its expression marks the haemangioblast that produces both endothelial and haematopoietic lineages (Gering *et al.,* 1998). Targeted deletion of scl/tal1 in mice leads to severe haematopoietic defects during both primitive and definitive haematopoiesis (Robb *et al.,* 1995; Shivdasani *et al.,* 1995)

while Lyl1 mutant mice had a reduced number of B cells but had normal blood count and were viable (Capron *et al.,* 2006).

Despite the similarities between Lyl1 and Scl/tal1, it is clear that both have distinct role in haematopoiesis. Although Lyl1 is dispensable for the early mouse development its precise role in primitive haematopoiesis has not been studied due to the complex experimental approach using the mouse system. To overcome such limitations we want to utilise zebrafish and determine Lyl1 function in primitive haematopoiesis and extend the current knowledge of Lyl1 function in adult HSCs ultimately establishing a *lyl1* gene regulatory network determining HSC fate. During zebrafish development, *scl/tal1* expression was first observed in the ALM and PLM at 3 somite stage. Its expression is also observed in the ICM (21hpf) and circulating blood cells (Gering *et al.,* 1998). Ectopic expression of *scl/tal1* can specify blood and endothelial cells (Gering *et al.,* 1998; Liao *et al.,* 1998). Loss-of-function studies using morpholinos for Scl/tal1 demonstrates that it is crucial for the development of haemangioblast and haemogenic endothelium (Patterson *et al.,* 2005). The function of Lyl1 in zebrafish haematopoiesis nor its expression was not studied. Using gain-of-function studies by overexpressing *lyl1* in zebrafish embryos we show that Lyl1 can promote erythroid differentiation. TALEN-mediated loss-of-function analysis shows that Lyl1 plays a role in both waves of haematopoiesis.

4.2 Lyl1 bHLH domain is highly conserved among different species

Lyl1 amino acid sequence was obtained from ENESMBL (ENSDARG00000091603) genome and compared with the other vertebrate. Zebrafish Lyl1 protein has 320 amino acids and the bHLH domain comprises from amino acid 188 to 243. Multiple sequence alignments of zebrafish lyl1 with, mouse, rat and human proteins show that the bHLH domain is highly conserved among vertebrates (Figure 4.1 A). Zebrafish Lyl1 bHLH domain is 92% identical to human bHLH domain of Lyl1 and 90% conserved in mouse and rat. In addition to the

bHLH domain other regions are also conserved across species. Entire Lyl1 amino acids are 43% identical to human Lyl1 and 40% identical to rat and mouse. As mouse Scl/Tal1 and Lyl1 have almost identical bHLH domains, we compared the amino acid in the bHLH region of zebrafish Lyl1 and scl/tal1. Similar to mouse the region is 90% identical to zebrafish scl/tal1 bHLH region (Figure 4.1 B). However as observed in mouse, regions other than the bHLH are much less conserved (33%). The function of lyl1 in zebrafish has not been studied yet.

A

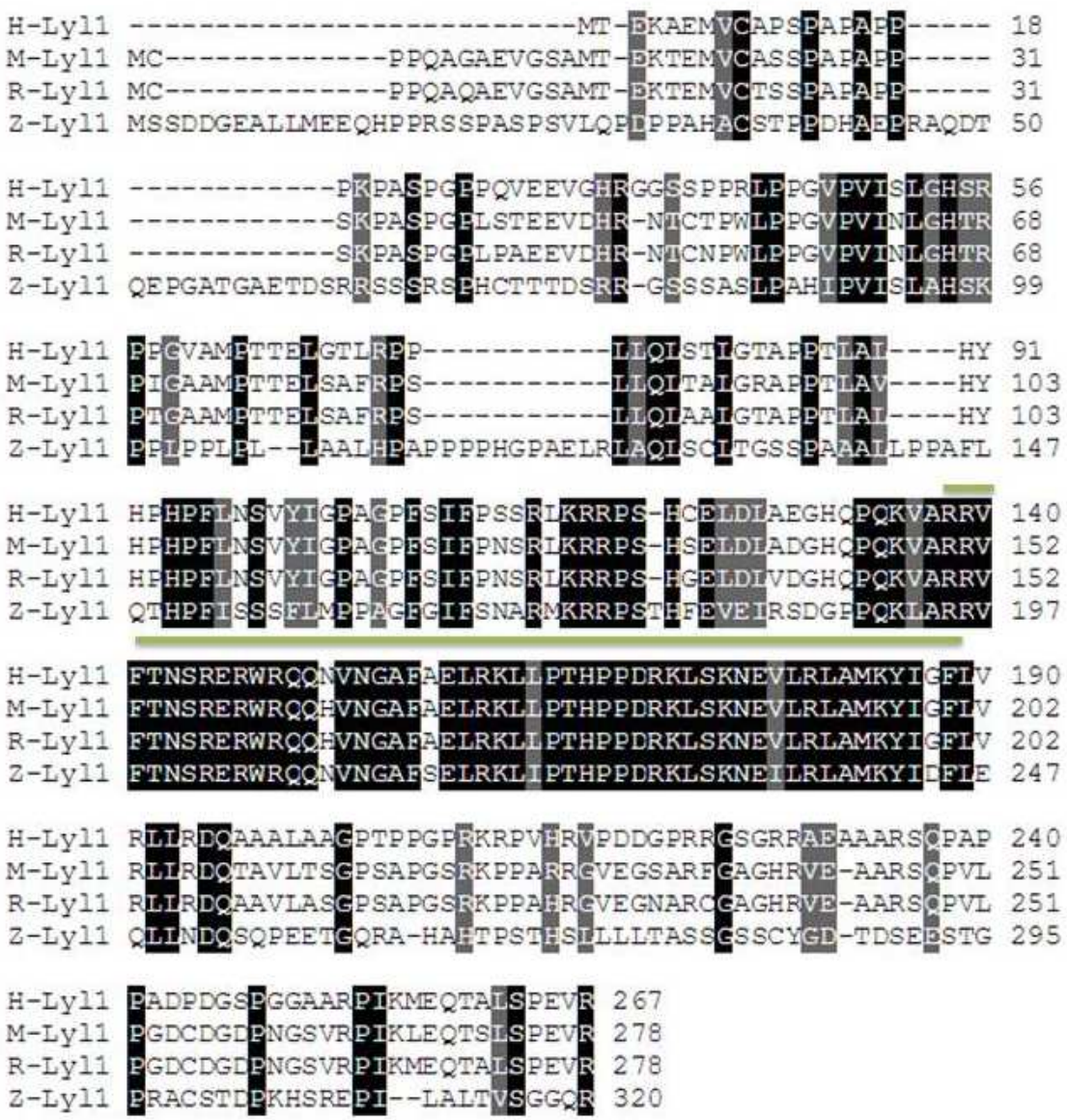
H-Lyl1 ----------MT-EKAEMVCAPSPAPAPP----- 18
M-Lyl1 MC----------PPQAGAEVGSAMT-EKTEMVCASSPAPAPP----- 31
R-Lyl1 MC----------PPQAQAEVGSAMT-EKTEMVCTSSPAPAPP----- 31
Z-Lyl1 MSSDDGEALLMEEQHPPRSSPASPSVLQPDPPAHACSTPPDHAEPRAQDT 50
H-Lyl1 ----------PKPASPGPPQVEEVGHRGGSSPPRLPPGVPVISLGHSR 56
M-Lyl1 ----------SKPASPGPLSTEEVDHR-NTCTPWLPPGVPVINLGHTR 68
R-Lyl1 ----------SKPASPGPLPAEEVDHR-NTCNPWLPPGVPVINLGHTR 68
Z-Lyl1 QEPGATGAETDSRRSSSRSPHCTTTDSRR-GSSSASLPAHIPVISLAHSK 99
H-Lyl1 PPGVAMPTTPLGTLRPP----------LLQLSTLGTAPPTLAI----HY 91
M-Lyl1 PIGAAMPTTPLSAFRPS----------LLQLTALGRAPPTLAV----HY 103
R-Lyl1 PTGAAMPTTPLSAFRPS----------LLQLAALGTAPPTLAI----HY 103
Z-Lyl1 PPLPPLPL--LAALHPAPPPPHGPAELRLAQLSCLTGSSPAAAILPPAFL 147
H-Lyl1 HPHPFLNSVYIGPAGPFSIPPSSRLKRRPS-HCELDLAEGHQPQKVARRV 140
M-Lyl1 HPHPFLNSVYIGPAGPFSIPPNSRLKRRPS-HSELDLADGHQPQKVARRV 152
R-Lyl1 HPHPFLNSVYIGPAGPFSIPPNSRLKRRPS-HGELDLVDGHQPQKVARRV 152
Z-Lyl1 QTHPFISSSFLMPPAGFGIPSNARMKRRPSTHFEVEIRSDGPPQKLARRV 197
H-Lyl1 FTNSRERWRQQNVNGAFAELRKLLPTHPPDRKLSKNEVLRLAMKYIGFLV 190
M-Lyl1 FTNSRERWRQQHVNGAFAELRKLLPTHPPDRKLSKNEVLRLAMKYIGFLV 202
R-Lyl1 FTNSRERWRQQHVNGAFAELRKLLPTHPPDRKLSKNEVLRLAMKYIGFLV 202
Z-Lyl1 FTNSRERWRQQNVNGAFSELRKLIPTHPPDRKLSKNEILRLAMKYIDFLE 247
H-Lyl1 RLLRDQAAALAAGPTPPGPPKRPVHRVPDDGPRRGSGRRAEAAARSQPAP 240
M-Lyl1 RLLRDQTAVLTSGPSAPGSPKPPARRGVEGSARPGAGHRVE-AARSQPVL 251
R-Lyl1 RLLRDQAAVLASGPSAPGSPKPPAHRGVEGNARCGAGHRVE-AARSQPVL 251
Z-Lyl1 QLLNDQSQPEETGQRA-HAPTPSTHSLLLLTASSGSSCYGD-TDSEESTG 295
H-Lyl1 PADPDGSPGGAARPIKMEQTALSPEVR 267
M-Lyl1 PGDCDGDPNGSVRPIKLEQTSLSPEVR 278
R-Lyl1 PGDCDGDPNGSVRPIKMEQTALSPEVR 278
Z-Lyl1 PRACSTDPKHSREPI--LALTVSGGQR 320

B

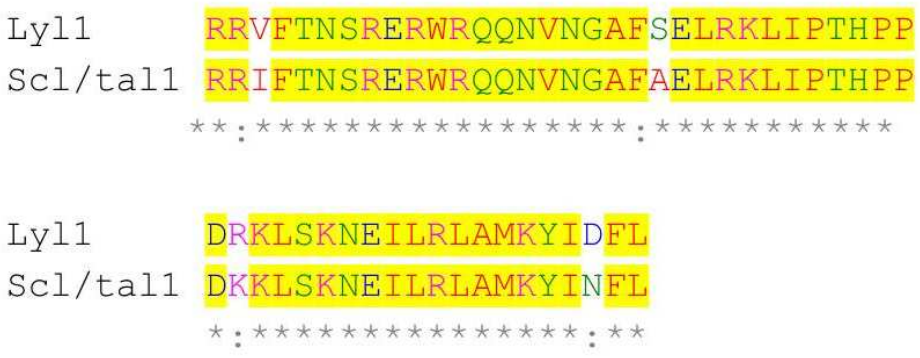
Lyl1 RRVFTNSRERWRQQNVNGAFSELRKLIPTHPP
Scl/tal1 RRIFTNSRERWRQQNVNGAFAELRKLIPTHPP
Lyl1 DRKLSKNEILRLAMKYIDFL
Scl/tal1 DKKLSKNEILRLAMKYINFL

Figure 4.1: Multiple sequence alignment of Zebrafish Lyl1. (A). Zebrafish Lyl1 protein sequence was aligned and compared to other vertebrates. bHLH domain was marked by black bar. (B) Amino acid in the bHLH domain of zebrafish Lyl1 and Scl/Tal1 were 90% identical. All the amino acid sequences are obtained from ENSEMBL. Human Lyl (ENSG00000104903); Mouse Lyl1(ENSGMUSG00000034041); Zebrafish Lyl1(EBSDARG00000091603); Rat Lyl1 (ENSRNOG00000002850); Zebrafish Scl/tal1 (ENSDARG00000019930)

4.3 Lyl1 RNA is detected during both primitive and definitive waves of zebrafish haematopoiesis

RNA was extracted from zebrafish embryos at different stages of development and reverse transcriptase PCR (RT-PCR) was performed to determine whether *lyl1* is expressed during zebrafish development. Primitive haematopoiesis in zebrafish is initiated at 2 somites stage (~10.6 hpf) coinciding with the start of *scl/tal1* expression (Gering *et al.,* 1998). In contrast, weak *lyl1* expression was first observed at 11 hpf (5 somites stage) and strong expression was observed from 14 hpf (10 somites) onwards (Figure 4.2 B). No PCR product was detected in RT^- control amplification (Figure 4.2). The *lyl1* PCR product was cloned and sequenced. Sequence comparison revealed that it was identical to ENESMBL *lyl1* cDNA confirming specificity of the PCR reactions (Appendix 2).

We next wanted to establish the expression pattern of lyl1 using whole mount *in situ* hybridization. However, several *lyl1* antisense probes were tested and all resulted in un-specific back ground signal (example at 24 hpf shown in Figure 4.2 C). As *lyl1* mRNA has high GC content, it might have been difficult to establish appropriate hybridization conditions for whole mount *in situs*. In contrast, *in situ* hybridization on kidney sections resulted in strong signals in regions where haematopoietic stem cells reside (Figure 4.2 D, D'). No signals were observed using a sense control probe (Figure 4.2 F & F'). As a positive control, *scl/tal1* expression was also analysed (Figure 4.2 E & E'). Comparing both signals, it appears as if *lyl1* gave rise to strong positive signals than scl/tal1 (Figure 4.2 E, E'). These preliminary data seem to suggest that *lyl1* expression is more widespread than scl/tal1 in adult HSCs and that it might therefore play a distinct role in adult HSC function and fate.

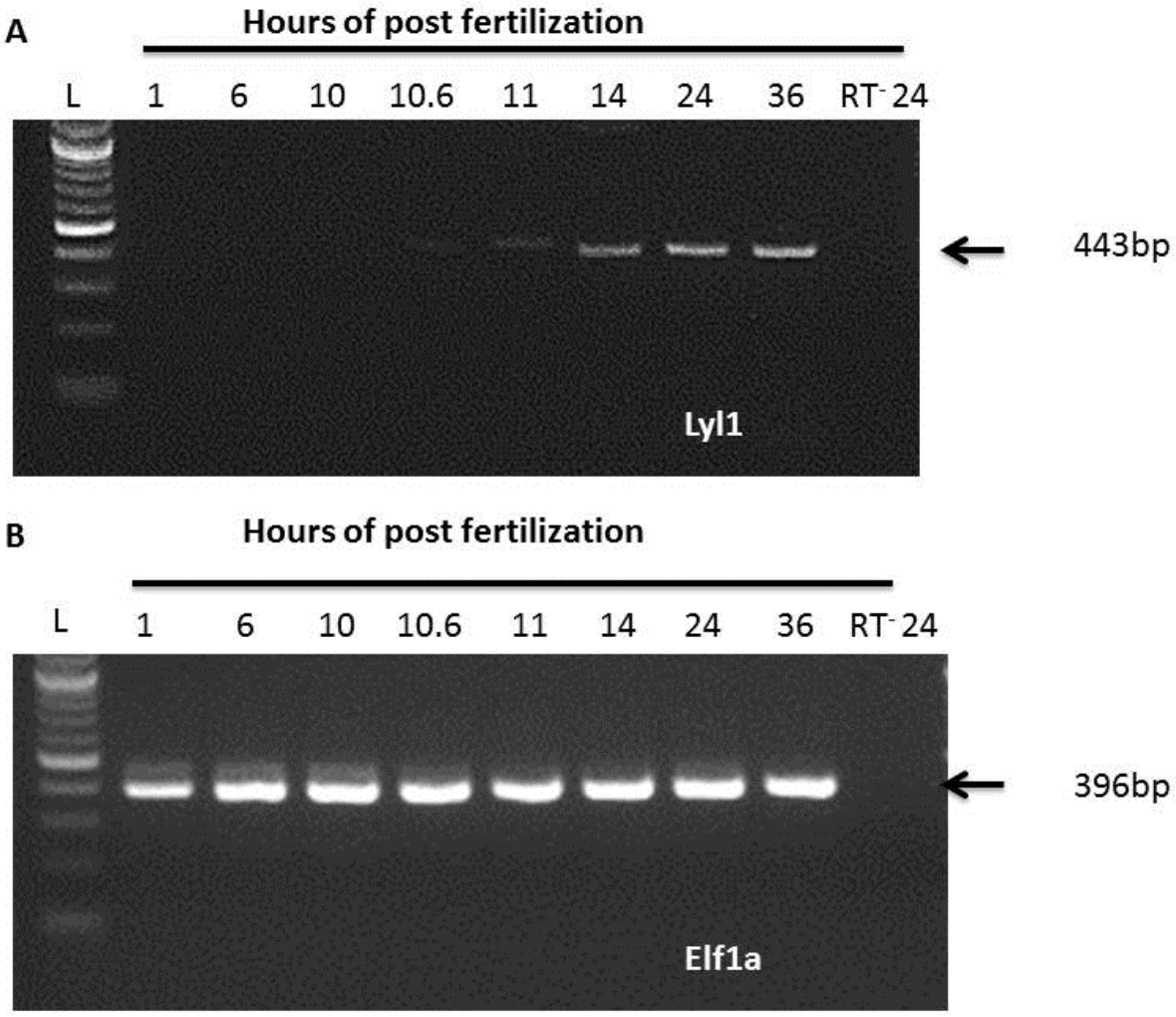
A
Hours of post fertilization
L
1
6
10
10.6
11
14
24
36
RT- 24
443bp
Lyl1
B
Hours of post fertilization
L
1
6
10
10.6
11
14
24
36
RT- 24
396bp
Elf1a

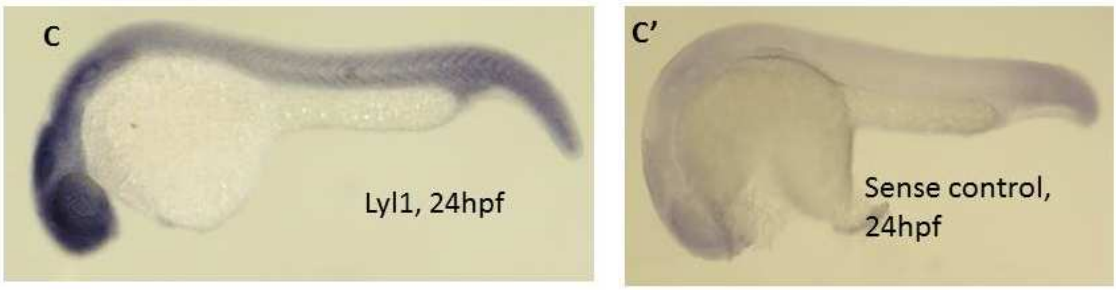
C
Lyl1, 24hpf
C'
Sense control,
24hpf

10/10 **10/10**

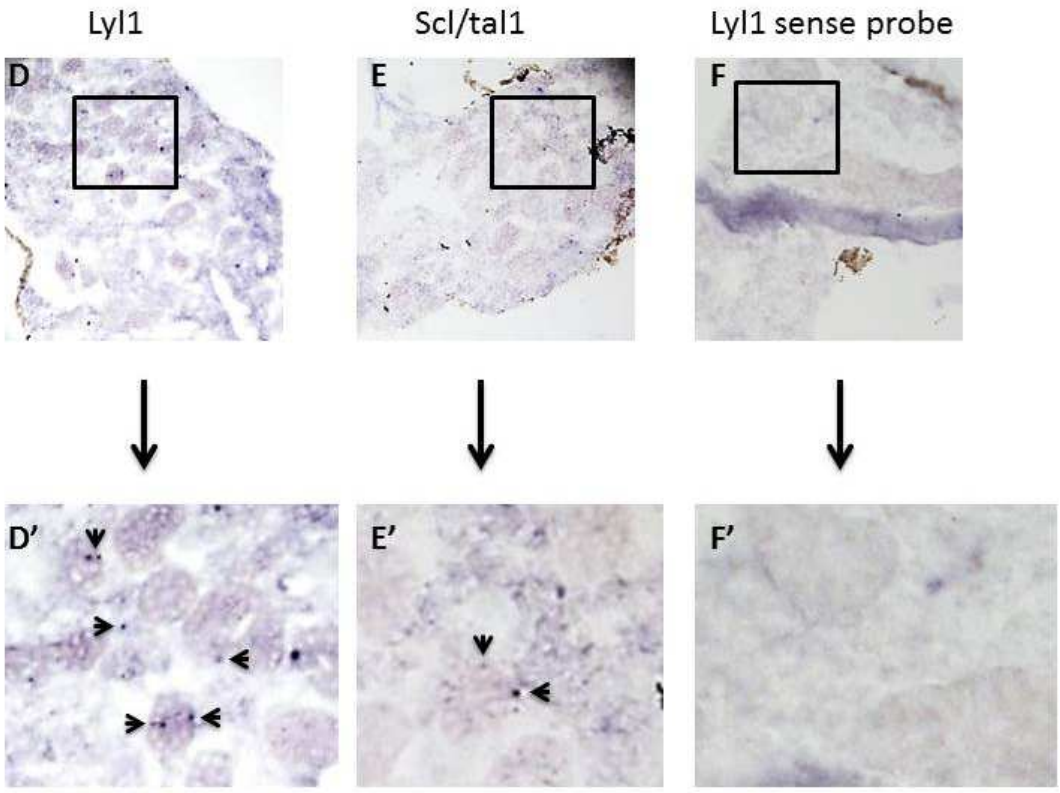

Figure 4.2 *Lyl1* expression profile in embryos and adult kidney sections. RT-PCR using RNA isolated from zebrafish embryos at different stages as indicated. **(A)** PCR using *lyl1*-specific primers produced a 443 bp weakly detectable at 11 hpf and clearly visible from 14 hpf onwards. **(B)** Control PCR using Elf1a-specifc primers resulted in amplification in all stages tested. RT^- : Reverse transcriptase negative control; L- 100 bp Ladder. **(C)** Whole mount *in situ* hybridization using 24 hpf zebrafish embryos with lyl1 mRNA probes did result in high background signal **(C')** sense control. **(D-E**) *In situ* hybridization on adult kidney sections comparing *lyl1* and *scl/tal1* expression. (F) *Lyl1* control sense probe did not give rise to any signal. **(D'-F')** Representative enlargement of marked areas from D, E and F. Arrows indicate positive cells for *lyl1* and *scl/tal1*.

4.4 Ectopic overexpression of *lyl1* in zebrafish embryos resulted in mild to moderate morphological phenotype

Gain-of-function studies in zebrafish can be achieved by microinjecting *in vitro* transcribed mRNA into 1 or 2 cell stage embryos (Chao *et al.,* 1991; Kelly *et al.,* 1995; Toyama *et al.,* 1995; Nikaido *et al.,* 1997; Koos and Ho, 1999). However, this approach results in ectopic overexpression of the protein in all cells that might give rise to ectopic phenotypes. Full length *in vitro* transcribed *lyl1* RNA (Section 2.2.2.1) was injected at different concentration (50 pg and 100 pg) into two cell stage embryos and at 24 hpf morphology of embryos was analysed. Out of 103 embryos injected with 50 pg *lyl1* mRNA, 72 embryos developed and at 24 hpf 47% (34/72) embryos displayed a similar morphology as wild type embryos (Figure 4.3 A). 26 out of 72 embryos (36%) displayed a mild phenotype with a slightly curved tail. 17% (12/72) of the embryos were classified as moderate as they possessed curved tail defect that resulted in reduced body axis and their head was not properly developed (Figure 4.3 A). 88 of the 130 embryos survived after injection of 100 pg *lyl1* mRNA. 35% (31/88) of these embryos looked normal, whereas 43% (38/88) exhibited a mild phenotype in the trunk (Figure 4.3 B). A moderate phenotype was observed in 19 out of 88 (22%) embryos injected with 100 pg *lyl1* mRNA. These results suggest that ectopic *lyl1* overexpression give rise to morphological alterations that are dose dependent (Figure 4.3 C).

A

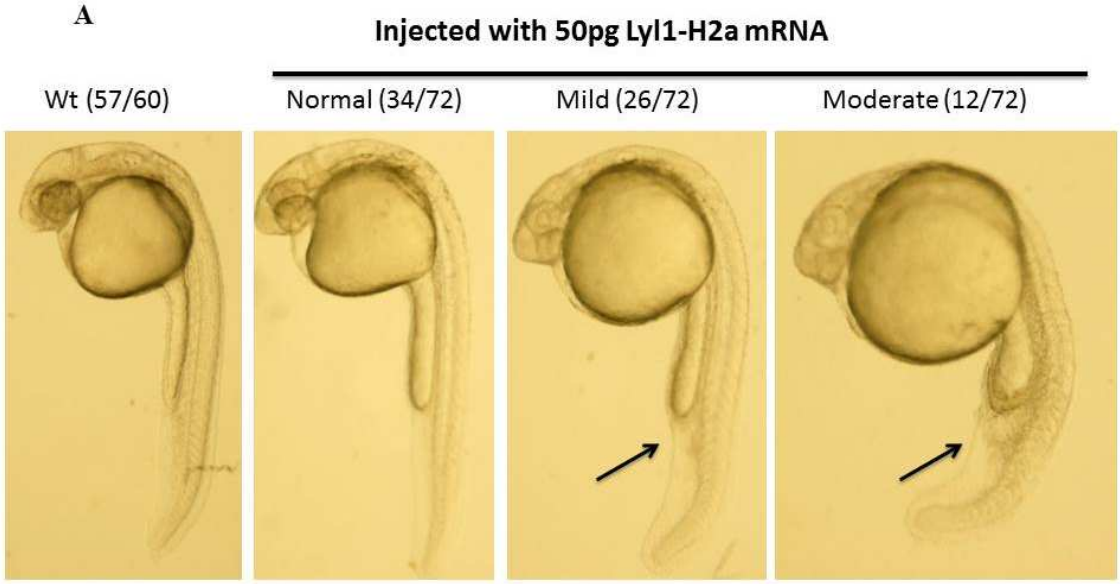
Injected with 50pg Lyl1-H2a mRNA
Wt (57/60)
Normal (34/72)
Mild (26/72)
Moderate (12/72)

B

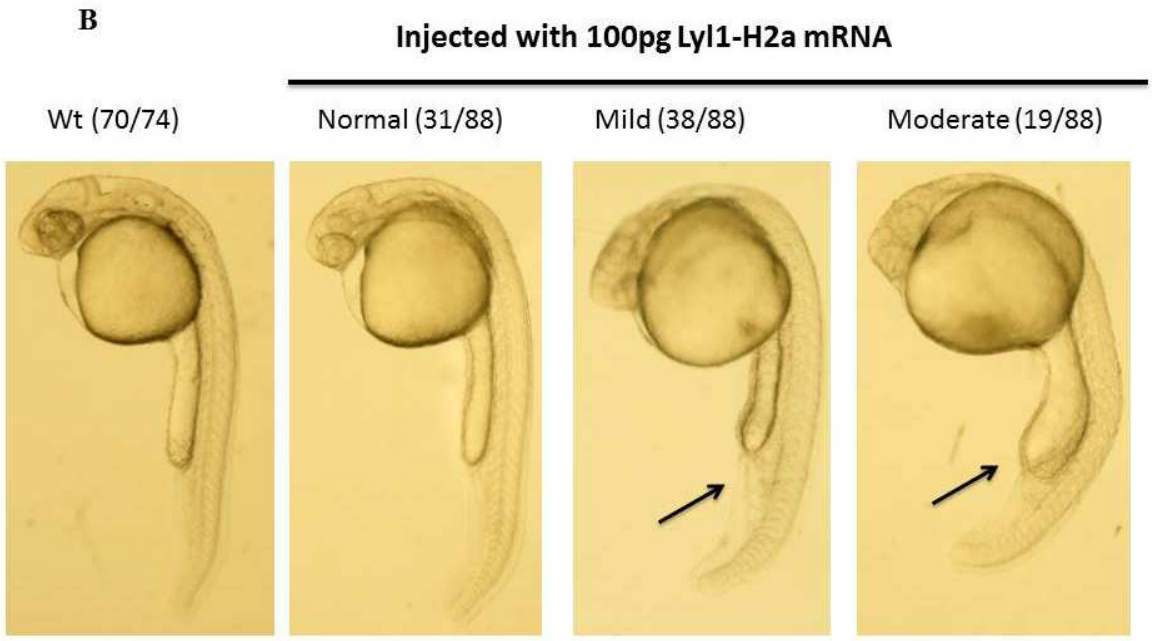
Injected with 100pg Lyl1-H2a mRNA
Wt (70/74)
Normal (31/88)
Mild (38/88)
Moderate (19/88)

C

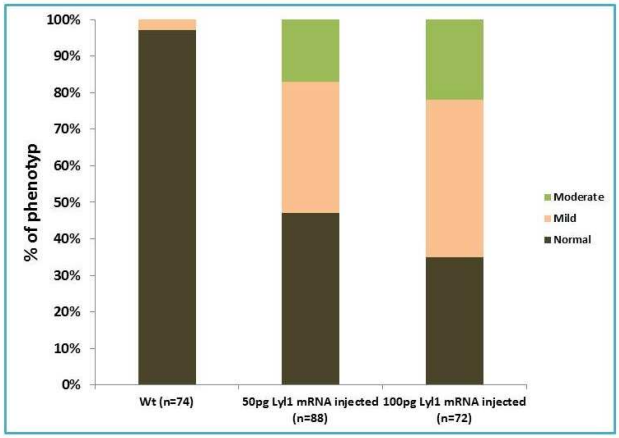
100%
90%
80%
70%
60%
50%
40%
30%
20%
10%
0%
% of phenotyp
Moderate
Mild
Normal
Wt (n=74)
50pg Lyl1 mRNA injected (n=88)
100pg Lyl1 mRNA injected (n=72)

Figure 4.3 Ectopic overexpression of *lyl1* in zebrafish embryos results in a dose dependent phenotype. Phenotypes observed in the embryos injected with 50 pg *lyl1* mRNA **(A)** and 100 pg *lyl1* mRNA **(B)** at 24 hpf. Based on the morphology they are divided into normal, mild and moderate. A representative embryo from each division is shown. (**C)** Quantification of the phenotypes in the *lyl1* mRNA injected embryos. About 47% of the embryos developed normally while 53% showed a phenotype in 50 pg injected embryos whereas 65% percentage of the embryos displayed a phenotype when 100 pg *lyl1* mRNA was injected.

4.5 Ectopic overexpression of *lyl1* leads to impaired primitive haematopoiesis

To check whether enforced expression of *lyl1* induces any haematopoietic alterations in the developing zebrafish embryos, the expression of several marker genes for haematopoiesis was determined at 14 hpf (for primitive wave). Primitive haematopoiesis in zebrafish occurs at the ALM (Anterior Lateral Mesoderm) and PLM (Posterior Lateral Mesoderm). PLM consist of vascular and erythroid cells whereas myelopoiesis occurs in the ALM.

At 14 hpf *scl/tal1* is expressed in both ALM and PLM as two stripes and its expression marks the initiation of haemangioblast formation that produces both vascular and blood cells. Ten out of 12 embryos injected with 100 pg of *lyl1* mRNA displayed an increase in *scl/tal1* expression whereas two out of 12 embryos did not show any change in the expression at 14 hpf (Figure 4.4 A, B). We next observed the expression of erythrocyte marker *gata1*, which is expressed by a subset of *scl/tal1* positive cells (Davidson *et al.*, 2004) in the PLM at 14 hpf. As observed for *scl/tal1*, expression of *gata1* was also increased in the PLM of lyl1 RNA-injected embryos at 14 hpf (Figure 4.4 C, D). In the ALM a subset of *scl/tal1* positive cells express *pu.1*, a myeloid cell marker (Bennett *et al.*, 2001). In contrast to the increase in the expression of *gata1*, expression of *pu.1* was reduced Figure 4 E, F).

As described above, endogenous *scl/tal1* expression occurs earlier than *lyl1* expression and therefore *lyl1* cannot be part of the early regulatory network. Nevertheless, ectopic overexpression of *lyl1* could still alter such network by for example synergising or competing with scl/tal function. The observed enhanced *scl/tal1* and *gata1* expression and reduced *pu.1* expression might therefore reflect Lyl1's contribution to the expansion of *scl/tal1* expressing cells and to the biased differentiation into erythroid fate to the expense of myeloid cells.

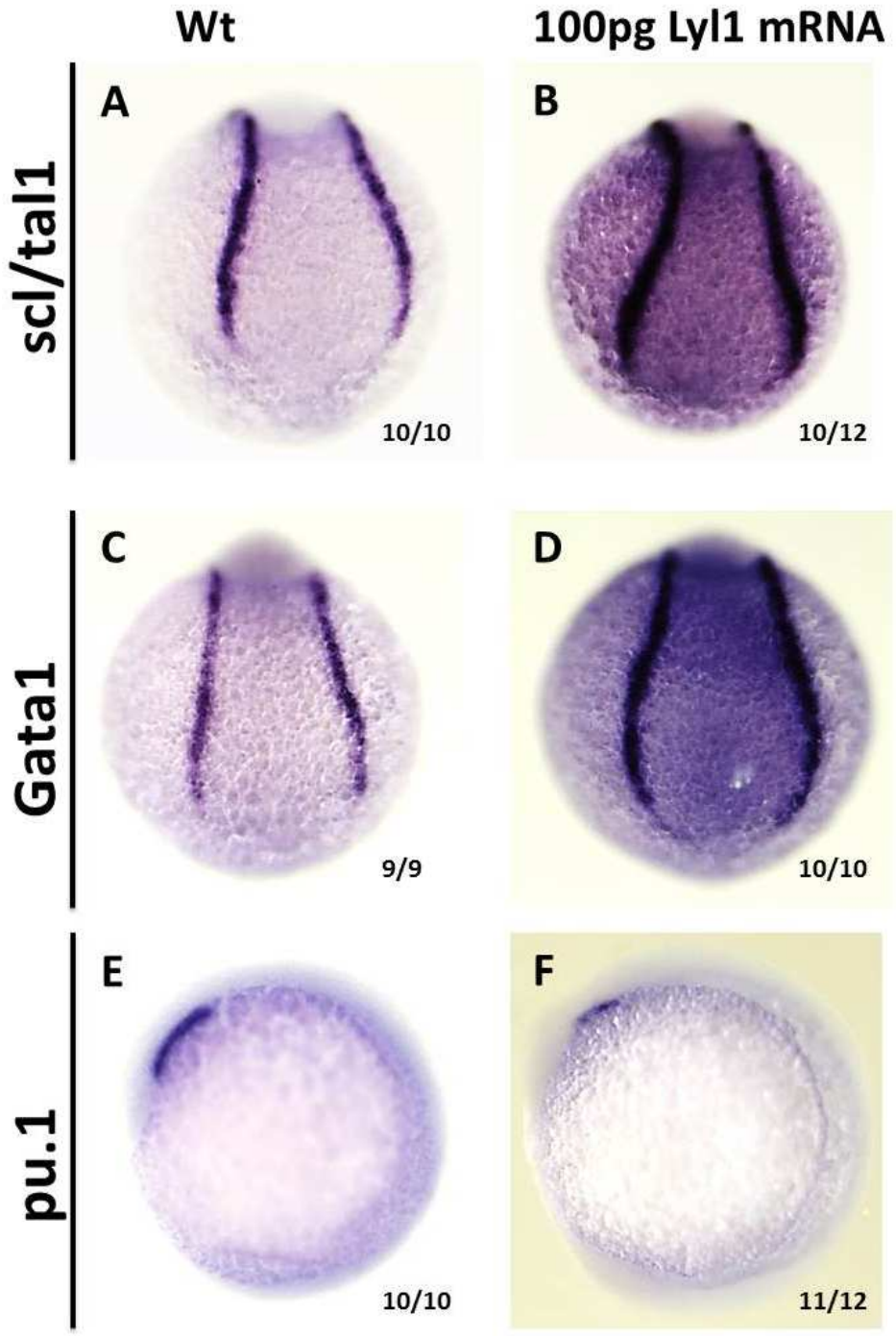
Wt
100pg Lyl1 mRNA
scl/tal1
A
10/10
B
10/12
Gata1
C
9/9
D
10/10
pu.1
E
10/10
F
11/12

Figure 4.4 Abnormal primitive haematopoiesis was observed in the 100 pg *lyl1* RNA injected embryos. (A-B) At 14 hpf *scl/tal1* is expressed in the PLM as two stripes in the wild type (A) and *lyl1* mRNA injected (B) embryos. **(C-D)** Expression of *gata1* is also elevated in the lyl1 mRNA injected embryos **(E-F)** Myeloid marker *pu.1* expression is reduced with elevated levels of *lyl1* when compared with wild type embryos. (A-D Dorsal view; E and F Lateral view).

4.6 Exogenous *lyl1* mRNA expression has enhanced the primitive red blood cells

Primitive erythropoiesis occurs in the ICM and produces the prRBC which is the only circulating RBC for the first four days of development (Weinstein *et al.*, 1996). Injection of *scl/tal1* into zebrafish embryos resulted in overproduction of blood and the most of the embryos also displayed circulation defect (Gering *et al.*, 1998). In order to check whether enforced expression of *lyl1* also resulted in the increased production of primitive erythrocytes, we observed the expression of various marker genes on *lyl1* injected embryo at 24-30 hpf. At 24 hpf, 13 out of the 14 embryos injected with 100 pg of *lyl1* RNA exhibited increased scl/tal1 expression (Figure 4.5 A, B) and 9 out of 12 embryos injected with *lyl1* mRNA also displayed an increased gata1 expression (Figure 4.5 C, D). Both *scl/tal1* and *gata1* at 24 hpf marks the primitive erythrocytes and this elevated expression of them indicates an increase in the blood cell production. At 30 hpf, expression of *c-myb* noticed in the ventral wall of the dorsal aorta, was increased in embryos injected with *lyl1* mRNA (Figure 4.5 E, F). Ikaros that is required for normal development of lymphocytes, which starts around 4 dpf (Willet *et al.*, 2001). It is also expressed in the ICM at 24 hours and in the embryos with enforced Lyl1 expression had an increased expression of *ikaros* in the ICM. These enhanced expressions of these two markers also suggest that the ICM is packed with prRBC. Unlike *scl/tal1* injected embryos which displayed an increase in the expression of angioblast marker *flk1*, the expression of *flk1* in all the *lyl1* mRNA injected embryos (10/10) was not altered (Figure 4.5 I, J).

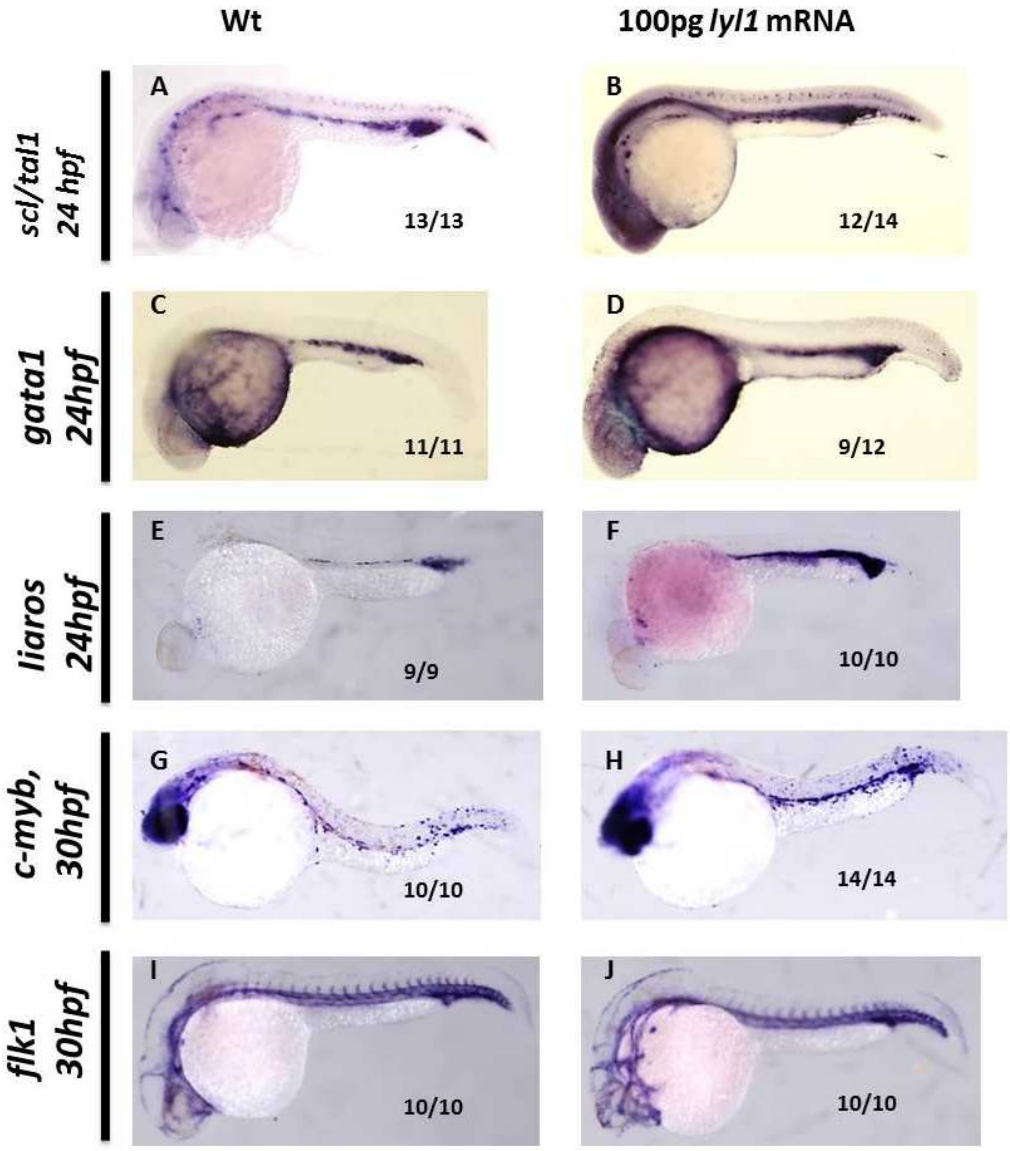

Figure 4.5 Expansion of prRBCs in embryos ectopically overexpressing *lyl1*. Injection of *lyl1* mRNA has increased the expression of prRBC markers (**A, B)** *scl/tal1* **(C, D)** *gata1* **(E, F)** *ikaros* at 24 hpf and **(G, H)** *c-myb* at 30 hpf. However the expression of endothelial marker **(I, J)** *flk1* was unaltered at 24 hpf (A-J Lateral view)

4.7 lyl1 homozygous mutant embryos exhibit normal morphology

To further analyse the role of Lyl1 in zebrafish haematopoiesis, TALEN-mediated mutation of the *lyl1* gene was performed. TALEN pairs targeting DNA upstream of the region encoding the bHLH domain created a mutation with 10bp deletion/26bp addition predicted to result in a truncated Lyl1 protein lacking the bHLH domain. Both heterozygous (*lyl1*$^{+/qmc801}$) and homozygous (*lyl1*$^{qmc801/qmc801}$) fish developed normally and produced embryos without obvious morphological defects. As example, a 24 hpf *lyl1* $^{qmc801/qmc801}$ embryos is shown in Figure 4.7, which appears morphologically identical to the wild type embryo.

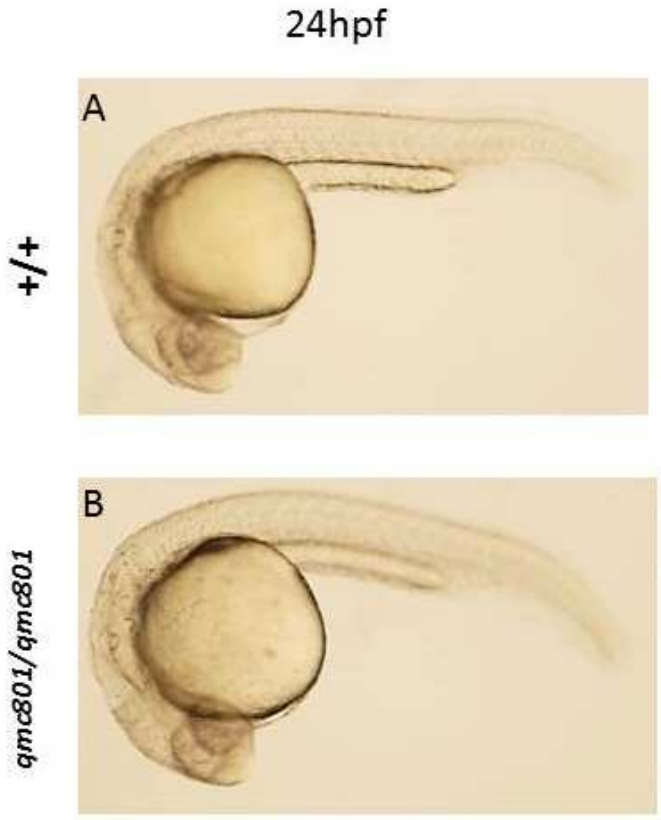

Figure 4.6 *lyl1*$^{qmc801/qmc801}$ embryos at 24 hpf are morphologically indistinguishable from wild type embryos. Lateral view of wild type embryo **(A)** and *lyl1*$^{qmc801/qmc801}$ embryo **(B)** at 24 hpf.

4.8 Loss of Lyl1 results in impaired haematopoiesis during both primitive and definitive haematopoiesis

As described above, *lyl1* expression was clearly detectable at 14 hpf by RT-PCR (Figure 4.2 A) so loss of Lyl1 function could have an impact on heamatopoiesis at this and later developmental stages. However, *in situ* hybridization using *scl/tal1* and *gata1* probes indicated that expression of these genes was unaltered in *lyl1*$^{qmc801/qmc801}$ embryos at 14 and 24 hpf (Figure 4.8). As *lyl1* is not expressed early on, haemangioblast formation and early production of primitive erythrocytes was not compromised in *lyl1* $^{qmc801/qmc801}$ embryos and their maintenance at 14 hpf seems independent of Lyl1. In contrast, expression of *pu.1* in the PBI and yolk sac of *lyl1* $^{qmc801/qmc801}$ embryos at 24 hpf was increased (Figure 4.9). Together with the results described above that overexpression of *lyl1* resulted in a reduction of *pu.1* expression, these results suggest that Lyl1 is antagonising myeloid differentiation. In addition, Lyl1 can promote erythrocyte differentiation but is not required during early phases of erythropoiesis.

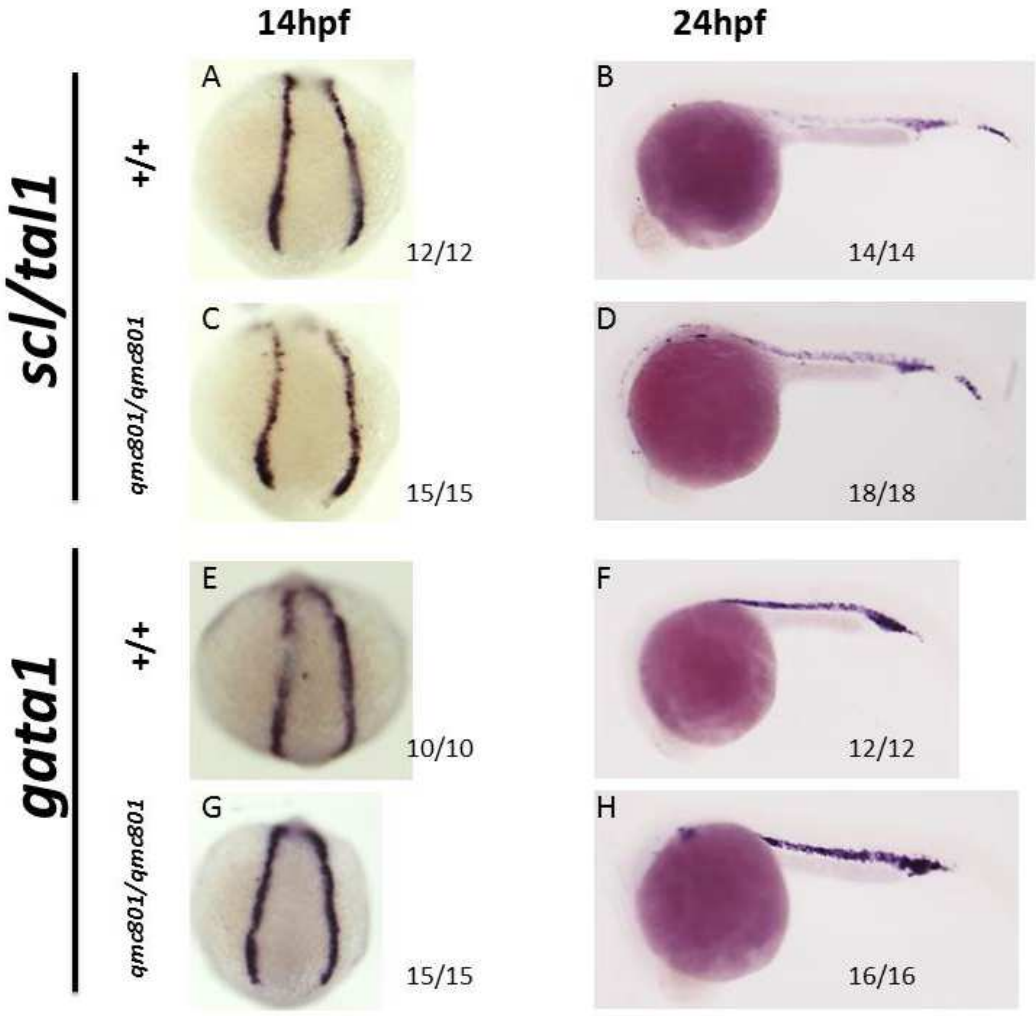

Figure 4.7 Loss of lyl1 does not alter the expression of *scl/tal1* and *gata1*. (A-D) Expression of *Scl/tal1* in Wt and *lyl1*$^{qmc801/qmc801}$ embryos at 10 somite (A, C) and 24 hpf (B, D). **(E-H)** No difference in the cells expressing Gata1 in the mutants (G and H) when compared with wild type (E and F) during zebrafish development. (A, C, E and F Dorsal view; B, D, E and F Lateral view)

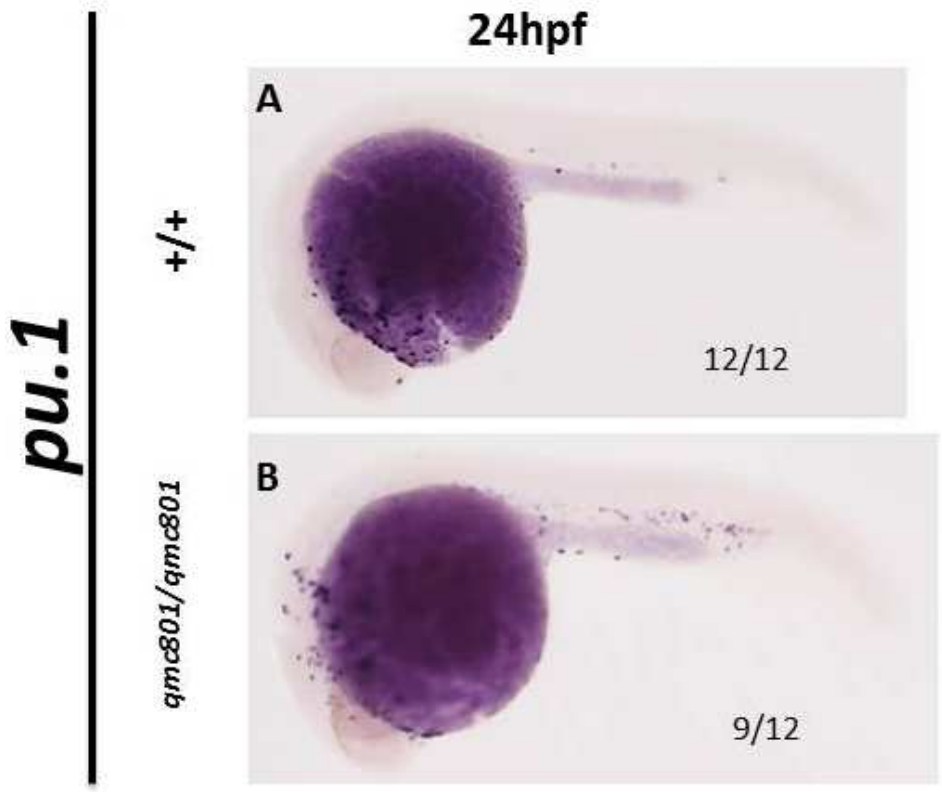

Figure 4.8 Elevated expression of *pu.1* in the *lyl1*$^{qmc801/qmc801}$ embryos. (A) *pu.1* is expressed in the yolk sac of wild type embryos at 24 hpf. **(B)** Increase in *pu.1* positive cells are noticed in the ventral wall of dorsal aorta and also in the PBI of the *lyl1*$^{qmc801/qmc801}$ embryos at 24 hpf. (A and B Lateral view)

4.9 Lyl1 is required for regulation of Gfi1aa during primitive and definitive haematopoiesis

In mammals, *gfi1* is expressed in HSCs and lymphoid cells. Deletion of *gfi1* suggested that it is critical for maintenance and self-renewal of HSCs (Grimes *et al.,* 2006; Zheng *et al.*, 2004; Hock *et al.*, 2004; Hock and Orkin, 2006). In addition, Lyl1 was shown to directly regulate *gfi1* expression during T cell lymphopoiesis (Zohren *et al.*, 2011). The zebrafish *gfi1aa* ortholog is also expressed in prRBC (Wei *et al.*, 2008). Therefore, expression of *gfi1aa* was determined. As shown in Figure 4.10 loss of lyl1 resulted in a clear reduction of *gfi1aa* in the ICM of 18 hpf as well as the ventral wall of 24 hpf *lyl1*$^{qmc801/qmc801}$ embryos (Figure 4.10).

Primitive haematopoiesis in zebrafish produces prRBC that starts to circulate around 24hpf. *Gfi1aa* expression was first observed in the prRBC progenitors at 5ss and its expression start to reduce in the ICM around 19-20hpf (Cooney *et al.*, 2013). *lyl1*$^{qmc801/qmc801}$ embryos seem to be slightly older which could be due to staging difference hence analysing the embryos at a much earlier time point (10ss) should validate the loss of *gfi1aa* expression during primitive haematopoiesis in *lyl1* $^{qmc801/qmc801}$. *Gfi1aa* expression was also reduced in the *lyl1* $^{qmc801/qmc801}$at 24 hpf. The expression of *gfi1aa* is restricted to ventral wall of the dorsal aorta and inner ear at 26hpf. As only a few cells express *gfi1aa* in the vDA at 22-24 hpf the observed reduction in the *lyl1* $^{qmc801/qmc801}$ embryo may be due to embryos being slightly younger. Hence, it is necessary to validate the *gfi1aa* expression at an earlier (5-10ss) and later (26 hpf) developmental stage.

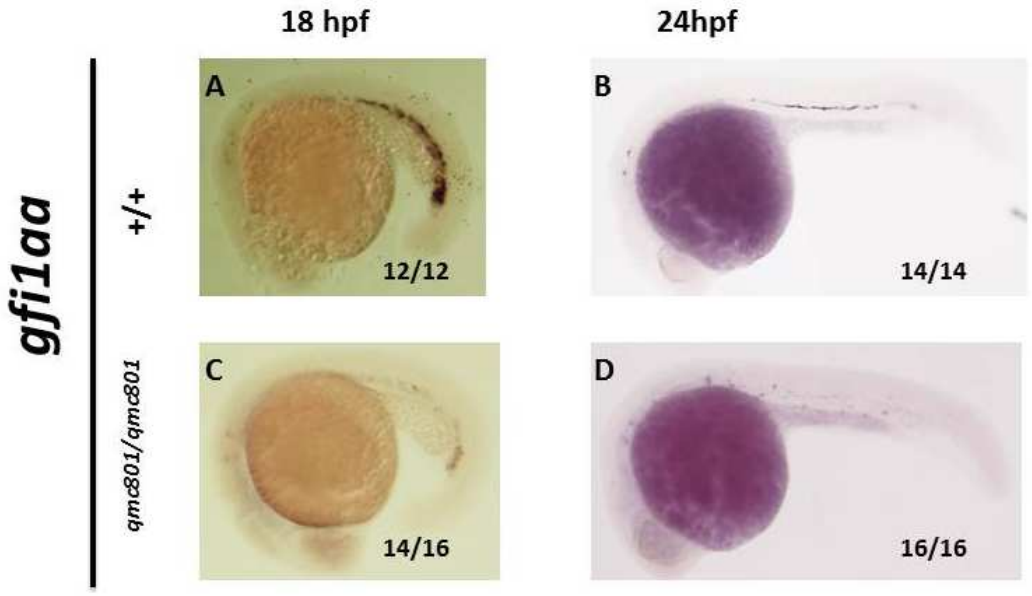

Figure 4.9 Disruption of lyl1 markedly reduces *gfi1aa* expression. Expression of *gfi1aa* in wild type (A, B) and *lyl1*$^{qmc801/qmc801}$ (C, D) embryos in the ICM (arrows) at 18 hpf (A, C) and in the ventral wall (arrows) at 24 hpf (B, D). A-D: lateral view.

4.10 Lyl1 is required for definitive haematopoiesis and lymphopoiesis

Studies using *lyl1* mutant mice showed that Lyl1 is not required for development of HSCs but essential for long-term repopulation ability of the HSCs. In addition, mutant mice displayed a reduction in the number of B cells (Capron *et al.*, 2006).

As shown in Figure 4.11, loss of Lyl1 function resulted in reduction in *c-myb* expression at 2 dpf in the caudal haematopoietic tissue that is formed from the PBI. It seems therefore that in zebrafish Lyl1 contributes to the formation and/or maintenance of definitive HSCs.

Although identified at chromosomal translocation sites in T cell acute lymphoblastic leukemia, *lyl1* is not expressed in mature T cells (Capron *et al.*, 2006). Lymphoid differentiation in zebrafish occurs from 4 dpf in the thymus. From 3 dpf HSCs/lymphoid progenitors from the CHT start to seed the thymus and expression of lymphoid markers are apparent from 4 dpf. *lyl1* $^{qmc801/qmc801}$ mutant embryos displayed a reduced expression of *rag1* in the thymus at 5 dpf (Figure 4.12). Given that expression of two HSC markers Gfi1aa and *c-myb* was reduced in the absence of Lyl1, it seems likely that lymphopoiesis and/or colonisation of the thymus by HSCs/lymphoid progenitors is impaired resulting in reduced lymphocytes.

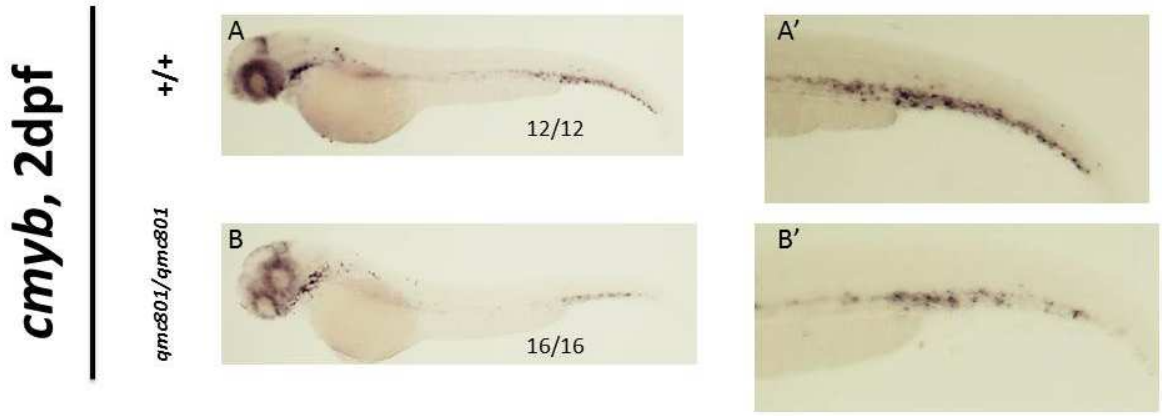

Figure 4.10 Reduction of definitive HSC in the *lyl1*$^{qmc801/qmc801}$ mutant (A) Expression of *c-myb* in the wild type embryos at 2dpf. **(A')** Expression in the CHT is highlighted **(B)** Loss of lyl1 resulted in the reduction of *c-myb* positive cells and CHT of the mutant embryo is highlighted in **B'.** (A, A', B and B'- Lateral view)

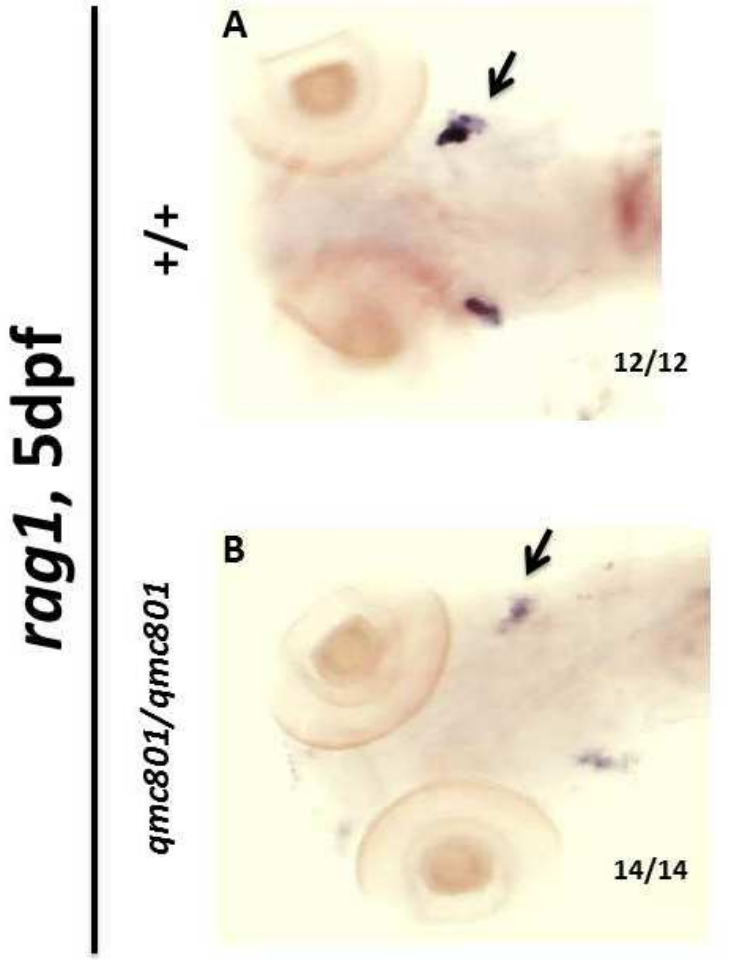

Figure 4.11 Lyl1 is required for lymphoid cell maintenance in the thymus (A) Expression of *rag1* thymus of wild type embryos at 5dpf. **(B)** Reduced expression of *rag1* in the thymus of *lyl1*$^{qmc801/qmc801}$ embryos at 5dpf**.** (A, A', B and B'- Lateral view)

4.11 Adult *lyl1*$^{qmc801/qmc801}$ mutant fish exhibit a reduced lymphopoiesis and increased myelopoiesis

By day 4 of zebrafish development HSCs in the CHT seed the kidney that serves as primary site of adult haematopoiesis producing all major blood cells. To determine whether lack of Lyl1 impaired adult haematopoiesis, kidneys from 8 month old wild type and *lyl1* $^{qmc801/qmc801}$ fish were isolated and whole kidney marrow cells analysed using flow cytometry. Forward and side scatter are sufficient to separate the kidney marrow cells into four different cell populations that have been identified as erythroid cells, myelomonocytes, lymphocytes and immature precursor cells (Traver *et al.*, 2003). As shown in Figure 4.13 (Appendix II), *lyl1*$^{qmc801/qmc801}$ fish exhibited a strikingly different flow cytometry profile compared to wild type fish. The myelomonocyte population that include neutrophils, granulocyte and monocytes was increased from 3.25% (±0.3%) in the wild type to 10% (±2.82%) in the *lyl1*$^{qmc801/qmc801}$ fish. Conversely, the lymphocyte population was decreased from 10% (±1.4%) in the wild type to 2.75 % (±1.06%) in mutant fish. In contrast, the erythrocyte population didn't show a marked difference (51% vs 49.5%) and the immature precursor cell population was only slightly reduced (3.65% (±0.2%) vs 2% (±1.4%)) in *lyl1*$^{qmc801/qmc801}$ (Figure 4.13 and Appendix II).

Taken together these results confirm and extend the data obtained from *lyl1* knockout mice demonstrating the functional role of Lyl1 in adult haematopoiesis suppressing myelopoiesis and driving lymphopoiesis.

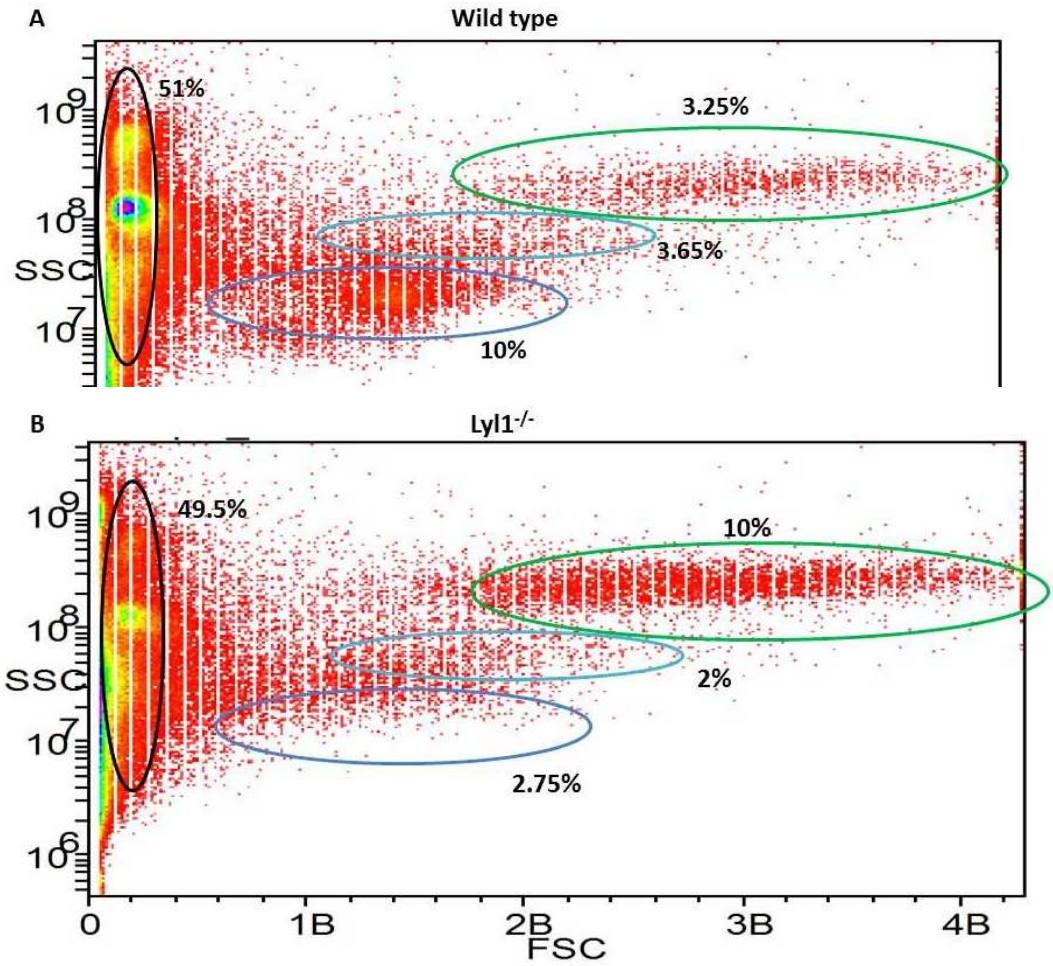

Figure 4.12 Separation of whole kidney marrow cells revealed the loss of lymphocyte and rise in myelomonocytes. FACS sorted whole kidney marrow cells from adult wild type (A) and lyl1 mutant (B) fish. SSC-Side scatter, FSC- Forward scatter. Myelomonocytes are highlighted in green, erythroid cells in black, blue denotes lymphocytes and immature precursor cells shown in light blue.

4.12 Summary

- Ectopic expression of *lyl1* enhanced primitive red blood cells production and suppressed the myeloid differentiation. The enhanced expression of marker genes suggests that these embryos produced an increase in primitive red blood cells.
- *lyl1*$^{qmc801/qmc801}$ embryos developed normally but displayed distinct marker gene expression during primitive and definitive haematopoiesis establishing a role for lyl1 in both waves of haematopoiesis.

    Primitive wave: Expression of *scl/tal1* and *gata1* was unaltered suggesting normal primitive erythropoiesis. However increased expression of *pu.1* indicates that Lyl1 antagonises myeloid differentiation.

    Reduction of *gfi1aa* expression in the *lyl1*$^{qmc801/qmc801}$ during primitive haematopoiesis (18 hpf) did not have any effect on primitive erythroid cells, which may be due to redundancy between Gfi1aa and Gfi1b.

    Definitive wave: Loss of Lyl1 resulted in reduction in the expression of *c-myb* (HSC) at 2dpf in the CHT and *rag1* (lymphocyte) at 5dpf in the thymus.

- In adult zebrafish Lyl1 regulates lineage choice driving lymphopoiesis and suppressing myelopoiesis

Chapter 5

5.1. Introduction

bHLH proteins have been shown to be crucial regulators of the development of the central nervous system. Id4 is a members of Id protein family that anatogonise bHLH protein function. Thus Id proteins in general drive cell proliferation and inhibit cell differentiation (Benezra *et al.,* 1990; Norton *et al.,* 2000). During mouse embryogenesis, Id4 is mainly expressed in the developing nervous system, but in the adult, Id4 expression is more widespread (Riechmann and Sablitzky, 1995; Riechmann *et al.,* 1993). Deletion of Id4 in the mouse resulted in impaired neurogenesis with significant reduction in neural stem cell proliferation and increased apoptosis (Yun et al., 2004; Bedford *et al.,* 2005). But it was later shown that loss of Id4 also resulted in impaired mammary cell development (Dong *et al.,* 2011) and premature differentiation of spermatogonial stem cells (Oatley *et al.,*2011). Furthermore, Id4 acts as a molecular switch promoting osteoblast differentiation (Tokuzawa *et al.,* 2010) and silencing of its expression contributes to the pathogenesis of mouse and human chronic lymphocytic leukaemia (CLL; Chen *et al.,* 2011).

5.2 Id4 expression in zebrafish embryos

Thisse *et al* (2001) showed that *id4* is also expressed in the developing central nervous system of zebrafish. However, this analysis did not cover early development and earlier RT-PCR had demonstrated that *id4* mRNA could be detected from 6 hpf onwards (Basir, 2010). Hence we cloned the full length zebrafish *id4* cDNA and used RNA probes (see Materials & Methods) for *in situ* hybridization to establish the expression pattern of Id4 at different developmental stages. *id4* expression was first observed throughout the embryo at 6hpf (Shield stage) (Figure 5.1 A). At 70% epiboly, *id4* expression was widespread including

the precordal plate (Figure 5.1 B). During somite stages (1-18) the expression of *id4* was noticed in multiple regions including the central nervous system and retina (Figure 5.1 C-E).At 24 and 48 hpf the expression of *id4* was again restricted to the developing nervous system; especially in various regions of the brain such as the midbrain, hindbrain, telencephalon, diencephalon, retina and tegmentum. These results indicate that *id4* is ubiquitously expressed in early stages (6 hpf) but its expression becomes restricted to the developing nervous system during later stages.

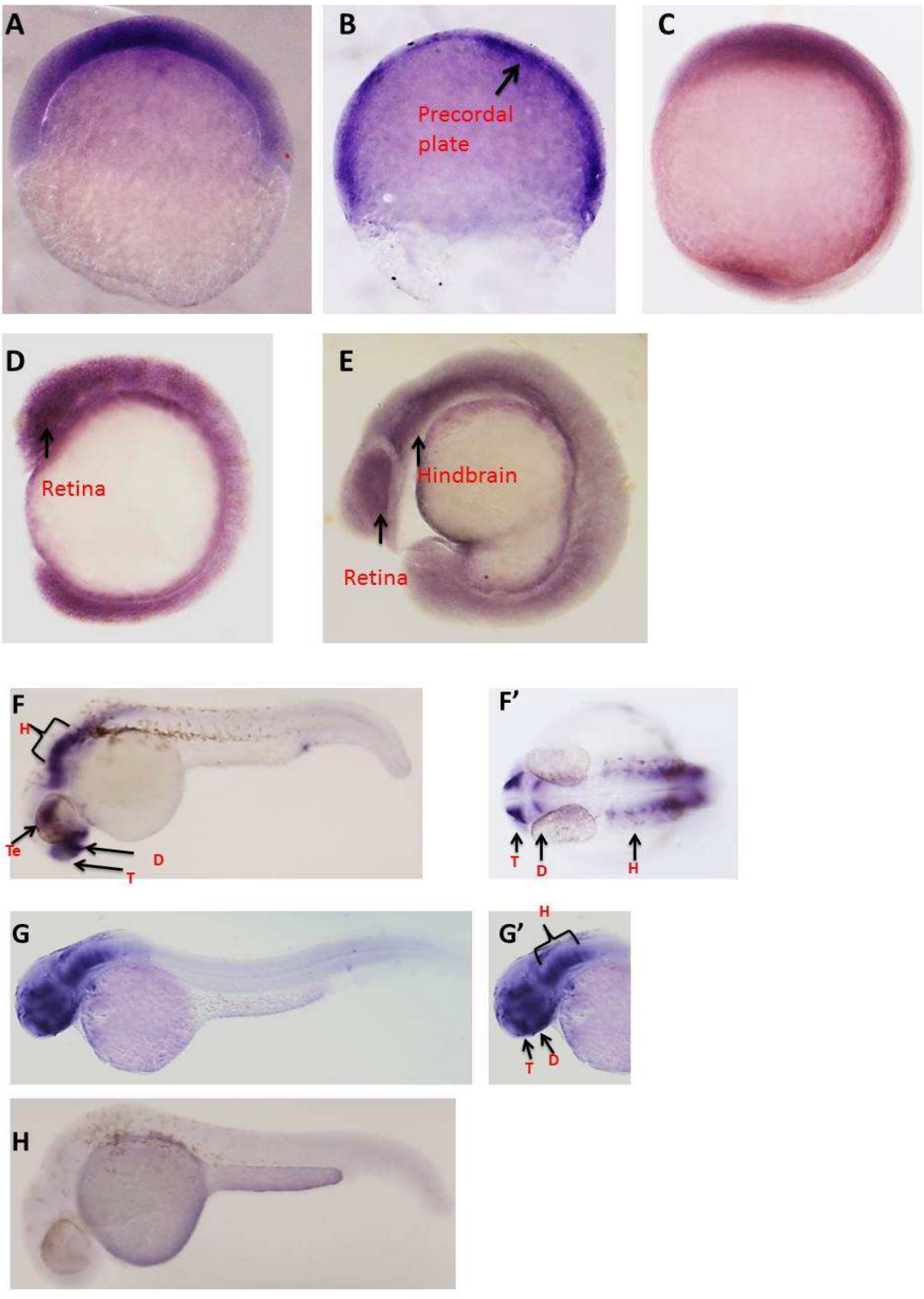
A
B
Precordal plate
C
D
Retina
E
Hindbrain
Retina
F
H
Te
D
T
F'
T
D
H
G
G'
H
T
D
H

Figure 5.1 *ID4* expression during zebrafish development.

Id4 is ubiquitously expressed during early stages of zebrafish development (A) Shield, (B) 70% epiboly. In later stages *id4* is expressed in the neural plate, Telencephalon (C) 2 somites (D) 5 somites (E) 18 somites stage and finally the expression is restricted to the developing nervous system (F, F'-Ventral view) 24 hpf (G, G'-Enlarged) 36 hpf. No expression was observed with the sense probe (H). T: Telencephalon; H: Hindbrain; D: Diencephalon; Te: Tegmentum (A-G Lateral View)

5.3 Id4 expression is regulated via notch signalling

Notch signalling pathway controls cell fate in many developmental processes and genome-wide transcriptome analysis of Notch-1 induced genes in murine embryonic stem cells have reported that activated Notch1 has upregulated *id1, id3* and *id4,* while *id2* is downregulated (Meier-Stiegen *et al.*,2010； Li *et al.,* 2012). Zebrafish mind bomb mutants have a defective notch signalling pathway due to a mutation in the E3 ubiquitin ligase gene. Reduced notch signalling in the mind bomb mutants resulted in complex phenotypes including aberrant neurogenesis (Itoh *et al.,* 2003). Due to premature differentiation of neural stem cells, primary neurons were increased while secondary neurons were reduced (Jiang *et al.,* 1996; Itoh *et al.,* 2003). Despite the complex phenotype, aberrant neurogenesis in mind bomb resembled somewhat the phenotype of Id4 knockout mice, as both displayed precocious neuronal differentiation (Yun *et al.,* 2004; Bedford *et al.,* 2005) which prompted us to test whether Id4 expression is regulated via notch signalling. Wild type embryos were treated with N-[N-3,5-difluorophenacetyl]-L-alanyl-S-phenylglycine methyl ester (DAPM), a well known inhibitor of notch signalling (de Strooper and Annaert, 2010), and Id4 expression was analysed by *in situ* hybridization. As shown in Figure 5.2, expression of *id4* appeared elevated in DAPM treated embryos at 25 hpf suggesting that notch signalling inhibits *id4* expression in zebrafish rather than driving it. In line with this observation are previous results showing that ectopic expression of *id4* in Su(H) morphants that exhibit a defective notch signalling (Sieger *et al.,* 2003) could not rescue the Su(H) morphant phenotype (premature neuronal differentiation) but in contrast enhanced it (Ganguly, 2013). Indeed it was shown that high level of ectopic overexpression of *id4* in wild type embryos also resulted in a severe neurogenic phenotype (Patlola, 2009; Bashir, 2010). In addition, mindbomb mutants and Su(H) morpholino treated embryos also displayed an eleaveted *id4* expression at 24hpf

(Figure 5.2 C, D)Together with the result above (Figure 1.5) that Id4 morphants exhibited a reduction in proliferative cells and an increase in cells undergoing apoptosis resulting in abnormal brain development (Dhanaseelan, 2011), these results strongly suggest that a tightly controlled expression of Id4 in time and space is essential for normal neurogenesis in zebrafish.

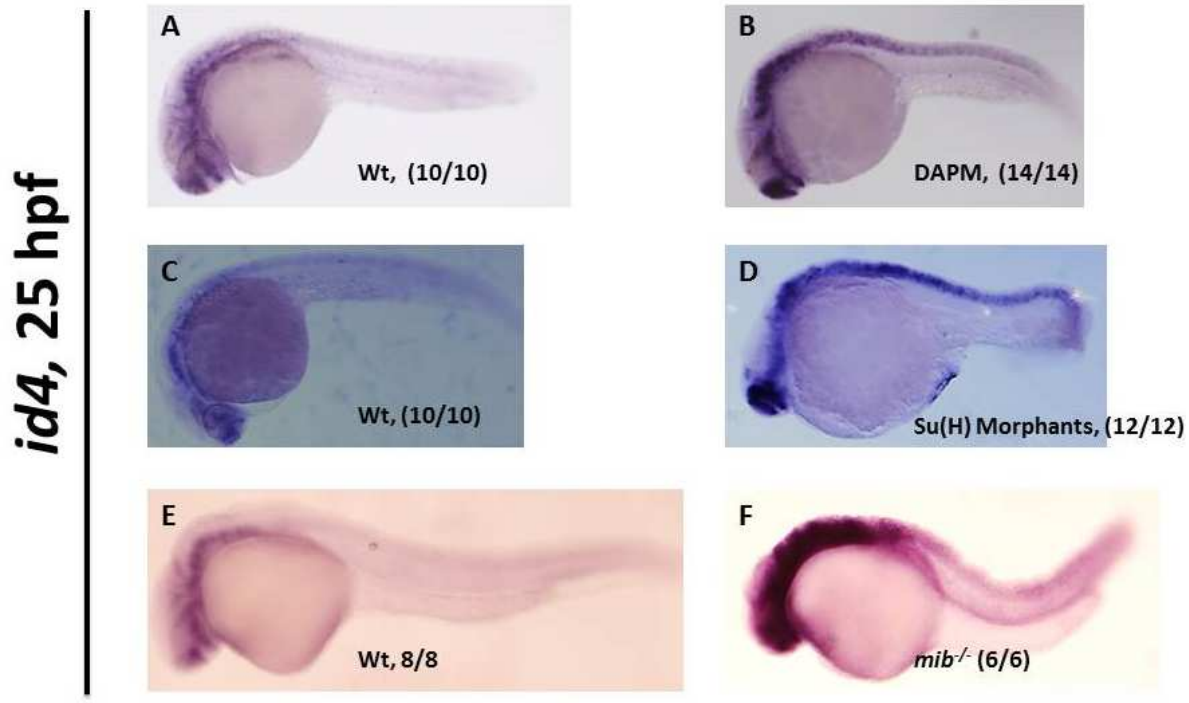

Figure 5.2 Id4 expression level is elevated in the absence of notch. Expression of *id4* in (A, C, E) Wild type embryo (B) DAPM-treated embryos (D) Su(H) morphants and (E) Mindbomb1 mutnats at 25 hpf . DAPM selectively blocks Notch activity resulting in an increased of Id4 expression. (A-F lateral view)

5.4 Id4 promotes neural progenitor proliferation and survival by suppressing p38 MAPK activity

We had earlier shown that morpholino-mediated knockdown of Id4 in zebrafish impaired neurogenesis. Id4 morphants exhibited a reduction in proliferative cells and an increase in cells undergoing apoptosis resulting in abnormal brain development (Figure 1.5; Dhanaseelan, 2011). To ensure that the observed phenotype was specific and not due to an artifical upregulation of the p53 pathway (Robb *et al.,* 2007), p53 morpholinos were co-injected with Id4 morpholinos. Indeed, the phenotypic effect in double morphants was less severe but significant decrease of cell proliferation and increase of apoptosis was still observed (Figure 1.5; Dhanaseelan, 2011). To further elucidate the downstream targets of Id4, we asked whether the observed phenotype in Id4 and Id4/p53 morphants was due to activation of p38MAPK function. p38MAPK is known to inhibit cell proliferation and promote apoptosis during development (Molnar *et al.,* 1997; Sarkar *et al.*, 2002). p38MAPK activation leads to cell cycle arrest by inhibiting cyclin D (Molnar *et al.,* 1997; Galibert *et al.,* 2001) and it was shown that Id4 regulates mammary gland development by surpressing p38MAPK activity (Dong *et al.,* 2011).

Hence to analyse whether the phenotypes observed in the Id4 and Id4/p53 morphants are indeed mediated through p38MAPK function, SB239063, a chemical specifically inhibiting p38MAPK, was used. Once the morphants and wild type control embryos reached 75% epiboly (8 hpf), the E3 medium/fish water was replaced with water containing 15 µM SB239063 and the embryos were allowed to develop further until they reached the 2 somites stage. Analysis using antibodies recognising pHH3, a marker for cells undergoing mitosis, revealed that wild type embryos treated with inhibitor had an average of 282 (±9) positive cells for pHH3.

The average number of proliferative cells in Id4 morphants treated with the inhibitor was 225 (±17) which is 20% less when compared with the treated wild type embryos ($p=7.6X10^{-8}$). Id4/p53 morphants treated with the p38MAPK inhibitor exhibited an even higher number of proliferative cells (272±13) that was similar to the treated wild type embryos (Figure 5.3).

Compared to the results established previously (Figure 1.5), both Id4 and Id4/p53 normal cell proliferation was rescued. While Id4 morphants showed a 50% reduction in proliferating cells compared to wild type, Id4 morphants treated with SB239063 exhibited a 20% reduction indicating a partial rescue. Id4/p53 morphants showed about 30% reduction of proliferating cells compared to wild type and inhibition of p38MAPK almost completely rescued this phenotype (Figure 1.5, Figure 5.3 D/E).

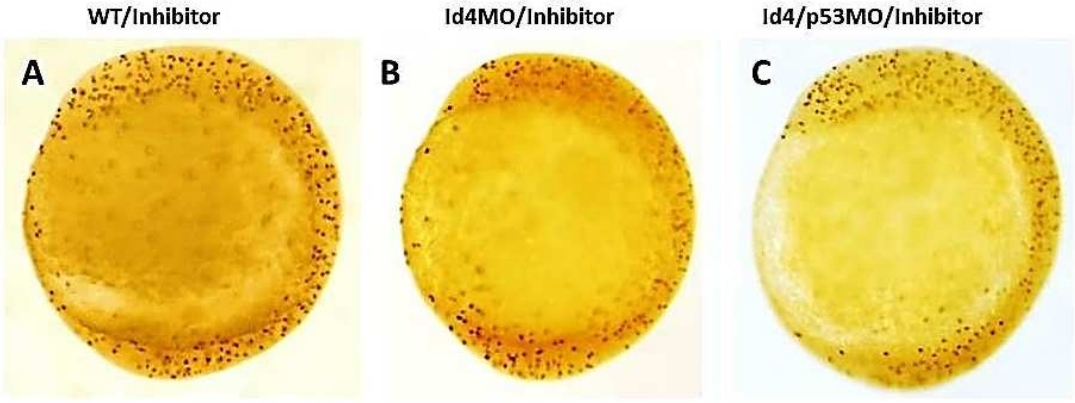
WT/Inhibitor
Id4MO/Inhibitor
Id4/p53MO/Inhibitor
A
B
C

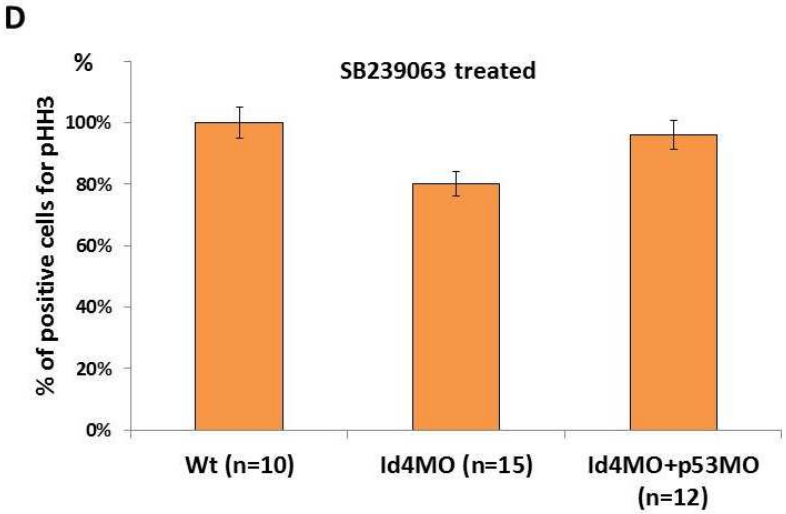
D
%
SB239063 treated
% of positive cells for pHH3
100%
80%
60%
40%
20%
0%
Wt (n=10)
Id4MO (n=15)
Id4MO+p53MO (n=12)

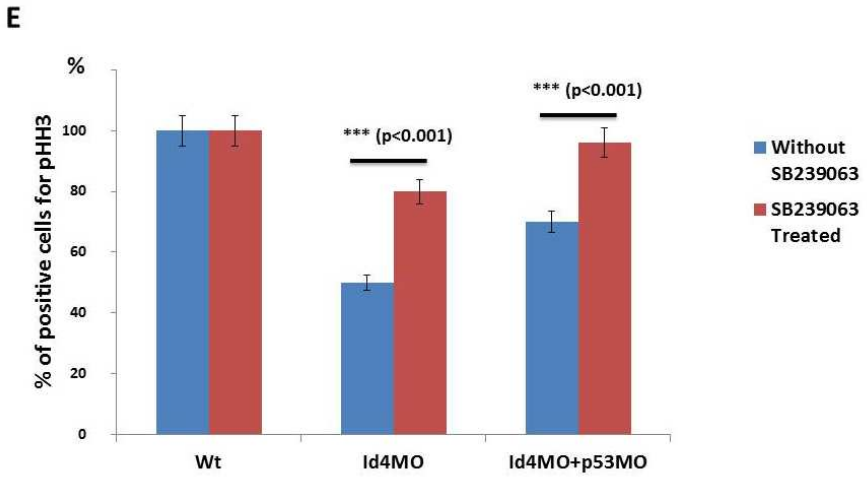
E
%
% of positive cells for pHH3
100
80
60
40
20
0
*** (p<0.001)
*** (p<0.001)
Wt
Id4MO
Id4MO+p53MO
Without SB239063
SB239063 Treated

Figure 5.3 Cell proliferation defects observed in Id4 and Id4/p53 morphants was partially rescued through inhibition of p38MAPK. Whole-mount pHH3 immunostaining on zebrafish embryos treated with SB239063 at 2 somites stage **(A)** wild type **(B)** Id4 morphants **(C)** Id4/p53 morphants. **(D)** Quantification of pHH3 positive cells from embryos treated with inhibitor. Average number of positive cells for pHH3 was determined for wild type, Id4 and Id4/p53 morphants and the ratio in percentage was calculated. **(E)** Comparison of cell proliferation between wild type, Id4 and Id4/p53 morphant embryos either untreated (taken from Figure 1.5) or treated with p38MAPK inhibitor A-D: Lateral view.

In addition to its role in cell proliferation and differentiation, p38MAPK also promotes cell death (Sarkar *et al.*, 2002). Both Id4 and Id4/p53 morphant embryos displayed an increase in apoptotic cells compare to the wild type (Figure 1.5; Dhanaseelan, 2011). Hence TUNEL staining was carried out on embryos grown in the presence of the p38MAPK inhibitor. In wild type embryos only a few apoptotic cells could be detected (21±12) and Id4 morphants treated with SB239063 still exhibited a much higher level of apoptosic cells (125±32) significantly different from wild type ($p=2.1X10^{-8}$) (Figure 5.4). However, compared to the number of apoptotic cells in untreated Id4 morphants (180±16) the number of apopotics cells in treated Id4 morphants (125±32) was significantly reduced ($p=1.041X10^{-5}$). Inhibition of p38MAPK in Id4/p53 morphants resulted in few apoptotic cells (28±15) similar to treated wild type embryos (Figure 5.4). In contrast, Id4/p53 morphant that had not been treated with the inhibitor displayed 8 times more apoptotic cells compared to the wild type ($p=3.9X10^{-13}$) again indicating that inhibition of p38MAPK resulted in a complete rescue of the Id4/p53 morphant phenotype.

Taken together, these experiments strongly suggest that the phenotype observed in Id4 morphants is indeed due to aberrant activation of p38MAPK and that the severity of the phenotype was enhanced by the accompanied up regulation of p53.

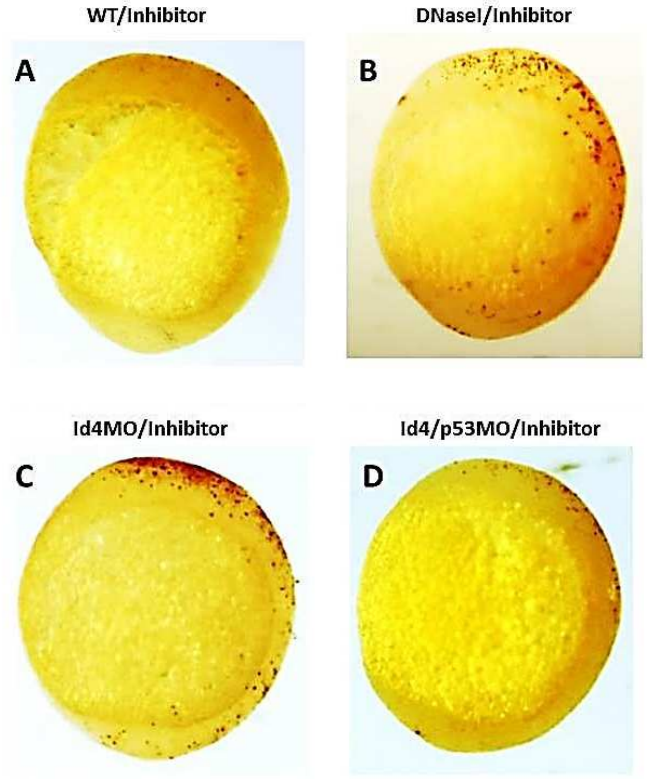
WT/Inhibitor
DNaseI/Inhibitor
A
B
Id4MO/Inhibitor
Id4/p53MO/Inhibitor
C
D

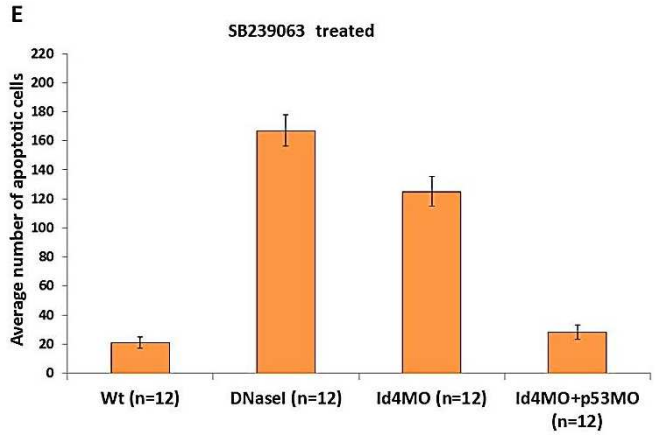
E
SB239063 treated
Average number of apoptotic cells
220
200
180
160
140
120
100
80
60
40
20
0
Wt (n=12)
DNaseI (n=12)
Id4MO (n=12)
Id4MO+p53MO (n=12)

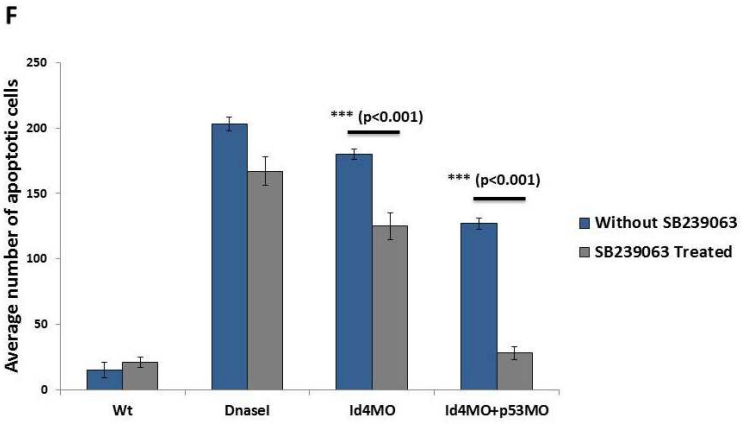
F
Average number of apoptotic cells
250
200
150
100
50
0
*** (p<0.001)
*** (p<0.001)
Without SB239063
SB239063 Treated
Wt
Dnasel
Id4MO
Id4MO+p53MO

Figure 5.4 Increased apoptosis observed in the Id4/p53 morphants are p38 MAPK mediated. Whole-mount TUNEL on zebrafish embryos injected with embryos with morpholinos at 2-4 cell stage, treated with SB239063 at 75% epiboly and staining was performed at 2 somites stage **(A)** wild type **(B)** DNaseI treated **(C)** Id4 morphants **(D)** Id4/p53 morphants. **(E)** Quantification of the number of apoptotic cells in wild type and morphant embryos treated with SB239063. Average number of TUNEL positive cells was calculated for wild type, Id4 morphants and Id4/p53 morphants. **(F)** Comparison of apoptotic cell death between wild type, Id4 and Id4/p53 morphant embryos either untreated (taken from Figure 1.5) or treated with p38MAPK inhibitor A-D: Lateral view.

5.5 *id4*$^{qmc803/qmc803}$ embryos displayed normal morphology

It was recently demonstrated that phenotypes observed in morpholino-mediated knockdown experiments could often (but not always) not been reproduced in mutant knockout fish (Kok *et al.*, 2015). To see whether the phenotype observed in Id4 morphants described above was specific, TALEN-mediated mutagenesis was employed to establish Id4 mutant zebrafish. TALEN pairs targeting the Id4 gene created a mutation that is predicted to produce a truncated Id4 protein lacking the HLH domain (Figure 3.7 C, D). In contrast to Id4 morphants, *id4*$^{qmc803/qmc803}$ embryos at 24 hpf were morphologically indistinguishable from wild type embryos (Figure 5.5 A, B). Especially brain boundaries that were severely affected in the morphants (Figure 1.4 E, F) looked normal in the mutant embryos. However, more detailed analysis shown in the next sections revealed that morpholino-mediated knockdown and TALEN-mediated knockout of Id4 resulted in a similar phenotype.

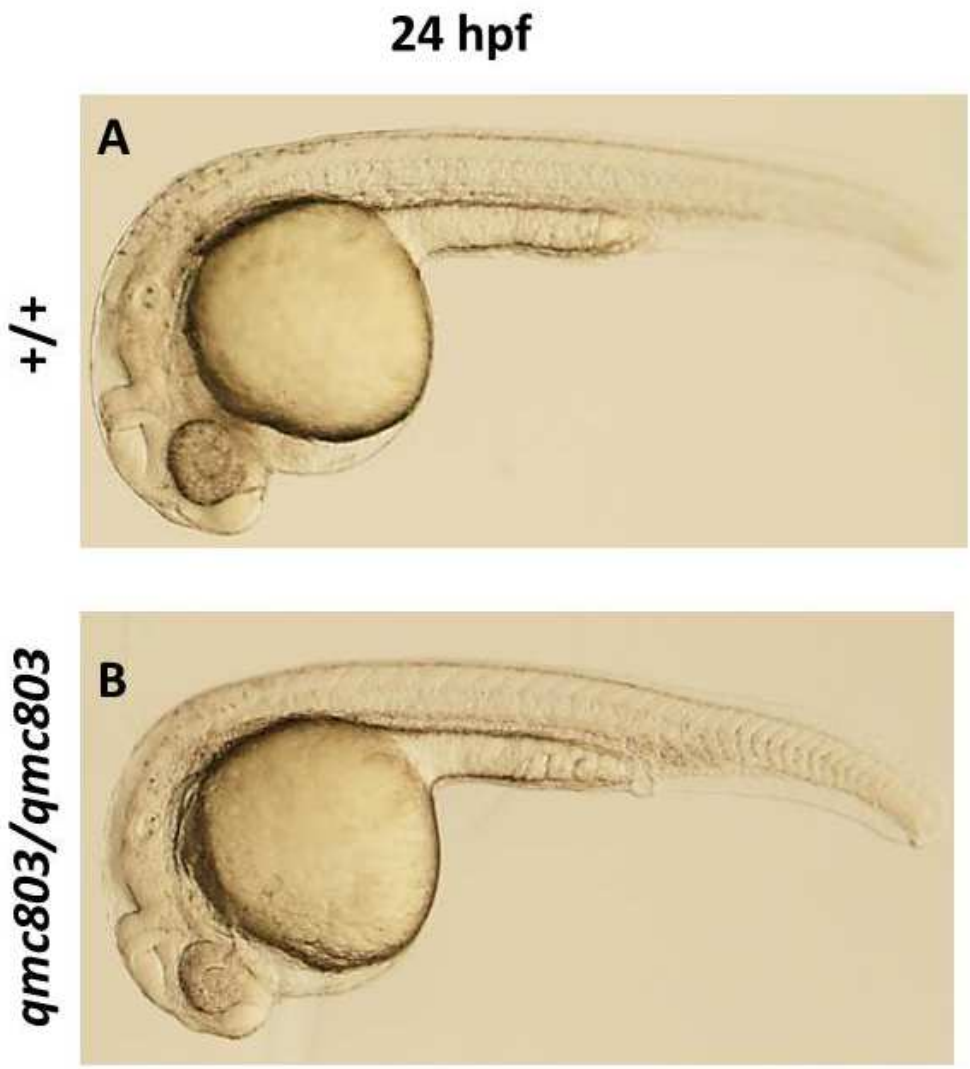

Figure 5.5 *id4*$^{qmc803/qmc803}$developed normally at 24 hpf. A. Later view of wild type embryo. **(B**) Embryos derived from *id4*$^{qmc803/qmc803}$fish did not show any phenotype.

5.6 Id4 knockout leads to premature neuronal differentiation

To determine whether the loss of Id4 had an effect on neurogenesis as it was described above, the expression pattern of neurogenin 1 (*ngn1*) and ELAV like neuron-specific RNA binding 3 (elavl3/*HuC*) was analysed in homozygous embryos and compared to wild type embryos.

Ngn1 is a pro neural bHLH protein, activating pan neuronal genes, driving differentiation of cortical progenitors into neurons. At 2-somite stage *ngn1* is expressed in the multiple regions of the developing central nervous system (CNS) including the proneural clusters which has a potential for a neural fate (Thisse *et al.,* 2001). Loss of Id4 had a marked effect on the expression pattern of *ngn1*. While the overall expression of *ngn1* at 2 somites stage was incomparable between the wild type and *id4*$^{qmc803/qmc803}$embryos, the pattern of expression seemed altered in the mutants and a slight increase in *ngn1* positive cells was observed in the pro neural clusters (Figure 5.6 A, A', B and B'). At 24 hpf the expression of *ngn1* was observed in telencephalon, diencephalon, hindbrain, tegmentum and spinal cord (Thisse *et al.,* 2001). At 24 hpf expression of ngn1 was clearly increased throughout the central nervous system (including telencephalon, midbrain, hindbrain and spinal cord) suggesting premature neurogenesis in *id4*$^{qmc803/qmc803}$ embryos (Figure 5.6 C, C', D and D').

To verify the above results, expression of *HuC/elavl3,* a marker for neuronal determination and differentiation, was also determined (Park *et al.,* 2000). *Huc* is also expressed along the proneural clusters at 2 somite stage and in the multiple regions of developing CNS like the telencephalon, diencephalon and hind brain at 18 hpf (Thisse *et al.,* 2001). Like in the case of *ngn1, HuC/elavl3* expression at 2 somite stage was similar in wild type and mutant embryos, perhaps with a small increase in the ventral pro neural clusters in the *id4*$^{qmc803/qmc803}$ (Figure 5.7 A, B). At 18 hpf, expression of *HuC/elavl3* in the telencephalon, ventral diencephalon, midbrain, and ventral hindbrain and in the spinal cord

regions was clearly increased in the *id4*$^{qmc803/qmc803}$embryos compared to the wild type embryos (Figure 5.7 C, D). Taken together, these results suggest that knockout of Id4 in zebrafish leads to premature neuronal differentiation.

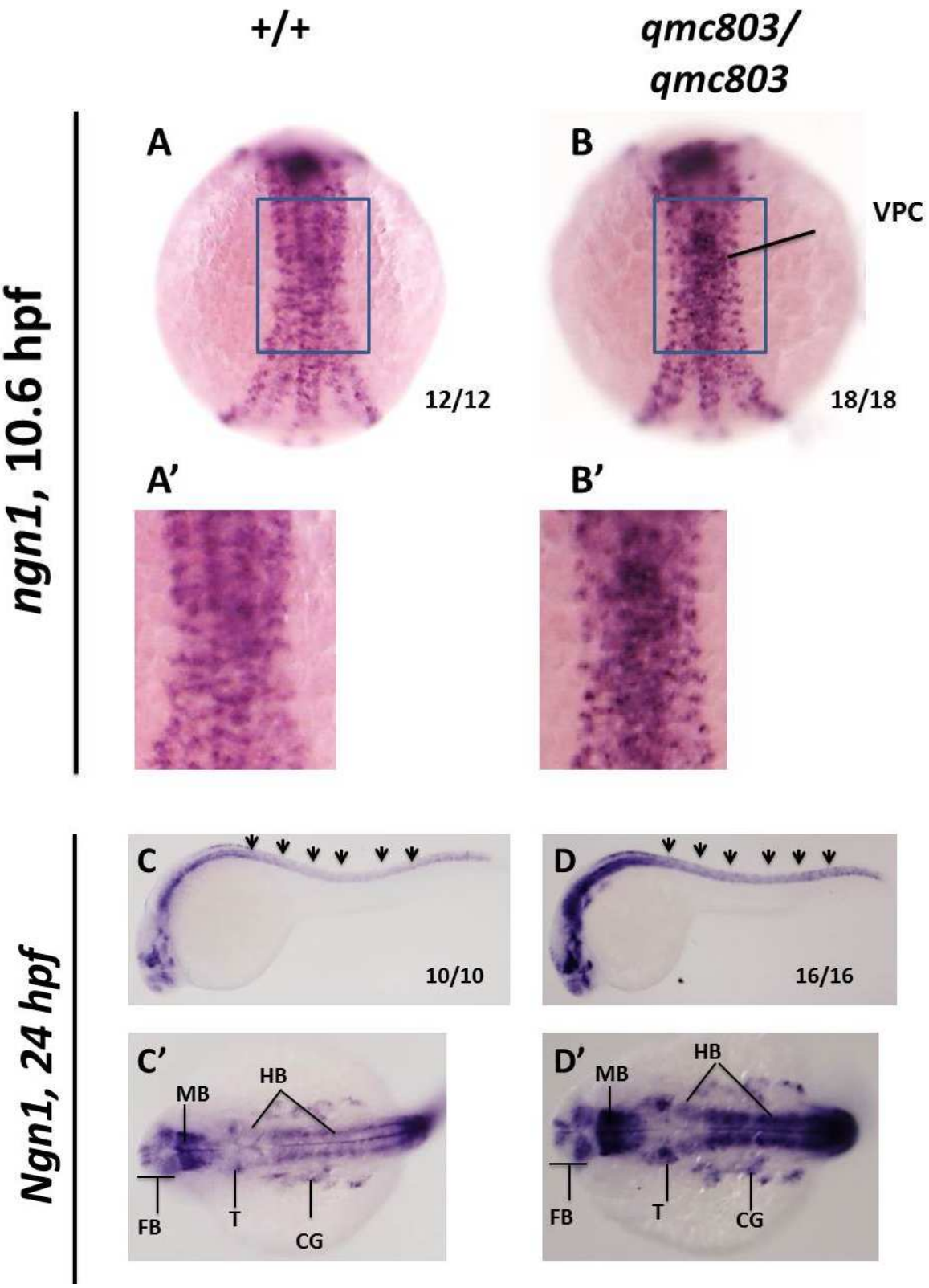
+/+
qmc803/
qmc803
ngn1, 10.6 hpf
A
B
VPC
12/12
18/18
A'
B'
Ngn1, 24 hpf
C
D
10/10
16/16
C'
D'
MB
HB
FB
T
CG

Figure 5.6 Expression of *ngn1* is elevated in *id4*$^{qmc803/qmc803}$mutants. (A-B) Ngn1 expression in wild type and *id4*$^{qmc803/qmc803}$ embryos at 2 somites stage. (**A'-B'**) Highlighted areas from A and B, respectively. **(C-D)** Elevated expression of neurogenin 1 in the developing central nervous system of *id4*$^{qmc803/qmc803}$ at 24 hpf. **(C'-D')** Dorsal view showing the expression of *ngn1* in different regions of the CNS in wild type and *id4*$^{qmc803/qmc803}$. VPC- ventral pro-neural clusters, FB- forebrain, HB- hindbrain, MB- midbrain, T-tectum, CG- cranial ganglia. Arrows indicate spinal cord. (A, A', B and B'- dorsal view; C, C', D and D'- ventral view)

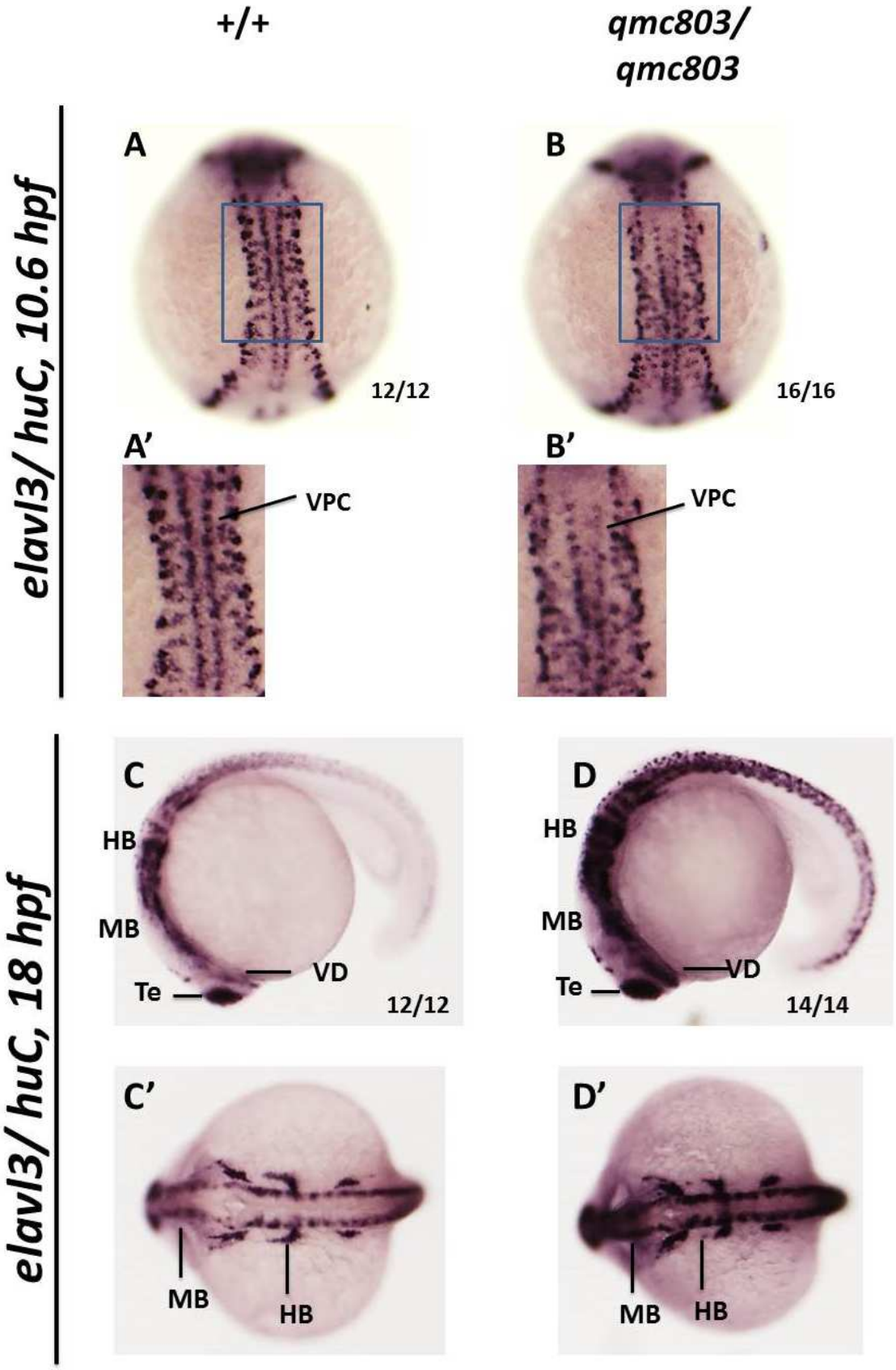
+/+
qmc803/
qmc803
elavl3/ huC, 10.6 hpf
A
12/12
B
16/16
A'
VPC
B'
VPC
elavl3/ huC, 18 hpf
C
HB
MB
Te
VD
12/12
D
HB
MB
Te
VD
14/14
C'
MB
HB
D'
MB
HB

Figure 5.7 Premature neuronal differentiation in the *id4*$^{qmc803/qmc803}$ embryos. (A-B) *HuC/elavl3* expression is similar in wild type and *id4*$^{qmc803/qmc803}$ at 2 somites stage. (**A'-B'**) Highlighted areas from A and B, respectively. **(C-D)** Elevated expression of *HuC/elavl3* in the *id4*$^{qmc803/qmc803}$ developing central nervous system at 24 hpf. **(C'-D')** *HuC/elavl3* expression in the dorsal CNS. VPC-ventral pro-neural clusters, FB- forebrain, HB- hindbrain, VD- ventral diencephalon, Te-telencephalon. (A, A', B and B'- dorsal view; C, C', D and D'- ventral view)

5.7 *id4*$^{qmc803/qmc803-}$ mutant embryos exhibit a decrease in cell proliferation and an increase in apoptosis

Knockout of Id4 in the mouse resulted in impaired neural stem cell proliferation and increased apoptosis (Yun et al., 20040; Bedford *et al.,* 2005) and Id4 morphants also exhibited reduced cell proliferation and increased apoptosis resulting in aberrant neurogenesis (Figure 1.5; Dhanaseelan, 2011).

To analyse whether zebrafish Id4 mutants had a defect in cell proliferation, whole mount pHH3 immuno-staining was performed on mutant and control wild type embryos at 2 somites stage. Phosphorylated histone H3 specifically marks the cells that are undergoing mitosis. Wild type embryos showed positive cells for pHH3 throughout (Figure 5.8A, A'), and on an average contained 370 (±11) proliferating cells. Similarly, *id4*$^{qmc803/qmc803}$ embryos exhibited proliferating cells but the number was reduced to 280 (±17) cells; a reduction of 24% compared to wild type ($p=2.1 \times 10^{-9}$) (Figure 5.8).

To test whether Id4 knockout in zebrafish also exhibited increased apoptosis, TUNEL assay was performed as before on 2 somites stage embryos comparing wild type and *id4*$^{qmc803/qmc803}$ mutants. As shown in Figure 5.9, control wild type embryos displayed on average of about 66 (±8) apoptotic cells but the number of apoptotic cells in the *id4*$^{qmc803/qmc803}$ embryos was increased up to 2.3 fold (average of about (158±10) ($p=3.9 \times 10^{-20}$)) again indicating that Id4 mutants display a similar (albeit not identical) phenotype to Id4 morphants.

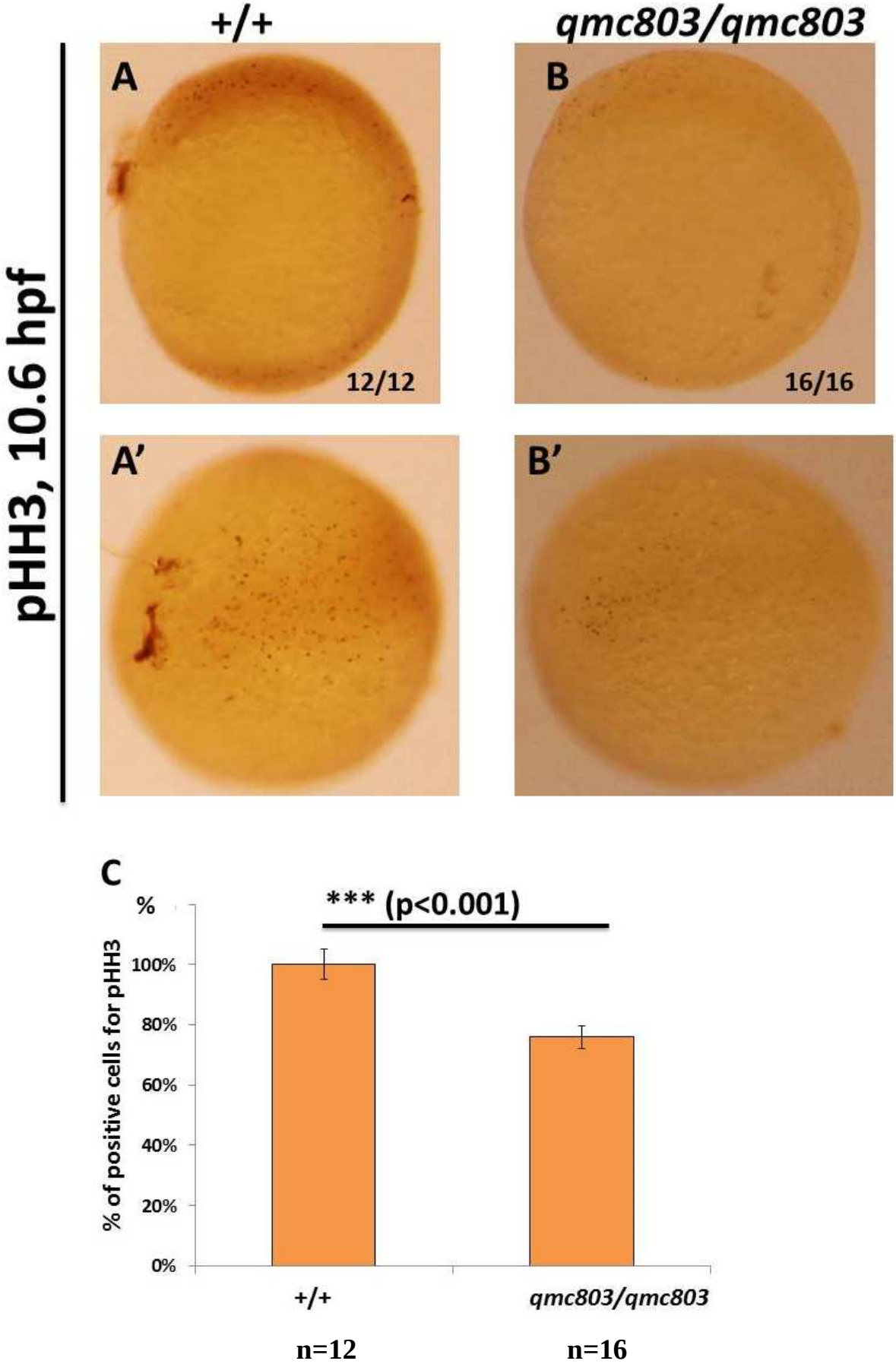
+/+
qmc803/qmc803
pHH3, 10.6 hpf
A
12/12
B
16/16
A'
B'
C
*** (p<0.001)
% of positive cells for pHH3
%
100%
80%
60%
40%
20%
0%
+/+
qmc803/qmc803
n=12
n=16

Figure 5.8: Id4 mutants displayed a reduction in the number of dividing cells. (A) Wild type embryos at 2 somites stage had positive cell throughout the embryo. **(A')** Dorsal view of the developing CNS showing the proliferating cells. **(B)** *id4*$^{qmc803/qmc803}$ embryos also had positive cells in the embryo and in the CNS **(B')**, but had fewer cells compared to the wild type. (**C)** Quantification of the positive cells for pHH3. Average number of positive cells for pHH3 was calculated for wild type and Id4 mutants. Percentage is the ratio of mutant to wild type. (A,B- Lateral view; A', B'- Dorsal view)

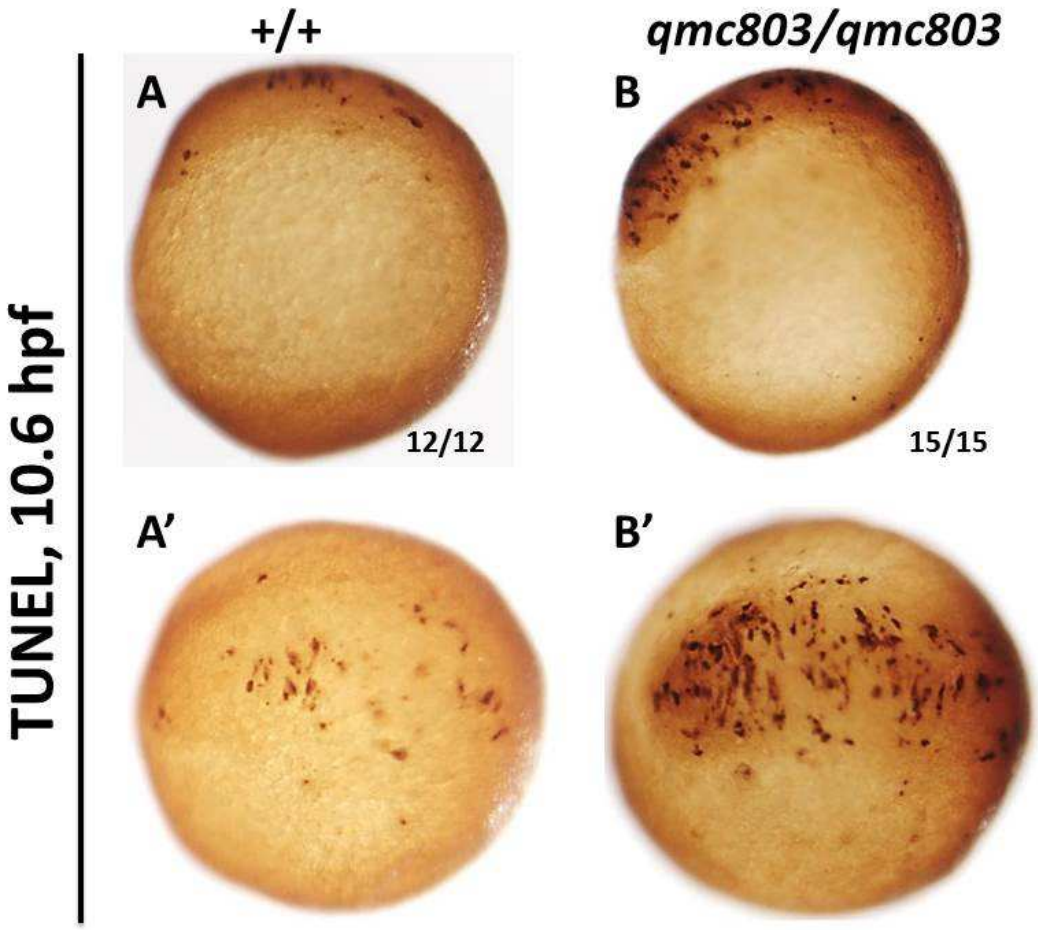
+/+
qmc803/qmc803
TUNEL, 10.6 hpf
A
B
12/12
15/15
A'
B'

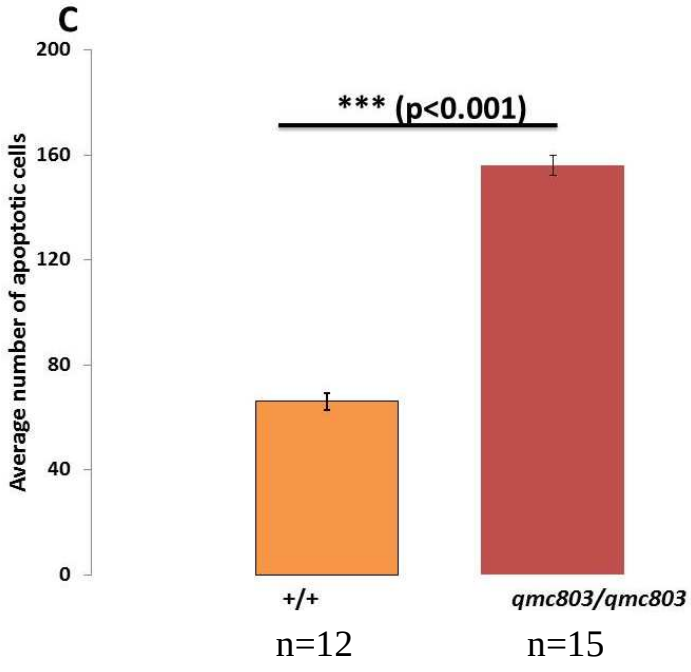
C
200
160
120
80
40
0
Average number of apoptotic cells
*** (p<0.001)
+/+
qmc803/qmc803
n=12
n=15

Figure 5.9 Id4 loss resulted in enhanced apoptosis in the developing brain. TUNEL assay in wild type **(A, A')** and *id4*$^{qmc803/qmc803}$ **(B, B')** embryos at 2 somite stage. (C) Quantification of the apoptotic cells. Average number of TUNEL positive cells was calculated for wild type (66±8) and Id4 mutants (158±10). Two-tailed Student's t-tests showed a significant ($p<0.001$; three asterisks) increase in the number of apoptotic cells in the mutants (A, B - Lateral view; A', B'- Dorsal view).

5.8 Impaired cell proliferation in the Id4 mutant embryos is mediated through elevated p38 MAPK activity

As shown above**,** inhibition of p38MAPK was sufficient to partially rescue Id4 morphants. To confirm the latter findings, p38MAPK activity was suppressed in the Id4 null embryos using 15 µM SB239063.

Both wild type and *id4*$^{qmc803/qmc803}$ embryos were treated with 15µM SB239063 at 75% epiboly, the embryos were raised until they reach 2 somites stage and pHH3/ TUNEL immuno staining was performed (Figure 5.10). The average number of mitotically active cells in the inhibitor treated *id4*$^{qmc803/qmc803}$ embryos was 397 (±24; n=17) which was similar to the wild type (400 (±25, n=17)) but significantly different from the untreated Id4 mutant embryos ($p=6.7 \times 10^{-13}$) that exhibited a 24% reduction in the number of proliferating cells compared to wild type (Figure 5.8; Figure 5.10 D). There was a significant reduction in the number of apoptotic cells in the *id4*$^{qmc803/qmc803}$ when p38MAPK is inhibited via chemical inhibitors. Average number of apoptotic cells in the inhibitor treated *id4*$^{qmc803/qmc803}$ embryos was 66 ((±14; n=17). This apoptosis r6ate is similar to the wild type embryos (60 ((±12; n=10)).

Overall, the analysis of *id4*$^{qmc803/qmc803}$ embryos reciprocated the phenotypic analysis of Id4 morphants and together revealed the novel finding that Id4 negatively regulates p38MAPK activity to ensure sufficient cell proliferation and expansion of neural stem and progenitor cells and preventing premature differentiation and cell death.

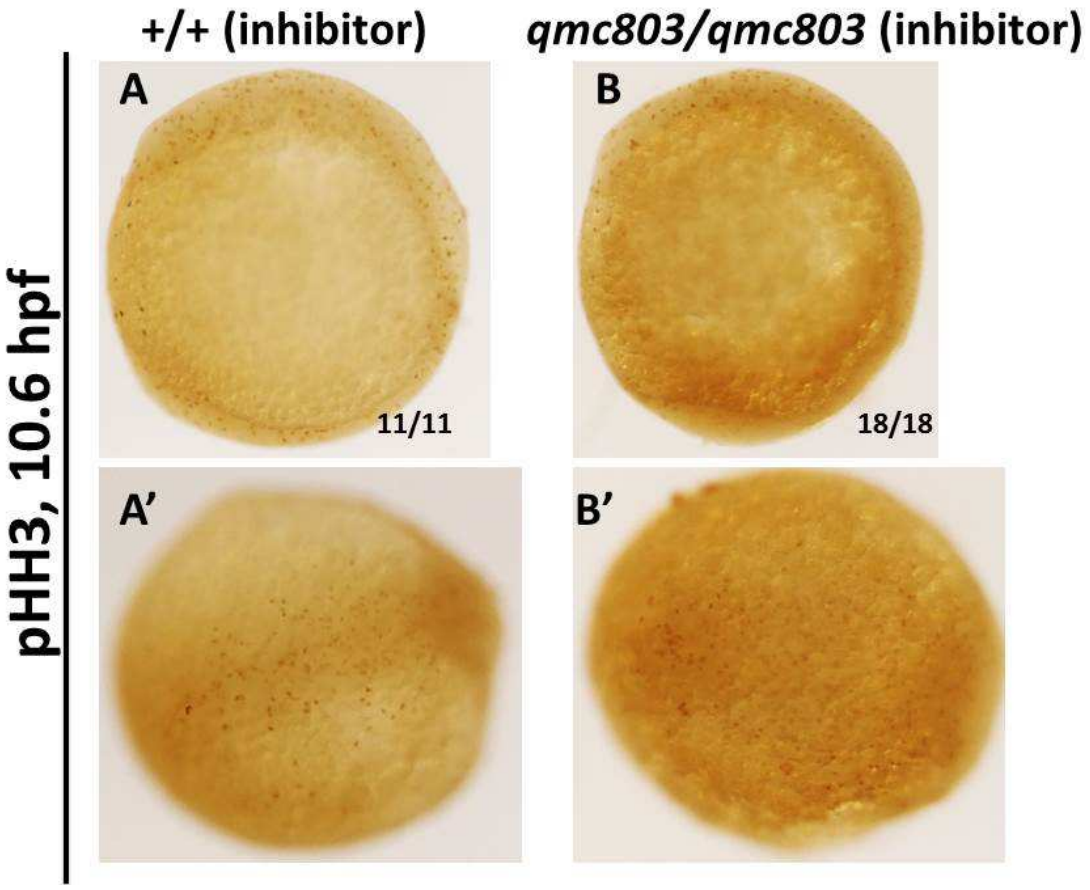
+/+ (inhibitor)
qmc803/qmc803 (inhibitor)
pHH3, 10.6 hpf
A
11/11
B
18/18
A'
B'

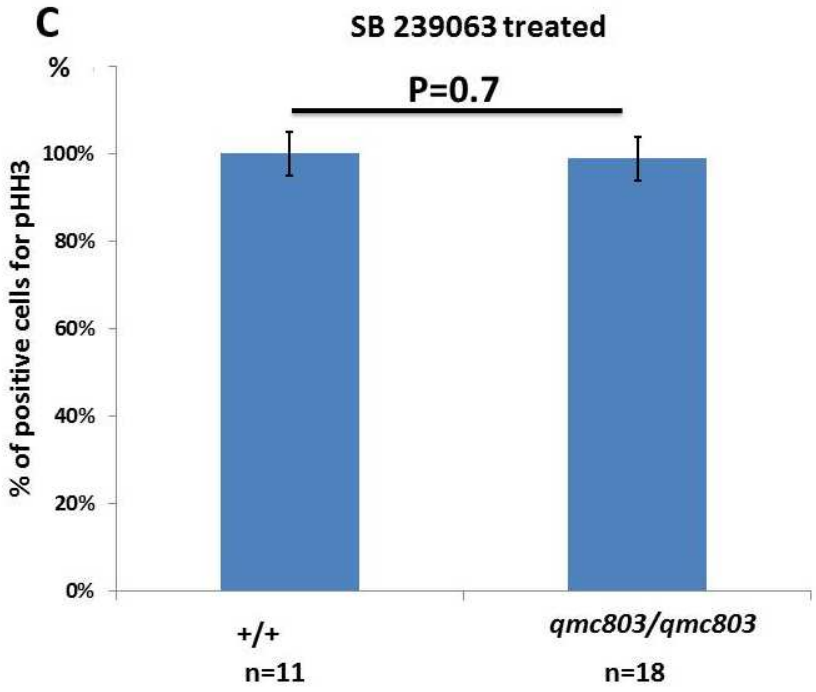
C
SB 239063 treated
P=0.7
%
100%
80%
60%
40%
20%
0%
% of positive cells for pHH3
+/+
n=11
qmc803/qmc803
n=18

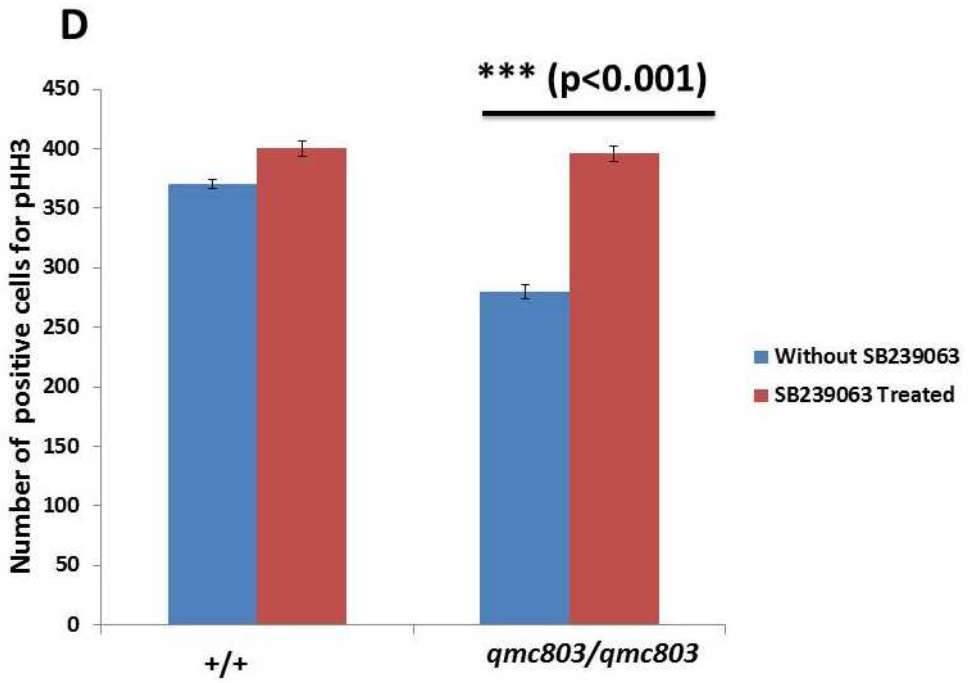

Figure 5.10 Inhibition of p38MAPK in Id4 mutants restores cell proliferation. (A) Wild type embryos treated with p38MAPK inhibitor exhibited proliferating cells throughout the embryo. **(A')** pHH3 positive cells in the developing nervous system. **(B-B')** Inhibition of p38MAPK in Id4 mutants rescues the proliferation defect, as pHH3 positive cells were observed throghtout the embryo including the developing brain. **(C)** Quantification of the $pHH3^{+}$ cells from embryos treated with inhibitor. Average number of positive cells for pHH3 was calculated for wild type and $id4^{qmc803/qmc803}$ embryos. Ratio (in persentage) of mutant to wild type is shown. **(D)** Comparison of cell proliferation between wild type and Id4 mutant embryos either untreated or treated with p38MAPK inhibitor (A,B- Lateral view; A', B'- Dorsal view)

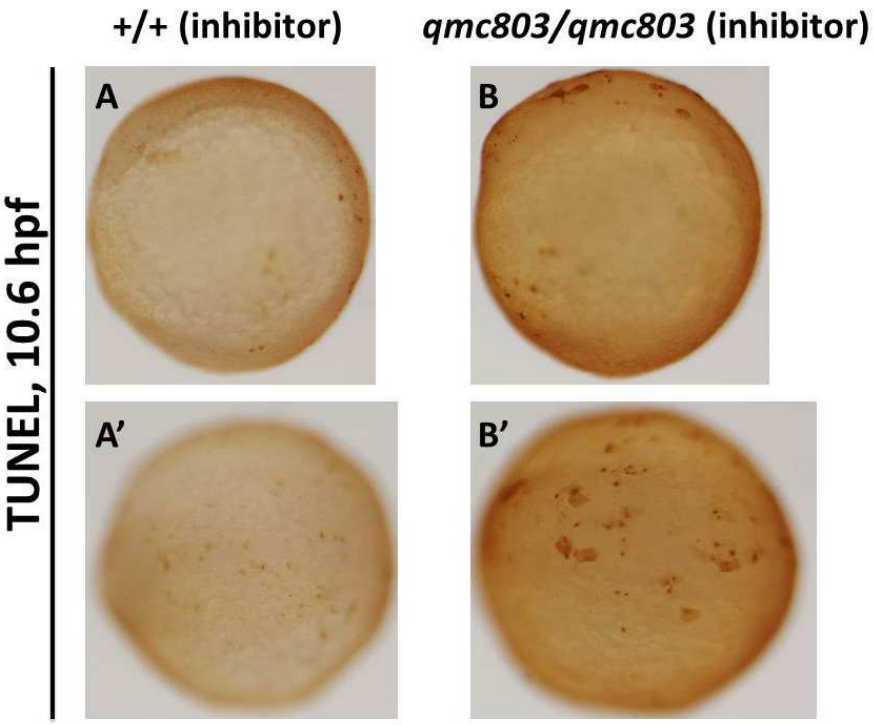
+/+ (inhibitor)
qmc803/qmc803 (inhibitor)
TUNEL, 10.6 hpf
A
B
A'
B'

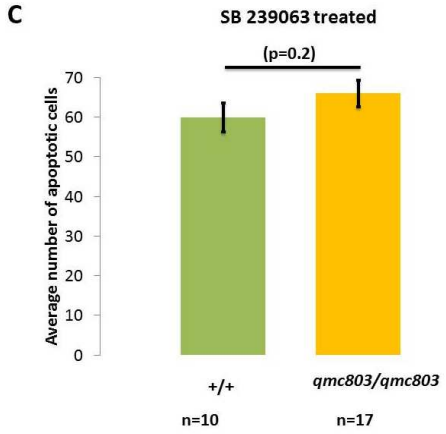
C
SB 239063 treated
(p=0.2)
Average number of apoptotic cells
70
60
50
40
30
20
10
0
+/+
qmc803/qmc803
n=10
n=17

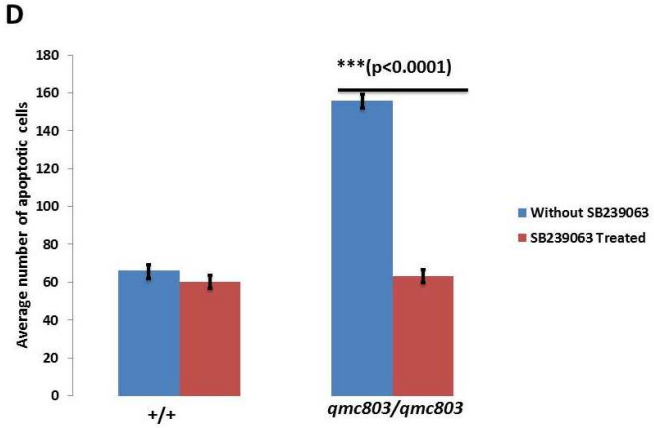
D
***(p<0.0001)
Average number of apoptotic cells
180
160
140
120
100
80
60
40
20
0
Without SB239063
SB239063 Treated
+/+
qmc803/qmc803

Figure 5.11 Inhibition of p38MAPK has rescued the survival defects in the *id4*$^{qmc803/qmc803}$ embryos. (A) Wild type embryo treated with SB239063 displayed a few TUNEL positive cells. **(A')** TUNEL positive cells in the developing nervous system **(B)** *id4*$^{qmc803/qmc803}$ embryos treated with inhibitor has very few apoptotic cells when compared to the *id4*$^{qmc803/qmc803}$ embryos when p38MAPK was not inhibited. **(B')** TUNEL positive cells in the developing nervous system**. (C)** Quantification of TUNEL positive cells. Average number of apoptotic cells was calculated for wild type and the *qmc803/qmc803*. **(D)** Comparison of apoptosis between wild type and *id4*$^{qmc803/qmc803}$ embryos either treated or untreated with inhibitor (A,B- Lateral view)

5.9 Summary

- Inhibition of p38MAPK resulted in a complete rescue of impaired cell proliferation and increased apoptosis in Id4/p53 morphants and to a partial rescue in Id4 morphants.

- *id4*$^{qmc803/qmc803}$ embryos at 24 hpf developed normally but displayed an increased expression of the pro neural bHLH protein *ngn1* as well as the *HuC*/*elavl3* protein suggesting precocious neuronal differentiation.

- *id4*$^{qmc803/qmc803}$ embryos exhibited decreased cell proliferation and increased apoptosis similar to to the Id4 and Id4/p53 morphants. Quantitative comparison between mutant and morphants would suggest that the enhanced phenotype observed in Id4 morphants is indeed due to artifical up regulation of p53.

- Impaired proliferation in the *id4*$^{qmc803/qmc803}$ embryos is p38MAPK mediated and inhibiton of p38 MAPK restored normal cell proliferation.

Chapter 6

Discussion

Using gain-of-function and loss-of-function approaches, the role of two cell fate regulators, lyl1 and Id4 was analysed using zebrafish as a model system. To this end, ectopic overexpression and morpholino-mediated knockdown as well as TALEN-mediated mutagenesis was employed. Phenotypic analysis of morphant and mutant zebrafish revealed potential mechanisms underlying the function of lyl1 and Id4 in haematopoiesis and neurogenesis, respectively. The data presented that *lyl1* role during zebrafish haematopoiesis. Gain-of-function studies suggest that if expressed at early during development they can promote erythrocyte differentiation. But the mutant displayed normal erythrocyte development. However, the mutant had a reduction in HSCs and an impaired lymphopoiesis. In addition, the data also demonstrate that *lyl1* regulates lineage choice driving lymphopoiesis and suppressing myelopoiesis

Id4 is required for maintenance and expansion of neural stem cells preventing premature cell differentiation and death through negatively regulating p38MAPK activity.

6.1 TALEN a powerful tool for genome editing

Site-specific programmable nucleases emerged as a powerful reverse genetic tool allowing genomic engineering in many model organisms including zebrafish. Here, we have targeted two different loci in the zebrafish genome and have successfully established mutant lines using TALENS. TALENS possessed various advantages as their targeting range is quite high compared to ZFNs and thus they can be used to target any region of the genome (Joung and Sander, 2013). While TALENS effectively generated somatic mutation in zebrafish, ZFNs failed to create deletions (Moore *et al.,* 2012).

Both Lyl1 and Id4 TALEN pairs were highly efficient resulting in site-directed mutagenesis in zebrafish somatic cells. The mutation was also transmitted through the germline. TALEN-mediated approach in zebrafish had a targeting efficiency ranging from 20%-77% (Moore *et al.,* 2011) and in some cases up to 100% (Bedell *et al.,* 2012). Targeting efficiency of the TALENS used in this study range from 11% to 90% and in few embryos, 100% efficiency was also observed. TALENs induce mutations at a particular target site in dose-dependent fashion (Dahlem *et al.,* 2012). When injected with 125 pg of *lyl1* TALEN RNA into zebrafish embryos we did not observe any gene disruption but increasing the amount of RNA resulted in targeted mutations. Injection of 50 pg of *id4* TALEN RNA into zebrafish had a mutation frequency of 50%-70% whereas the mutation frequency in 125 pg injected embryos was 90%. This suggests the frequency of mutation is dose-dependent and increasing amounts of RNA will increase the frequency of mutations. However injecting too much of TALEN RNA also increases the toxicity leading to developmental defects or even death of the embryos. For example, injecting 500 pg of each *id4* TALEN RNA resulted in morphological phenotypes in all embryos within 48 hours of injection. Hence for every TALENS pairs it is important to establish the amount of TALEN RNA required to cause gene disruption without causing developmental defects.

Both Lyl1 and Id4 TALENS created targeted mutations in zebrafish somatic cells and screening of F_0 adults revealed that mutations were transmitted to the germline. However, only 2 lyl1 F_0 founder displayed heritable mutations and the frequency of mutation is only 11 and 23%. On the other hand, 66% of the embryos analysed had transmitted the Id4 mutation to their offspring with a 40-60% frequency. A similar frequency was also observed by others targeting different loci of the zebrafish genome and in these cases founder fish displayed transmission frequencies ranging from 6-75% with some had 100% mutation frequency (Dahlem *et al.,* 2012; Cade *et al.,* 2012). Usually F_0 founder fish are mosaic harbouring a

number of different mutations (Dahlem *et al.,* 2012; Ansai *et al.,* 2013; Ota *et al.,* 2013) but most of our founders exhibited only single mutations.

We did not observe any large deletions in the F1 embryos as all deletions observed were in the range of 6-18 bp while in one instance deletion and insertion occurred. All the deletions observed in Lyl1 embryos were out-of-frame deletions but the majority of the mutations in Id4 F1 embryos were in-frame. Genotyping revealed that Lyl1 F1 fish carried a mutation in one of the alleles with 10 bp deletion and 26 bp insertion. In addition to two type of in-frame mutations, Id4 F1 fish also had out-of-frame deletions (10 bp and 8 bp). The mutant allele are inherited in mendelian fashion and the F1 adult fish were viable and fertile.

DNA-binding specificity of TALENS is high due to the long DNA-binding domain reducing off-target effects frequently observed with other programmable nucleases like ZFNs and CRISPR cas9 (Meng *et al.,* 2008; Cradick *et al.,* 2013). This is due to the fact that TALENS fail to cleave 3-6 base mismatches and only partially cleave 2-base mismatch. We did not find any potential off-target sites by using the online TALEN off-site predictor suggesting that the TALENS used are specific for their targets.

Several assays are available to detect mutations caused by programmable nucleases. Genomic DNA extracted from TALEN injected and control embryos are amplified with primers spanning the target site. The template can be analysed by surveyor nucleases such as the T7 endonuclease or Cel-I which can detect and cleaves heteroduplex DNA (Mussolino *et al.,* 2011). High resolution melt analysis (HRMA) can also be used to identify the hetero-duplex (Dahlem *et al.,* 2012). To detect the TALEN-mediated mutations we use PCR followed by restriction enzyme digestion. This approach requires the presence of a restriction site in the spacer region that will be destroyed through TALEN-mediated DSB and NHEJ repair; hence the enzyme cannot digest the PCR product. Recently it has been reported that TALEN-mediated DSB occur in the middle of the spacer region in 70% of cases targeting 4-5

bp (Yu *et al.,* 2014). The spacer regions of lyl1 and Id4 TALEN target sites contain restriction sites at these 4-5 bp and hence identifying the TALEN-mediated mutations at these loci by restriction enzyme digestion was very effective.

Lyl1 (Qmc801) and Id4 (Qmc803) mutant lines were established to study their role in haematopoietic and neural stem cell fate, respectively.

6.2 Lyl1 is required for HSC function and lymphoid differentiation

6.2.1 Lyl1 RNA is present during both waves of haematopoiesis

In zebrafish, RT-PCR analysis using whole embryos indicated that *lyl1* was expressed albeit weakly from 11 hpf; slightly later than *scl/tal1* that was expressed in the lateral mesoderm from 10.5 hpf onwards (Gering *et al.,* 1998). Unfortunately, *in situ* hybridization using several different anti sense RNA probes produced high background and therefore it was not possible to determine Lyl1 expression during zebrafish embryogenesis in more detail. Nevertheless, the RT-PCR analysis indicated that *lyl1* RNA was detectable in zebrafish embryos at developmental time points when primitive and definitive haematopoiesis.

6.2.2 Ectopic overexpression of *lyl1* enhanced primitive red blood cells production

Ectopic expression of *scl/tal1* mRNA resulted in overproduction of primitive erythrocytes that displayed increased expression of *gata1* in the ICM at 22 hpf (Gering *et al.,* 1998). Similarly, injection of *lyl1* mRNA resulted in an increase of *scl/tal1* and *gata1* expressing cells at 14 hpf (Figure 4.4) suggesting that Lyl1 can promote primitive haematopoietic progenitors and enhance primitive erythrocyte differentiation. A clear increase in *scl/tal1* and *gata1* expression was also observed at 24 hpf (Figures 4.5 and 4.6). Given that blood cell circulation starts around 24 hpf it is possible that the observed increase

in *scl/tal1* and *gata1* expressing cells was due to increase in blood cell production. *Scl/tal1* and *gata1* are known to express in circulating blood cells and together with their elevated expression in 14 hpf suggest that there is an increase in the primitive red blood cell production. The expression of *ikaros* in the ICM at 24 hpf and *c-myb* at 30 hpf further suggest that the primitive red blood production has enhanced in the *lyl1* mRNA injected embryos. This enhanced expression of marker genes of primitive erythrocytes suggest that overexpression of Lyl1 resulted in an increase in primitive blood cell production.

6.2.3 Ectopic overexpression of *lyl1* had no effect on expression of endothelial cell marker flk1

In contrast to *scl/tal1* mRNA injected embryos that displayed an increase in the expression of the endothelial marker *flk1* (Gering *et al.*, 1998), *flk1* expression appeared normal in *lyl1* injected embryos (Figure 4.5). Both, Scl/tal1 and Lyl1 are expressed in mouse endothelium (Giroux *et al*., 2007) and given the potential for redundancy (as discussed above) this result seems surprising. Injection of increasing amounts of Lyl1 RNA is needed to see whether flk1 expression will increase with increasing amounts of Lyl1. This seems unlikely though, given that Gering *et al.* (1998) inject 70 pg *Scll/tal1* RNA compared to 100 pg *Lyl1* RNA injected here. It seems therefore that ectopic overexpression of Lyl1 has no effect on flk1 expression suggesting a non-redundant role for Scl/tal1 and Lyl1 in endothelial cells.

6.2.4 Lyl1 mutant fish (*qmc 801/qmc801*) had normal primitive haematopoiesis

Targeted deletion of Scl/tal1 in the mouse resulted in the absence of haematopoiesis in the yolk sac and Scl/tal1$^{-/-}$ embryos died around 9.5 dpc (Robb *et al.*, 1995). Similarly, morpholino-mediated knockdown of Scl/tal1 failed to develop primitive haematopoiesis

(Patterson *et al.,* 2005). In contrast, Lyl1 mutant embryos displayed normal yolk-sac haematopoiesis and mutant mice were viable (Capron *et al,* 2006). Similarly, primitive haematopoiesis seemed unaltered in *lyl1*$^{qmc801/qmc801}$ zebrafish embryos (normal expression of the *scl/tal1* and *gata1*; Figure 4.7) suggesting that in contrast to Scl/tal1, Lyl1 function is not required for primitive haematopoiesis in both mice and zebrafish.

6.2.5 Lyl1 mutant fish (*qmc 801/qmc801*) had impaired definitive haematopoiesis

In the mouse Lyl1 expression was high in the immature haematopoietic and pro-B cells at embryonic day 14 and Lyl1 mutant displayed a 2-fold reduction in immature B-cell. Bone marrow multipotent HSC population is also reduced in the *lyl1*$^{-/-}$ animals indicating that it is important for HSC maintenance. Reconstitution assays demonstrate that *Lyl1*$^{-/-}$ bone marrow cells displayed a severe defect in their ability to reconstitute lymphoid lineages (Capron *et al.,* 2006). *lyl1* $^{qmc801/qmc801}$ embryos also displayed a marked reduction in the *c-myb* expressing blood progenitors in the CHT at 2 dpf (Figure 4.10). In addition, there was a clear reduction in the *rag1* expressing lymphoid cells in the thymus of *lyl1* $^{qmc801/qmc801}$ embryos at 5dpf suggesting that Lyl1 function is required for definitive HSC maintenance as well as T cell development.

The reduction of blood progenitors and lymphocytes in the CHT and thymus respectively, can be validated by analysing the expression of these genes by qRT-PCR. Another possibility would be to cross *qmc801* with *qmc551*:GFP that expresses GFP in prRBCs, HSCs (dorsal aorta) and lymphocytes (thymus) (Dr Gering, personal communication). This would allow to visualise GFP-expressing blood cells in live embryos and to quantify them using flow cytometry.

6.2.6 Lyl1 antagonises myeloid differentiation

Lyl1 mutant mice had normal myeloid cell number (Capron *et al.,* 2006). At 24 hpf the number of *pu.1* positive cells throughout the ventral wall was increased in *lyl1* $^{qmc801/qmc801}$ embryos when compared with the wild-type (Figure 4.8). Overexpression of *lyl1* mRNA has suppressed the expression of *pu.1* at 14hpf (Figure 4.4 E, F). In line with the overexpression data this enhanced expression of *pu.1* in *lyl1* $^{qmc801/qmc801}$ embryos suggests that Lyl1 might antagonize myeloid differentiation. Circulation in zebrafish starts around 24 hpf and hence there is possibility that the observed cells may be the circulating cells rather than the elevated *pu.1* expression. To avoid this confusion and to validate the observed upregulation of *pu.1* it is important to check their expression around 27-30 hpf. Yet, the data here presents a possible role of Lyl1 in suppressing myeloid cell differentiation.

6.2.7 Lyl1 regulate lineage specification promoting lymphopoiesis and suppressing myelopoiesis

In the mouse, transplantation of *Lyl1*$^{-/-}$ bone marrow cells failed to engraft into lymphoid lineage (Souroullas *et al.*, 2009; Capron *et al.*, 2006). Although the number of MPP remains unaltered in the *lyl1*$^{-/-}$ animals the frequency of LMPP was severely reduced. *Lyl1*$^{-/-}$ LMPP achieved only partial thymic engraftment and failed to generate T cells (Zohren *et al.*, 2012).

Flow cytometric analysis of kidney marrow cells from wild type and *lyl1*$^{qmc801/qmc801}$ adult fish has revealed that Lyl1-deficiency supported an alternative lineage fate choice as a 4-fold reduction in lymphocyte population and a 3-fold increase in myeloid population was observed in *lyl1*$^{qmc801/qmc801}$. This is consistent with the earlier observation of reduced *rag1* expression in the thymus at 5 dpf (Figure 4.10) and enhanced *pu.1* expression in the ventral wall at 24 hpf (Figure 4.8). Thus the analysis of kidney marrow cells suggests that lyl1

regulate lineage specification promoting lymphocyte differentiation and suppressing myeloid differentiation.

6.2.8 Lyl1 may regulate Gfi1aa expression

Gfi1 is expressed in mouse HSC and in mice lacking *gfi1*, differentiation of lymphocytes was blocked (Hock *et al.,* 2006; Hock *et al.,* 2003). Gfi1 plays important role in regulating self-renewal and maintenance of adult HSCs (Zeng *et al.,* 2004; Hock *et al.,* 2004). We observed a reduced expression of *gfi1aa* at 18 hpf and 24 hpf *in* the *lyl1* $^{qmc801/qmc801}$ (Figure 4.9). At 18 hpf *gfi1aa* is expressed in the prRBC and the reduction of *gfi1aa* does not alter the primitive erythrocyte differentiation in *lyl1*$^{qmc801/801}$ as the marker for primitive erythrocyte looked normal (*gata1*; figure 4.7). Morpholino-mediated knockdown of Gfi1aa resulted in impaired primitive haematopoiesis (Cooney *et al.,* 2013). However, more recent analysis of *gfi1aa* mutant zebrafish revealed that *gfi1aa, gfi1ab* and *gfi1b* play redundant roles during primitive and definitive haematopoiesis compensating for each other's loss (D Ucanok and M Gering, personal communication). Hence it is important to check the expression of other *gfi1* genes in *lyl1*$^{qmc801/801}$. Also the expression of *gfi1* was significantly reduced in mouse LMPP. Transduction of *Lyl1*$^{-/-}$ cells with retrovirus expressing lyl1 or gfi1 rescued the impaired T-cell development suggesting that Gfi1 acts downstream of Lyl1 during T-cell development (Zohren *et al.,* 2012). This is consistent with our observation of reduced *gfi1aa* expression in the *lyl1*$^{qmc801/qmc801}$ embryos. Together these suggest Lyl1 might play a role in regulating Gfi1aa expression. However, our observation on the expression of *gfi1aa* in *lyl1*$^{qmc801/qmc801}$ was hampered by the staging difference of the embryos. As the expression of *gfi1aa* leaves the prRBC from 19 hpf and it start to express in the ventral wall at 24 hpf, the selected stage to observe the expression of *gfi1aa* in the mutants was not ideal. To overcome this staging difference it is necessary to check the expression of *gfi1aa* during

10ss (for primitive haematopoiesis) and 27 hpf or later (for definitive haematopoiesis) which will give a clear idea about the Lyl1 role in regulating Gfi1aa.

6.3 Id4 promotes neuronal proliferation by suppressing p38MAPK activity

6.3.1 Expression of *id4* is conserved in vertebrates

It is known that Id proteins are highly expressed in the undifferentiated proliferating cells and their expression starts to decline once the cell starts to differentiate (Lasorella *et al.,* 2001). In the mouse central nervous system, Id4 expression was observed in the lateral ventricles, epithalamus and optic recesses at 12.5 dpc. Id4 expression was detected in the telencephalon at 14.5 dpc and at 17.5 dpc its expression was restricted to the developing central nervous system (Riechmann and Sablitzky, 1995). In the developing chick embryos the expression of *id4* was observed from stage 5 in the neural plate and at stage 10 in the neural tube. At day 3 (stage 19) the expression of *id4* is restricted to telencephalon, hind brain, mid brain and in the eye (Kee and Bronner-Fraser, 2001). In Xenopus, the expression of Id4 is noticed in the neural plate, eye, and in trigerminal ganglia (Liu and Harland, 2003). Similar to other vertebrate, expression of *id4* is also restricted to the developing central nervous system in zebrafish at 24 and 48 hpf (Figure 5.1; Thisse *et al.,* 2001). *Id4* is mainly expressed in the telencephalon, diencephalon, tectum and in the hindbrain. The expression of *id4* was also noticed in the precordal plate and in the presumptive neural tube (6-10 hpf; Figure 5.1 A-C). This clearly suggests that the expression of Id4 is conserved with other vertebrates and during early development Id4 play a role in promoting the proliferation of neural epithelial cells. *Id4* expression was also observed in other tissue such as mammary gland, spermatogonial stem cells, adipocytes, osteoblast and prostrate epithelial cells (Oatley *et al.,* 2011; Sharma *et al.,* 2013; Dong *et al.,* 2011; Patel *et al.,* 2015). During early

development Id4 is critical for central nervous system and at later stages Id4 might promote the development of other developmental processes.

6.3.2 *id4*$^{qmc804/qmc804}$ phenocopied the mouse Id4 mutant

Two Id4 knockout mouse models are known and they exhibited a similar phenotype in the developing central nervous system (Yun *et al.,* 2004; Bedford *et al.,* 2005). Both mouse models displayed a reduction in forebrain due to precocious neuronal differentiation. The mice also displayed 20-30% reduction in proliferation and 3 fold increase in apoptosis (Yun *et al.,* 2004; Bedford *et al.,* 2005). Morpholino-mediated knockdown of Id4 in zebrafish resulted in various phenotypes in the developing embryos. The morphants displayed an impaired proliferation as the number of proliferating cells was decreased by 50%. In addition, an 8-fold increase in the cells undergoing apoptosis was observed (Dhanaseelan, 2011). However, this analysis was hampered by the fact that injection of Id4 morpholinos resulted in up-regulation of p53. Nevertheless, injection of Id4 and p53 morpholinos still exhibited a similar phenotype albeit with less severity (Dhanaseelan, 2011). Hence to overcome this disadvantage with morpholinos, Id4 mutant zebrafish (*id4*$^{qmc803/qmc803}$) were generated using TALEN-mediated mutagenesis. Cell proliferation was reduced by 24% and apoptosis was enhanced by 2.3 fold in *id4*$^{qmc803/qmc803}$ embryos at 10.6 hpf (Figure 5.8 and 5.9). Comparing this impaired proliferation and survival defects with the Id4-deficient mice it is clear that *id4*$^{qmc803/qmc803}$ also exhibited a similar proliferative defects. In addition Yun *et al.,* (2004) indicated that the Id4 mutant mice displayed precocious neurogenesis as the expression of marker genes for neurogenesis was up-regulated (*ngn2*, *neurod*). Expression of post-mitotic neuronal marker βIII tubulin was also increased in the developing forebrain at E12.5 and 14.5 in the Id4 mutants which suggest that loss of Id4 resulted in premature differentiation to neurons (Bedford *et al.,* 2005). Analysis of marker genes for neuronal differentiation (*ngn1,*

huC) in *id4*$^{qmc803/qmc803}$ embryos suggests that their expression looked normal during 2 somite stage however a clear increase in their expression was observed during later stages of development in *id4*$^{qmc803/qmc803}$ (Figure 5.6 and 5.7). Together these results clearly indicate that Id4 function is required for neural stem cell expansion and timing of differentiation. In this regard, the data are in line with earlier work showing that Id4 knockout mice exhibited a reduction in neural stem cells accompanied with premature neurogenesis and increased cell death (Yun *et al.,* 2004; Bedford *et al.,* 2005).

6.3.3 Id4 function by negatively regulating p38MAPK activity

The observed phenotype in Id4 morphants and mutant embryos is mediated through enhanced activity of p38MAPK. p38MAPK activation was observed when Id4 was silenced in the mammary gland and in cultured mammary tumour cells. p38MAPK is known to arrest cell cycle by phosphorylating p21 (cyclin-dependent kinase inhibitor), upregulating p16 (inhibitor of cyclin-dependent kinase 4 and 6) and by phosphorylating cyclin D1 leading to its degradation (Kim *et al.,* 2002; Bulavin *et al.,* 2004; Casanovas *et al.,* 2000). However the molecular mechanism through which Id4 negatively regulates the activity of p38MAPK is not clear but it was shown in Id4-deficient mice that Id4 regulates mammary gland development by suppressing p38MAPK activity (Dong et al., 2011).

Id4-deficient mice (six week old) exhibited impaired mammary development that include irregular terminal end bud (TEB), disorganized cap cell layer and shorten ductal branching. Similar to the impaired proliferation observed in the central nervous system of Id4 mutant mice (Bedford *et al.,* 2005; Yun *et al.,* 2004), Id4 null mammary gland also displayed a reduced proliferation and increased apoptosis in the TEB and ducts. The observed phenotype in the *id4*$^{-/-}$ mammary gland is mediated by p38MAPK as the expression of p38MAPK in mature ducts and TEB of Id4 mutant animal is very high when compared with

wild type. Inhibition of p38MAPK has rescued the impaired proliferation and apoptotic defects observed in the mammary gland (Dong *et al.*, 2011).

Inhibition of p38MAPK using chemical inhibitor has rescued the proliferation defects observed in the *id4*$^{qmc803/qmc803}$embryos (Figure 5.10). In addition, inhibition of p38MAPK also reversed the survival defects as the apoptotic rate in the *id4*$^{qmc803/qmc803}$ was completely rescued once p38MAPK activity was inhibited. A similar observation was also observed in the Id4 and Id4/p53 morphants. Average number of proliferation was reduced by 50% and 8 times more apoptosis was observed in the Id4 morphants (Dhanaseelan, 2011). Inhibition of p38MAPK in the Id4 morphants was rescued only partially which is due to the p53 activity. However, inhibition of p38MAPK in the Id4/p53 morphants has completely rescued the proliferation and surviving defects (Figure 5.3).

p38MAPK like other MAP kinases are activated by MAP kinase kinases (MKK) such as MKK3 and MKK6. Overexpression of p38MAPK is known to inhibit cell proliferation (Yee *et al.,* 2003) and in addition to their function in apoptosis and cell cycle control p38MAPK is also known to promote differentiation of adipocytes, cardiomyocytes, myoblast, erythroblast and neurons (Yehia *et al.,* 2001). p38MAPK expression was observed throughout zebrafish early development. At 24 and 48 hpf p38MAPK is expressed in the different areas of the developing central nervous system such as tegmentum, diencephalon, cerebellum and hindbrain (Krens *et al.,* 2006). Activation of p38MAPK by expressing MKK6 during zebrafish cardiogenesis has reduced the proliferation and enhanced the differentiation of cardiomyocytes leading to a severely disturbed cardiogenesis (Jopling *et al.,* 2012). Hence, Id4 might negatively regulate p38MAPK activity not only to promote proliferation of the NPC but also to inhibit differentiation. Although it is clear that inhibition of p38MAPK by Id4 is necessary for NPC proliferation and differentiation, the mechanism how Id4 orchestrate this p38MAPK regulation remains to be determined. ID4 is known to

downregulate matrix metalloproteinases (MMPs) by directly binding to Twist1 a bHLH protein that mediates MMPs expression and tumor invasion (Rahme and Israel, 2015). Hence, it is important to check whether Id4 regulates p38MAPK by directly binding to p38MAPK or by binding to other bHLH proteins that are required for p38MAPK activity.

In conclusion, this study presents the successful employment of TALEN-mediated mutagenesis to generate Id4 and Lyl1 mutant lines. It was shown that Lyl1 may play a role during primitive haematopoiesis suppressing myelopoiesis and is required to maintain blood and T-cell progenitors. It also presents the role of Id4 in regulating NPC proliferation and differentiation by negatively regulating p38MAPK activity.

References

Adolfsson J, Mansson R, Buza-Vidas N, Hultquist A, Liuba K, Jensen CT, et al. Identification of Flt3+ lympho-myeloid stem cells lacking erythro-megakaryocytic potential a revised road map for adult blood lineage commitment. Cell. 2005 22;121(2):295–306.

Akazawa C, Sasai Y, Nakanishi S, Kageyama R. Molecular characterization of a rat negative regulator with a basic helix-loop-helix structure predominantly expressed in the developing nervous system. *J. Biol. Chem*. 1992; 267; 21879–21885.

Al-Adhami MA and Kunz YQ. Ontogenesis of hematopoietic sites in Brachydanio rerio.Development, Growth and Differentiation 1997: 19: 171–179.

Amack JD and Yost HJ. The T box transcription factors no tail in ciliated cells controls zebrafish left-right asymmetry. *Curr. Biol*. 2004; 14, 685–690.

Amsterdam A, Hopkins N. Mutagenesis strategies in zebrafish for identifying genes involved in development and disease. *Trends Genet.* 2006; 22:473–478.

Anderson DJ.Stem cells and pattern formation in the nervous system: the possible versus the actual. *Neuron* 2001; 30: 19–35.

Ansai S, Kinoshita M. Targeted mutagenesis using CRISPR/Cas system in medaka. *Biology Open*. 2014; 3(5): 362-371.

Aplan PD, Jones CA, Chervinsky DS, Zhao X, Ellsworth M, Wu C. An scl gene product lacking the transactivation domain induces bony abnormalities and cooperates with LMO1 to generate T-cell malignancies in transgenic mice. *EMBO J* 1997; 16: 2408–2419.

Artavanis-Tsakonas S, Rand MD & Lake RJ. Notch signaling: cell fate control and signal integration in development. Science 284, 770–776 (1999)

Auer TO, Duroure K, De Cian A, Concordet J-P, Del Bene F. Highly efficient CRISPR/Cas9-mediated knock-in in zebrafish by homology-independent DNA repair. *Genome Research*. 2014; 24(1):142-153.

Bain G, Engel I, Robanus Maandag EC, te Riele HP, Voland JR, Sharp LL. E2A deficiency leads to abnormalities in alphabeta T-cell development and to rapid development of T-cell lymphomas. *Mol Cell Biol* 1997; 17: 4782–4791.

Bakkers J. Zebrafish as a model to study cardiac development and human cardiac disease. *Cardiovasc. Res*.2011; 91, 279–288.

Bao S, Wu Q, McLendon RE, Hao Y, Shi Q, Hjelmeland AB, et al. Glioma stem cells promote radioresistance by preferential activation of the DNA damage response. *Nature*. 2006; 444(7120): 756–60.

Barrangou R, Fremaux C, Deveau H, Richards M, Boyaval P, Moineau S, Romero DA, Horvath P. CRISPR provides acquired resistance against viruses in prokaryotes. *Science*. 2007; 315: 1709–1712.

Bashir, S. Role of Id4 in neural stem cell fate during early zebrafish development. Masters in Research thesis. University of Nottingham. 2010.

Bassett AR, Tibbit C, Ponting CP, Liu J-L. Highly Efficient Targeted Mutagenesis of *Drosophila* with the CRISPR/Cas9 System. *Cell Reports*. 2013; 4(1): 220-228.

Bayer SA, Altman J. Neocortical Development. *New York: Raven Press* 1999.

Bedell VM, Wang Y, Campbell JM, et al. *In vivo* Genome Editing Using High Efficiency TALENs. *Nature*. 2012; 491(7422): 114-118.

Bedford L, Walker R, Kondo T, van Crüchten I, King ER, Sablitzky F. Id4 is required for the correct timing of neural differentiation. *Dev. Biol*. 2005; 280:386–395.

Beger C, Pierce LN, Krüger M, et al. Identification of *Id4* as a regulator of*BRCA1* expression by using a ribozyme-library-based inverse genomics approach. *Proceedings of the National Academy of Sciences of the United States of America*. 2001; 98(1):130-135.

Benezra R, Davis R, Lockshon D, Turner D, Weintraub H. The protein ID – a negative regulator of helix-loop-helix DNA binding proteins. *Cell*. 1990; 61; 49-59.

Bennett CM, Kanki, JP, Rhodes, J. *et al.* Myelopoiesis in the zebrafish, Danio rerio. *Blood*. 2001; 98:643–651.

Berman JN, Kanki JP, Look AT. Zebrafish as a model for myelopoiesis during embryogenesis.*Experimental Hematology*. 2005;33(9):997–1006.

Bertrand JY, Chi NC, Santoso B, Teng S, Stainier DY, Traver D (2010) Haematopoietic stem cells derive directly from aortic endothelium during development. Nature 464: 108–111

Bertrand JY, Giroux S, Golub R, Klaine M, Jalil A, Boucontet L, Godin I, Cumano A. Characterization of puriWed intraembryonic hematopoietic stem cells as a tool to deWne their site of origin. *PNAS* 2005; 102; 134–139.

Bertrand N, Castro DS, Guillemot F. Proneural genes and the specification of neural cell types. *Nat. Rev. Neurosci*. 2002; 3; 517–530.

Bhaya D, Davison M, Barrangou R. CRISPR-Cas systems in bacteria and archaea: versatile small RNAs for adaptive defense and regulation. Annu Rev Genet. 2011;45:273–297.

Bibikova M, Golic M, Golic KG, Carroll D. Targeted chromosomal cleavage and mutagenesis in Drosophila using zinc-finger nucleases. *Genetics* 2002; 161, 1169–1175.

Bill, B.R., Petzold, A.M,., Clark, K.J., Schimmenti, L.A., and Ekker, S.C. A primer for morpholino use in zebrafish. *Zebrafish* 2009; 6; 69–77.

Bitinaite, J., Wah, D.A., Aggarwal, A.K., and Schildkraut, I. FokI dimerization is required for DNA cleavage. *Proc. Natl. Acad. Sci. USA* 1998; 95, 10570– 10575.

Blackwood E M and, Eisenman R N. Max: a helix-loop-helix zipper protein that forms a sequence-specific DNA-binding complex with Myc. *Science*. 1991; 251:1211–1217.

Blank U and Karlsson S. TGF-β signalling in the control of haematopoietic stem cells. Blood 2015: 125 (3).

Boch J, Bonas U. Xanthomonas AvrBs3 family-type III effectors: discovery and function. *Annu. Rev. Phytopathol*. 2010; 48:419–436.

Boch J, Scholze H, Schornack S, Landgraf A, Hahn S, Kay S, Lahaye T, Nickstadt A, Bonas U. Breaking the code of DNA binding specificity of TAL-type III effectors. *Science*. 2009; 326:1509–1512.

Bogdanove AJ and Voytas DF (2011). TAL effectors: customizable proteins for DNA targeting.Science 333: 1843–1846.

Bogdanove AJ, Schornack S, Lahaye T. TAL effectors: finding plant genes for disease and defense. Curr. Opin. Plant Biol. 2010;13:394–401.
Brain Res. Mol. Brain Res., 1995; 30, 312-326.

Bray S. Notch signalling in Drosophila: three ways to use a pathway. Semin Cell Dev Biol. 1998: 9(6): 591-597.

Brou C, Logeat F, Gupta N, Bessia C, LeBail O, Doedens JR, Cumano A, Roux P, Black RA, Israël A. A novel proteolytic cleavage involved in Notch signaling: the role of the disintegrin-metalloprotease TACE. Mol Cell. 2000;5:207–216.

Brouns SJ, Jore MM, Lundgren M, Westra ER, Slijkhuis RJ, Snijders AP, Dickman MJ, Makarova KS, Koonin EV, van der Oost J. Small CRISPR RNAs guide antiviral defense in prokaryotes.*Science*. 2008; 321:960–964.

Bulavin DV, Phillips, C., Nannenga, B., Timofeev, O., Donehower, L. A., Anderson, C. W., Appella, E. and Fornace, A. J., Jr (2004). Inactivation of the Wip1 phosphatase inhibits mammary tumorigenesis through p38 MAPKmediated activation of the p16(Ink4a)-p19(Arf) pathway. Nat. Genet. 36, 343- 350.

Burns CE, DeBlasio T, Zhou Y, Zhang J, Zon LI, Nimer SD. Isolation and characterization of runxa and runxb, zebrafish members of the runt family of transcriptional regulators. *Exp. Hematol*. 2002; 30(12), 1381-1389.

Bussmann, J., Wolfe, S.A., and Siekmann, A.F. Arterial-venous network formation during brain vascularization involves hemodynamic regulation of chemokine signaling. *Development* 138, 2011; 1717–1726.

Cade L, Reyon D, Hwang WY, et al. Highly efficient generation of heritable zebrafish gene mutations using homo- and heterodimeric TALENs. *Nucleic Acids Research*. 2012; 40(16):8001-8010.

Capron C, Lacout C, Lecluse Y, Wagner-Ballon O, Kaushik AL, Cramer-Borde E, Sablitzky F, Dumenil D, Vainchenker W. LYL-1 deficiency induces a stress erythropoiesis. *Exp Hematol*. 2011; 39:629–642.

Capron C, Lecluse Y, Kaushik AL, Foudi A, Lacout C, Sekkai D, Godin I, Albagli O, Poullion I, Svinartchouk F, et al. The SCL relative LYL-1 is required for fetal and adult hematopoietic stem cell function and B-cell differentiation. *Blood*. 2006; 107:4678–4686

Carey JP, Asirvatham AJ, Galm O, Ghogomu TA, Chaudhary J. Inhibitor of differentiation 4 (Id4) is a potential tumor suppressor in prostate cancer. *BMC Cancer*. 2009; 9:173.

Carroll D. Genome Engineering With Zinc-Finger Nucleases. Wahl LM, ed.*Genetics*. 2011;188(4):773-782.

Casanovas, O., Miro, F., Estanyol, J. M., Itarte, E., Agell, N. and Bachs, O. (2000). Osmotic stress regulates the stability of cyclin D1 in a p38SAPK2- dependent manner. J. Biol. Chem. 275, 35091-35097.

Castro M, Grau L, Puerta P, Gimenez L, Venditti J, Quadrelli S, Sanchez-Carbayo M. Multiplexed methylation profiles of tumor suppressor genes and clinical outcome in lung cancer. *Journal of translational medicine*. 2010; 8:86.

Cermak T, Doyle EL, Christian M, Wang L, Zhang Y, Schmidt C, Baller JA, Somia NV, Bogdanove AJ, Voytas DF. Efficient design and assembly of custom TALEN and other TAL effector-based constructs for DNA targeting. *Nucleic Acids Res*. 2011; 39:e82

Chakrabarti S, Streisinger G, Singer F, Walker C. Frequency of gamma-ray induced specific locus and recessive lethal mutations in mature germ cells of the zebrafish, Brachydanio rerio. *Genetics* 1993; 103, 109–123.

Chan AS, Tsui WY, Chen X, Chu KM, Chan TL, Li R, So S, Yuen ST, Leung SY. Downregulation of ID4 by promoter hypermethylation in gastric adenocarcinoma. *Oncogene*. 2003; 22(44):6946–6953.

Chan F, Oatley MJ, Kaucher AV, et al. Functional and molecular features of the $Id4^{+}$ germline stem cell population in mouse testes. *Genes & Development*. 2014; 28(12):1351-1362.

Chan WY, Follows GA, Lacaud G, Pimanda JE, Landry JR, Kinston S, Knezevic K, Piltz S, Donaldson IJ, Gambardella L, et al. The paralogous hematopoietic regulators Lyl1 and Scl are coregulated by Ets and GATA factors, but Lyl1 cannot rescue the early Scl−/− phenotype. Blood.2007; 109:1908–1916.

Chang N, Sun C, Gao L, et al. Genome editing with RNA-guided Cas9 nuclease in Zebrafish embryos. *Cell Research*. 2013;23(4):465-472.

Chapman MA, et al. Comparative and functional analyses of LYL1 loci establish marsupial sequences as a model for phylogenetic footprinting. Genomics. 2003;81(3):249–259.

Chen L, Obryan JP, Smith HS, Liu E. Overexpression of matrix Gla protein messenger-Rna in malignant human breast cells—isolation by differential Cdna hybridization. *Oncogene* 1990; 5: 1391–1395.

Chen SS, Claus R, Lucas DM, et al. Silencing of the inhibitor of DNA binding protein 4 (ID4) contributes to the pathogenesis of mouse and human CLL.*Blood*. 2011;117(3):862-871.

Chervinsky DS, Zhao XF, Lam DH, Ellsworth M, Gross KW, Aplan PD. Disordered T-cell development and T-cell malignancies in SCL LMO1 double-transgenic mice: parallels with E2A-deficient mice. *Mol Cell Biol* 1999; 19: 5025–5035.

Chetty R, Dada MA, Boshoff CH, Comley MA, Biddolph SC, et al. TAL-1 protein expression in vascular lesions. *J Pathol*. 1997; 181:311–315.

Cho KW, Blumberg B,Steinbeisser H, De Robertis EM. Molecular nature of Spemann's organizer: the role of the Xenopus homeobox gene goosecoid. *Cell* 1991;67:1111–1120.

Christensen JL, Weissman IL. Flk-2 is a marker in hematopoietic stem cell differentiation: A simple method to isolate long-term stem cells. *Proceedings of the National Academy of Sciences of the United States of America*. 2001;98(25):14541-14546.

Christian M, Cermak T, Doyle EL, Schmidt C, Zhang F, Hummel A, Bogdanove AJ, Voytas DF. Targeting DNA double-strand breaks with TAL effector nucleases. Genetics. 2010;186:757–761.

Ciau-Uitz A, Monteiro R, Kirmizitas A & Patient R. Developmental hematopoiesis: ontogeny, genetic programming and conservation. Exp. Hematol. 42, 669–683 (2014).

Cleary ML, Mellentin JD, Spies J, Smith SD. Chromosomal translocation involving the beta T cell receptor gene in acute leukemia. *J Exp Med* 1988; 167:682–687.

Cooney JD, Hildick-Smith GJ, Shafizadeh E, et al. Teleost *growth factor independence* (*gfi*) genes differentially regulate successive waves of hematopoiesis. *Developmental biology*. 2013;373(2):431-441. doi:10.1016/j.ydbio.2012.08.015.

Cradick TJ, Fine EJ, Antico CJ, Bao G. CRISPR/Cas9 systems targeting β-globin and *CCR5* genes have substantial off-target activity. *Nucleic Acids Research*. 2013;41(20):9584-9592.

Crews S. Control of cell lineage-specific development and transcription by bHLH-PAS proteins. *Genes Dev*. 1998;12:607–620.

Curtis DJ, Hall MA, Van Stekelenburg LJ, Robb L, Jane SM, Begley CG. SCL is required for normal function of short-term repopulating hematopoietic stem cells. Blood. 2004;103:3342–3348.

Dahlem TJ, Hoshijima K, Jurynec MJ, Gunther D, Starker CG, Locke AS, Weis AM, Voytas DF, Grunwald DJ 2012. Simple methods for generating and detecting locus-specific mutations induced with TALENs in the zebrafish genome. *PLoS Genet* 8: e1002861

Davidson AJ, Ernst P,Wang Y. *et al.,* cdx4 mutants fail to specify blood progenitors and can be rescued by multiple hox genes. *Nature* 2003;425:300–306.

de Bruijn MF, Speck NA, Peeters MC, Dzierzak E. Definitive hematopoietic stem cells first develop within the major arterial regions of the mouse embryo. Embo J. 2000;19:2465–2474.

de Candia P, Akram M, Benezra R, Brogi E.Id4 messenger RNA and estrogen receptor expression: inverse correlation in human normal breast epithelium and carcinoma. *Hum. Pathol.* 2006: 37: 1032–1041

de Rooij DG, Russell LD. All you wanted to know about spermatogonia but were afraid to ask. *J Androl* 2000; 21: 776–79.

de Strooper B, Annaert W. Novel research horizons for presenilins and γ-secretases in cell biology and disease. Annu Rev Cell Dev Biol. 2010;26:235–260.

Dean M, Fojo T, Bates S. Tumour stem cells and drug resistance. *Nat Rev Cancer* 2005;5: 275–284.

del Corral RD and Storey KG. Markers in vertebrate neurogenesis. Nat Rev Neurosci. 2001 2(11): 835–839.

Deleuze V, El-Hajj R, Chalhoub E, et al. *Angiopoietin-2* Is a Direct Transcriptional Target of TAL1, LYL1 and LMO2 in Endothelial Cells. *PLoS ONE*. 2012;7(7):e40484.

Dhanaseelan, T. Role of Id4 in neural stem cell development in zebrafish. Masters in Research thesis. University of Nottingham. 2011.

DiCarlo JE, Norville JE, Mali P, Rios X, Aach J, Church GM. Genome engineering in *Saccharomyces cerevisiae* using CRISPR-Cas systems.*Nucleic Acids Research*. 2013;41(7):4336-4343.

Dietrich, HW, Kieran MW, Chan FY, et al. Intraembryonic haematopoietic cell migration during vertebrate development. *Proc Natl Acad Sci* 1995;92: 10713-10717.

Doitsidou, M., Reichman-Fried, M., Stebler, J., Ko¨ prunner, M., Do¨ rries, J., Meyer, D., Esguerra, C.V., Leung, T., and Raz, E. Guidance of primordial germ cell migration by the chemokine SDF-1. *Cell* 2002; 111, 647–659.

Dong J, Huang S, Caikovski M, et al. ID4 regulates mammary gland development by suppressing p38MAPK activity. *Development* 2011;138(23):5247-5256.

Dooley W, Zon LI. (2000). Zebrafish: a model system for the study of human disease. *Curr. Opin. Genet. Dev.* 10, 252-256.

Doyon, Y., McCammon, J.M., Miller, J.C., Faraji, F., Ngo, C., Katibah, G.E., Amora, R., Hocking, T.D., Zhang, L., Rebar, E.J., *et al*.,. Heritable targeted gene disruption in zebrafish using designed zinc-finger nucleases. *Nat. Biotechnol*. 2008;26, 702–708.

Draper, BW, Morcos PA, Kimmel CB. Inhibition of zebrafish fgf8 pre-mRNA splicing with morpholino oligos: a quantifiable method for gene knockdown. *Genesis* 2011;30, 154–156.

Driever, W., Solnica-Krezel, L., Schier, A.F., Neuhauss, S.C., Malicki, J., Stemple, D.L., Stainier, D.Y., Zwartkruis, F., Abdelilah, S., Rangini, Z., *et al.*, (1996). A genetic screen for mutations affecting embryogenesis in zebrafish. Development 123, 37–46.

Duncan M, DiCicco-bloom EM, Xiang X, Benezara R, Chada, K. The gene for the helix-loop-helix protein, Id, is specifically expressed in neural precursors. *Dev. Biol.*1992; 154(1); 1-10.

Dzierzak E, Speck NA. Of lineage and legacy – the development of mammalian hematopoietic stem cells. *Nature immunology*. 2008;9(2):129-136.

Eisen JS, Smith JC. Controlling morpholino experiments: don't stop making antisense. *Development* 2008; 135, 1735–1743.

Elefanty AG, Begley CG, Metcalf D, Barnett L, Kontgen F, Robb L. Characterization of hematopoietic progenitor cells that express the transcription factor SCL, using a lacZ "knock-in" strategy. *Proc Natl Acad Sci U S A.* 1998;95: 11897-11902.

Ellis H M, Spann D R, Posakony J W. *extramacrochaetae*, a negative regulator of sensory organ development in *Drosophila*, defines a new class of helix-loop-helix proteins. *Cell*. 1990;61:27–38.

Ellmeier W, Aguzzi A, Kleiner E, Kurzbauer R, Weith A. Mutually exclusive expression of a helix-loop-helix gene and N-myc in human neuroblastomas and in normal development. *EMBO J* 1992; 11 (7): 2563-71.

Evans SM, O'Brien TX. Expression of the helix-loop-helix factor Id during mouse embryonic development. *Dev. Biol* 1993; 159(2): 485-99.

Fairman R, Beran-Steed RK, Anthony-Cahill SJ, Lear JD, Stafford WF, Degrado WF, Benfield PA, Brenner SL. Multiple oligomeric states regulate the DNA-binding of helix-loop-helix peptides. *Proc Natl Acad Sci USA.* 1993;90:10429–10433.

Flicek, P., Amode, M.R., Barrell, D., Beal, K., Brent, S., Chen, Y., Clapham, P., Coates, G., Fairley, S., Fitzgerald, S., et al. Ensembl 2011. *Nucleic Acids Res. 39* 2011(Database issue), D800–D806.

Fode C, Ma Q, Casarosa S, Ang SL, Anderson DJ Guillemot F. A role for neural determination genes in specifying the dorsoventral identity of telencephalic neurons. *Genes Dev*. 2000;14; 67–80.

Foley, J.E., Yeh, J.R., Maeder, M.L., Reyon, D., Sander, J.D., Peterson, R.T., and Joung, J.K. Rapid mutation of endogenous zebrafish genes using zinc finger nucleases made by Oligomerized Pool ENgineering (OPEN). PLoS ONE 2009; 4, e4348.

Fong S, Itahana Y, Sumida T, et al. *Id-1* as a molecular target in therapy for breast cancer cell invasion and metastasis. *Proceedings of the National Academy of Sciences of the United States of America*. 2003;100(23):13543-13548.

Friedland AE, Tzur YB, Esvelt KM, Colaiácovo MP, Church GM, Calarco JA. Heritable genome editing in *C. elegans* via a CRISPR-Cas9 system. *Nature methods*. 2013;10(8):10.

Frisen J, and Lendahl U. Oh no, Notch again! *BioEssays* 2001; 23: 3 – 7.

Fu Y, Foden JA, Khayter C, et al. High frequency off-target mutagenesis induced by CRISPR-Cas nucleases in human cells. *Nature biotechnology*. 2013;31(9):822-826.

Fujita S. The discovery of the matrix cell, the identification of the multipotent neural stem cell and the development of the central nervous system. *Cell Struct Funct*. 2003; 28(4): 205–228.

Gage F H. Mammalian neural stem cells. *Science* 2000 ; 287 (5457): 1433-1438.

Galibert M-D, Carreira S, Goding CR. The Usf-1 transcription factor is a novel target for the stress-responsive p38 kinase and mediates UV-induced*Tyrosinase* expression. *The EMBO Journal*. 2001;20(17):5022-5031.

Galloway JL, Zon, LI. Ontogeny of hematopoiesis: examining the emergence of hematopoietic cells in the vertebrate embryo. *Curr Top Dev Biol* 2003;53:139–158.

Ganguly, M. Masters in Research thesis. University of Nottingham. 2013.

Garcia-Porrero, JA, Godin IE, Dieterlen-Lievre F. Potential intraembryonic hemogenic sites at pre-liver stages in the mouse. *Anat. Embryol. (Berl)* 1995; 192, 425–435.

Gering M, Rodaway AR, Göttgens B, Patient RK, Green AR. The SCL gene specifies haemangioblast development from early mesoderm. *The EMBO Journal*. 1998;17(14):4029-4045. doi:10.1093/emboj/17.14.4029.

Giroux S, Kaushik AL, Capron C, Jalil A, Kelaidi C, Sablitzky F, Dumenil D, Albagli O, Godin I. lyl-1 and tal-1/scl, two genes encoding closely related bHLH transcription factors, display highly overlapping expression patterns during cardiovascular and hematopoietic ontogeny. Gene Expr Patterns. 2007;7:215–226.

Godin I, Garcia-Porrero JA, Dieterterlen-Lievre F, Cumano A. Stem cell emergence and hemopoietic activity are incompatible in mouse intraembryonic sites. *J Exp Med* 1999;190(1): 43-52.

Gokhan S, Marin-Husstege M, Yung SY, Fontanez D,Casaccia-Bonnefil P,Mehler MF.Combinatorial profiles of oligodendrocyte-selective classes of transcriptional regulators differentially modulate myelin basic protein gene expression. *J Neurosci* 2005;25: 8311–8321.

Grandori C, Eisenman RN. Myc target genes. Trends Biochem Sci. 1997;22:177–181.

Gratz SJ, et al. Genome engineering of Drosophila with the CRISPR RNA-guided Cas9 nuclease.*Genetics*. 2013

Gregory T, Yu C, Ma A, Orkin SH, Blobel GA, Weiss MJ. GATA-1 and erythropoietin cooperate to promote erythroid cell survival by regulating bcl-xL expression. *Blood*. 1999;94:87–96.

Grimes HL, Chan TO, Zweidler-Mckay PA, Tong B, Tsichlis PN. The Gfi-1 proto-oncoprotein contains a novel transcriptional repressor domain, SNAG, and inhibits G1 arrest induced by interleukin-2 withdrawal. Molecular and Cellular Biology. 1996;16:6263–6272.

Guillemot F. Cellular and molecular control of neurogenesis in the mammalian telencephalon. *Curr. Opin. Cell Biol.*, 2005;17; 639–647.

Haffter, P., Granato, M., Brand, M., Mullins, M.C., Hammerschmidt, M., Kane, D.A., Odenthal, J., van Eeden, F.J., Jiang, Y.J., Heisenberg, C.P., et al. (1996). The identification of genes with unique and essential functions in the development of the zebrafish, Danio rerio. Development 123, 1–36.

Hagiwara K, Nagai H, Li Y, Ohashi H, Hotta T, Saito H. Frequent DNA methylation but not mutation of the ID4 gene in malignant lymphoma. Journal of clinical and experimental hematopathology : *JCEH*.2007;47(1):15–18.

Hall MA, Curtis DJ, Metcalf D, Elefanty AG, Sourris K, Robb L, Gothert JR, Jane SM, Begley CG. The critical regulator of embryonic hematopoiesis, SCL, is vital in the adult for megakaryopoiesis, erythropoiesis, and lineage choice in CFU-S12. *Proc Natl Acad Sci U S A*. 2003;100:992–997.

Hanahan D, Weinberg RA. The hallmarks of cancer. *Cell*. 2000;100:57–70. doi: 10.1016/S0092-8674(00)81683-9.

Hashmat A. **Sikder HA**, Meghann K. Devlin, Shariff Dunlap, Byungwoo Ryu, Rhoda M. Alani. Id proteins in cell growth and tumorigenesis. *Cancer Cell*. 2003 June; 3(6): 525–530.

He S, Nakada D, Morrison S J. Mechanisms of stem cell self-renewal. *Annu Rev Cell Dev Biol* 2009;25: 377-406.

He W, Dorn DC, Erdjument-Bromage H, Tempst P, Moore MA, Massague J. Hematopoiesis controlled by distinct TIF1gamma and Smad4 branches of the TGFbeta pathway. *Cell* 2006;125: 929–941.

Heasman J, Kofron M, Wylie C. Beta-catenin signaling activity dissected in the early Xenopus embryo: a novel antisense approach. *Dev. Biol*. 2000; 222, 124–134.

Henthorn P, Stewart C, Kadesch T, Puck J. The gene encoding human TFE3, a transcription factor that binds the immunoglobulin heavy-chain enhancer, maps to xp11;22. *Genomics*. 1991;11:374–378.

Herbomel P, Thisse B, Thisse C. Ontogeny and behaviour of early macrophages in the zebrafish embryo. *Development* 1999;126:3735–3745.

Hock H, Hamblen MJ, Rooke HM, et al. Intrinsic requirement for zinc finger transcription factor Gfi-1 in neutrophil differentiation. Immunity 2003; 18:109-120.

Hock H, Hamblen MJ, Rooke HM, Schindler JW, Saleque S, Fujiwara Y, Orkin SH. Gfi-1 restricts proliferation and preserves functional integrity of haematopoietic stem cells. Nature. 2004;431:1002–1007.

Hock H, Orkin SH. Zinc-finger transcription factor Gfi-1: versatile regulator of lymphocytes, neutrophils and hematopoietic stem cells. *Curr Opin Hematol* 2006; **13**:1–6.

Hockemeyer D, Wang H, Kiani S, Lai CS, Gao Q, Cassady JP, Cost GJ, Zhang L, Santiago Y, Miller JC, et al. Genetic engineering of human pluripotent cells using TALE nucleases. *Nat. Biotechnol*.2011;29:731–734.

Hojo M, Ohtsuka T, Hashimoto N, Gradwohl G, Guillemot F, Kageyama R. Glial cell fate specification modulated by the bHLH gene Hes5 in mouse retina. *Development.* 2000;127; 2515–2522

Hsia N, Zon LI. Transcriptional regulation of haematopoietic stem cell development in zebrafish. *Exp Hematol*. 2005;33: 1007-1014.

Hsu PD, Scott DA, Weinstein JA, Ran FA, Konermann S, Agarwala V, Li Y, Fine EJ, Wu X, Shalem O, et al. DNA targeting specificity of RNA-guided Cas9 nucleases. *Nat Biotechnol*.2013;31:827–832.

Huang H. T., Zon L. I. Regulation of stem cells in the zebra fish hematopoietic system. *Cold Spring Harb. Symp. Quant. Biol* 2008;73: 111–118.

Huang P, Zhu Z, Lin S, Zhang B. Reverse genetic approaches in zebrafish. J Genet Genomics.2012;39(9):421–33.

Hwang WY, Fu Y, Reyon D, et al. Efficient *In Vivo* Genome Editing Using RNA-Guided Nucleases. *Nature biotechnology*. 2013;31(3):227-229.

Hyde DR, Godwin AR, Thummel R. *In vivo* Electroporation of Morpholinos into the Regenerating Adult Zebrafish Tail Fin. *JoVE*. 2012;(61):3632.

Inman KE, and Downs KM. The murine allantois: emerging paradigms in development of the mammalian umbilical cord and its relation to the fetus. Genesis. 2007;45:237–258.

Ishibashi M, Ang SL, Shiota K, Nakanishi S, Kageyama R, Guillemot F. Targeted disruption of mammalian hairy and Enhancer of split homolog-1 (HES-1) leads to up-regulation of neural helix-loop-helix factors, premature neurogenesis, and severe neural tube defects. Genes Dev. 1995;9:3136–3148.

Itoh M, Kim C-H, Palardy G, Oda T, Jiang Y-J, Maust D, Yeo S-Y, Lorick K, Wright GJ, Ariza-McNaughton L, Weissman AM, Lewis J, Chandrasekharappa SC, Chitnis AB. Mind bomb is a ubiquitin ligase that is essential for efficient activation of notch signaling by delta. Developmental Cell.2003.

Iwasaki H, Akashi K. Myeloid lineage commitment from the hematopoietic stem cell. *Immunity*.2007;26:726–740.

Jan YN, Jan LY. HLH proteins, fly neurogenesis and vertebrate myogenesis. Cell. 1993;75:827–830.

Jao L-E, Wente SR, Chen W. Efficient multiplex biallelic zebrafish genome editing using a CRISPR nuclease system. *Proceedings of the National Academy of Sciences of the United States of America*. 2013;110(34):13904-13909.

Jen Y, Manova K, Benezra R. Each member of the Id gene family exhibits a unique expression pattern in mouse gastrulation and neurogenesis. *Dev Dyn*. 1997;208:92–106.

Jeon H-M, Jin X, Lee J-S, et al. Inhibitor of differentiation 4 drives brain tumor-initiating cell genesis through cyclin E and notch signaling. *Genes & Development*. 2008;22(15):2028-2033. doi:10.1101/gad.1668708.

Jeon HM, Sohn YW, Oh SY, Kim SH, Beck S, Kim S, et al. ID4 imparts chemoresistance and cancer stemness to glioma cells by derepressing miR-9*-mediated suppression of SOX2. *Cancer Res*.2011;71(9):3410–3421.

Jiang YJ, Brand M, Heisenberg CP, Beuchle D, Furutani-Seiki M, Kelsh RN, et al. Mutations affecting neurogenesis and brain morphology in the zebrafish, Danio rerio. Development. 1996;123:205–216.

Jin H, Sood R, Xu J, Zhen F, English MA, Liu PP, Wen Z (2009) Definitive hematopoietic stem/progenitor cells manifest distinct differentiation output in the zebrafish VDA and PBI.Development 136: 647–654.

Jinek M, Chylinski K, Fonfara I, Hauer M, Doudna JA, Charpentier E. A programmable dual-RNA-guided DNA endonuclease in adaptive bacterial immunity. *Science*. 2012;337:816–821.

Jing L and Zon L,. Zebrafish as a model for normal and malignant hematopoiesis. *Disease Models and Mechanism*. 2011;4, 433-438.

Jones S. An overview of the basic helix-loop-helix proteins. *Genome Biology*. 2004;5(6):226.

Jopling C, Suñè G, Morera C, Izpisua Belmote JC. p38α MAPK regulates myocardial regeneration in zebrafish. *Cell Cycle*. 2012;11(6):1195-1201. doi:10.4161/cc.11.6.19637.

Jordan CT, Mckearn JP, Lemischka IR. Cellular and developmental properties of fetal haematopoietic stem cells. *Cell.* 1990;61(6): 953-963.

Junankar S, Baker LA, Roden DL, Nair R, Elsworth, B et al. ID4 controls mammary stem cells and marks breast cancers with a stem cell-like phenotype. *Nat. Commun*. 2015;6, 6548.

Kabos P, Kabosova A, Neuman T. Blocking Hes1 expression initiates GABAergic differentiation and induces the expression of p21(CIP1/WAF1) in human neural stem cells. *J. Bio. Chem.* 2002;277; 8763–8766.

Kageyama R, Ohtsuka T, Hatakeyama J, Ohsawa R. Roles of bHLH genes in neural stem cell differentiation. *Exp. Cell Res*. 2005; 306, 343–348.

Kallianpur AR, Jordan JE, Brandt SJ. The SCL/TAL-1 gene is expressed in progenitors of both the hematopoietic and vascular systems during embryogenesis. *Blood* 1994;83: 1200–1208.

Kataoka H, Ochi M, Enomoto K, Yamaguchi A. Cloning and embryonic expression patterns of the zebrafish Runt domain genes, runxa and runxb. *Mech. Dev*.2000; 98:139– 43

Kee Y and Bronner-Fraser M. Id4 expression and its relationship to other Id genes during avian embryonic development. Mechanism of development 2001; 109; 341-345.

Kelly GM, Erezyilmaz DF,Moon RT. Induction of a secondary embryonic axis in zebrafish occurs following the overexpression of beta-catenin. *Mech Dev* 1995;53:261–273.

Kim H and Kim JS. A guide to genome engineering with programmable nucleases. Nat Rev Gen. 2014:15: 321-334.

Kim YG, Cha J, Chandrasegaran S Hybrid restriction enzymes: zinc finger fusions to Fok I cleavage domain. *Proc. Natl. Acad. Sci. USA* 1996;93, 1156–1160.

Kim, G. Y., Mercer, S. E., Ewton, D. Z., Yan, Z., Jin, K. and Friedman, E. (2002). The stress-activated protein kinases p38 alpha and JNK1 stabilize p21(Cip1) by phosphorylation. J. Biol. Chem. 277, 29792-29802.

Kissa K, Murayama E, Zapata A, Cortés A, Perret E, Machu C and Herbomel P. 2008. Live imaging of emerging hematopoietic stem cells and early thymus colonization. Blood. 111:1147–1156.

Klambt C, Knust E, Tietze K, Campos-Ortega J A. Closely related transcripts encoded by the neurogenic gene complex enhancer of split of Drosophila melanogaster. *EMBO J*. 1989;8:203–210.

Kok FO, Shin M, Ni C-W, et al. Reverse genetic screening reveals poor correlation between Morpholino-induced and mutant phenotypes in zebrafish.*Developmental cell*. 2015;32(1):97-108.

Kondo M, Weissman IL, Akashi K. Identification of clonogenic common lymphoid progenitors in mouse bone marrow. Cell. 1997 28;91(5):661–72.

Kondo T, and Raff M. The Id4 HLH protein and the timing of oligodendrocyte differentiation. *The EMBO Journal*. 2000;19(9):1998-2007.

Koo BK, Lim HS, Song R, Yoon MJ, Yoon KJ, Moon JS, Kim YW, Kwon MC, Yoo KW, Kong MP, Lee J, Chitnis AB, Kim CH, Kong YY. Mind bomb 1 is essential for generating functional Notch ligands to activate Notch. Development. 2005;132:3459–3470.

Koos DS, Ho RK (1999) The *nieuwkoid/dharma* homeobox gene is essential for *bmp2b* repression in the zebrafish pregastrula. Dev Biol 215: 190–207.

Kopan R and Ilagan MX. The canonical Notch signaling pathway: unfolding the activation mechanism. Cell.2009

Krens SG, Spaink HP, Snaar-Jagalska BE. Functions of the MAPK family in vertebrate-development.FEBS Lett. 2006;580:4984–4990.

Kuo YY, Chang ZF. GATA-1 and Gfi-1B interplay to regulate bcl-xl transcription. *Mol Cell Biol.* 2007;27:4261.

Kuzontkoski PM, Mulligan-Kehoe MJ, Harris BT, Israel MA. Inhibitor of DNA binding-4 promotes angiogenesis and growth of glioblastoma multiforme by elevating matrix GLA levels. *Oncogene* 2010;*29*: 3793–3802.

Lai, E. C. (2004). Notch signaling: control of cell communication and cell fate. *Development* **131**,965 -973.

Langenau DM, Ferrando AA, Traver D, Kutok JL, Hezel JP. *et al.,* In vivo tracking of T cell development, ablation, and engraftment in transgenic zebrafish. *Proc. Natl. Acad. Sci. USA* 2004; 101:7369–74

Lasorella A, Uo T, Iavarone A. Id proteins at the cross-road of development and cancer.*Oncogene* 2001;20: 8326–8333.

Le Guyader D, Redd MJ, Colucci-Guyon E, et al. Origins and unconventional behavior of neutrophils in developing zebrafish. *Blood*. 2008;111(1):132–141.

Lei Y, Guo X, Liu Y, Cao Y, Deng Y, Chen X, Cheng CH, Dawid IB, Chen Y, Zhao H. Efficient targeted gene disruption in Xenopus embryos using engineered transcription activator-like effector nucleases (TALENs) *Proc. Natl Acad. Sci. USA*. 2012;109:17484–17489

Li T, Huang S, Zhao X, Wright DA, Carpenter S, Spalding MH, Weeks DP, Yang B. Modularly assembled designer TAL effector nucleases for targeted gene knockout and gene replacement in eukaryotes. *Nucleic Acids Res*. 2011;39:6315–6325.

Lieschke GJ, Oates AC, Paw BH, *et al.,* Zebrafish SPI-1 (PU.1) marks a site of myeloid development independent of primitive erythropoiesis: implications for axial patterning. *Dev Biol*. 2002;246:274–295.

Lim E, Vaillant F, Wu D, Forrest NC, Pal B, Hart AH, et al. Aberrant luminal progenitors as the candidate target population for basal tumor development in BRCA1 mutation carriers. *Nat Med*. 2009;15(8):907–913.

Lin MI, Yu J, Murata T, Sessa WC. Caveolin-1-deficient mice have increased tumor microvascular permeability, angiogenesis, and growth. Cancer Res. 2007;67:2849–2856.

Liu KJ and Harland RM. Cloning and characterization of Xenopus Id4 reveals differing role of Id genes. Dev. Biol 2003; 339-351.

Lombardo A. *et al.* Gene editing in human stem cells using zinc finger nucleases and integrase-defective lentiviral vector delivery. Nat Biotechnol 25, 1298–306 (2007).

Long Q, Meng A, Wang H., *et al.* GATA-1 expression pattern can be ecapitulated in living transgenic zebrafish using GFP reporter gene. *Development* 1997;124:4105–4111.

Lu QR, Yuk D, Alberta JA, Zhu Z, Pawlitzky I, Chan J McMahon AP, Stiles CD, Rowitch DH, Sonic hedgehog regulated oligodendrocyte lineage genes encoding bHLH proteins in the mammalian central nervous system. *Neuron* 2000; 25; 317–329.

Lukov GL, Rossi L, Souroullas GP, Mao R, Goodell MA. The expansion of T-cells and hematopoietic progenitors as a result of overexpression of the Lymphoblastic leukemia gene, Lyl1 can support leukemia formation. *Leukemia research*. 2011;35(3):405-412.

Lyden D, Young AZ, Zagzag D, Yan W, Gerald W, *et al.*, Id1 and Id3 are required for neurogenesis, angiogenesis and vascularization of tumour xenografts. *Nature*. 1999; 401: 670–677.

Marin-Husstege M, He Y, Li J, Kondo T, Sablitzky F, Casaccia-Bonnefil P. Multiple roles of Id4 in developmental myelination: predicted outcomes and unexpected findings. *Glia*. 2006;54:285–296.

Marraffini LA, Sontheimer EJ. CRISPR interference limits horizontal gene transfer in staphylococci by targeting DNA. *Science*. 2008;322:1843–1845.

Massari ME, Murre C. Helix-Loop-Helix Proteins: Regulators of Transcription in Eucaryotic Organisms. *Molecular and Cellular Biology*. 2000;20(2):429-440.

Mellentin JD, Smith SD, Cleary ML. lyl-1, a novel gene altered by chromosomal translocation in T cell leukemia, codes for a protein with a helix-loop-helix DNA binding motif. Cell. 1989;58:77–83.

Meng YS, Khoury H, Dick JE, Minden MD. Oncogenic potential of the transcription factor LYL1 in acute myeloblastic leukemia. *Leukemia*. 2005;19:1941–1947.

Meng, X., Noyes, M.B., Zhu, L.J., Lawson, N.D., and Wolfe, S.A. Targeted gene inactivation in zebrafish using engineered zinc-finger nucleases. *Nat. Biotechnol*. 2008; 26, 695–701.

Mikkola HK, Klintman J, Yang H, Hock H, Schlaeger TM, Fujiwara Y, Orkin SH. Haematopoietic stem cells retain long-term repopulating activity and multipotency in the absence of stem-cell leukaemia SCL/tal-1 gene. *Nature*. 2003;421:547–551.

Miller JC, Tan S, Qiao G, Barlow KA, Wang J, Xia DF, Meng X, Paschon DE, Leung E, Hinkley SJ, et al. A TALE nuclease architecture for efficient genome editing. *Nat. Biotechnol*. 2011;29:143–148.

Miyamoto A, Cui X, Naumovski L, Cleary ML. Helix-loop-helix proteins LYL1 and E2a form heterodimeric complexes with distinctive DNA-binding properties in hematolymphoid cells. *Mol Cell Biol*. 1996;16:2394–2401.

Molnar A, Theodoras A M, Zon L I, Kyriakis J M. Cdc42Hs, but not Rac 1, inhibits serum-stimulated cell cycle progressin at G1/S through a mechanism requiring p38/RK. *J Biol Chem* 1997; **272**:13229–35.

Molyneux G. *et al*. BRCA1 basal-like breast cancers originate from luminal epithelial progenitors and not from basal stem cells. *Cell Stem Cell* 2010;7; 403–17.

Monteiro R, Pouget C, Patient R. The gata1/pu.1 lineage fate paradigm varies between blood populations and is modulated by tif1γ. *The EMBO Journal*. 2011

Moore FE, Reyon D, Sander JD, et al. Improved Somatic Mutagenesis in Zebrafish Using Transcription Activator-Like Effector Nucleases (TALENs). Bonkowsky JL, ed. *PLoS ONE*. 2012;7(5):e37877.

Moore MA, Metcalf D. Ontogeny of the haemopoietic system: yolk sac origin of in vivo and in vitro colony forming cells in the developing mouse embryo. *Br J Haematol*. 1970;18:279–296.

Morrison, S.J. & Weissman, I.L. The long-term repopulating subset of hematopoietic stem cells is deterministic and isolatable by phenotype. *Immunity*1, 661−673 (1994).

Muller AM, Medvinsky A, Strouboulis J, Grosveld F, Dzierzak E. Development of hematopoietic stem cell activity in the mouse embryo. *Immunity*. 1994;1:291–301.

Mullins, M.C., Hammerschmidt, M., Haffter, P., and Nu¨ sslein-Volhard, C. Large-scale mutagenesis in the zebrafish: in search of genes controlling development in a vertebrate. *Curr. Biol.* 19944, 189–202.

Murayama E, Kissa K, Zapata A, et al. Tracing hematopoietic precursor migration to successive hematopoietic organs during zebrafish development. *Immunity*. 2006;25(6):963–975.

Murre C, Bain G, Vandijk MA, Engel I, Furnari BA, Massari ME, Matthews JR, Quong MW, Rivera RR, Stuiver MH. Structure and function of helix-loop-helix proteins. *Biochim Biophys Acta.*1994;1218:129–135.

Murre C, Mc Caw PS, Baltimore D. A new DNA binding and dimerizing motif in immunoglobulin enhancer binding, Daughterless, MyoD and Myc proteins. *Cell*. 1989;56:777–783.

Mussolino C, Morbitzer R, Lutge F, Dannemann N, Lahaye T, Cathomen T. A novel TALE nuclease scaffold enables high genome editing activity in combination with low toxicity. *Nucleic Acids Res*.2011;39:9283–9293.

Nair SK, Burley S. X-ray structures of Myc-Max and Mad-Max recognizing DNA: molecular bases of regulation by proto-oncogenic transcription factors. *Cell*. 2003;112:193–205.

Nakamura Y, Sakakibara S, Miyata T, Ogawa M, Shimazaki T, Weiss S, Kageyama R, Okano H. The bHLH gene hes1 as a repressor of the neuronal commitment of CNS stem cells *J. Neurosci.* 2000;12; 283–293.

Nasevicius, A and, Ekker SC. Effective targeted gene 'knockdown' in zebrafish. *Nat. Genet.* 2000; 26, 216–220.

Neugebauer JM, Amack JD, Peterson AG, Bisgrove BW, Yost HJ. FGF Signaling during embryo development regulates cilia length in diverse epithelia.*Nature*. 2009;458(7238):651-654.

Neuman T, Keen, A Zuber MX, Kristjansson GI, Gruss P, Nornes HO. Neuronal expression of regulatory helix–loop–helix factor Id2 gene in mouse, *Dev. Biol.* 1993; 160(1); 186–195.

Nieto M, Schuurmans C, Britz O, Guillemot F. Neural bHLH genes control the neuronal versus glial fate decision in cortical progenitors. 2001;*Neuron* 29, 401–413.

Nikaido M, Tada M, Saji T and Ueno N.. Conservation of BMP signaling in zebrafish mesoderm patterning. *Mech Dev* 1997: 61, 75-88.

Noetzel E, Veeck J, Niederacher D, Galm O, Horn F, Hartmann A, Knuchel R, Dahl E. Promoter methylation-associated loss of ID4 expression is a marker of tumour recurrence in human breast cancer.BMC Cancer. 2008;8:154.

North TE, de Bruijn M F, Stacy T, Talebian, L. *et al.* Runx1 expression marks long-term repopulating hematopoietic stem cells in the midgestation mouse embryo. *Immunity* 12002;6:661–72

Norton JD, Craggs G, Deed RW, Sablitzky F. ID helixloop-helix proteins in cell growth and differentiation. *Trends Cell Biol* 1998;8; 58-65.

Norton JD. ID helix-loop-helix proteins in cell growth, differentiation and tumorigenesis. *Development.* 2000; 113: 3897-3905.

Oatley JM, Brinster RL 2012. The germline stem cell niche unit in mammalian testes. *Physiol Rev* 92: 577–595.

Oatley MJ, Kaucher AV, Racicot KE, Oatley JM. Inhibitor of DNA Binding 4 Is Expressed Selectively by Single Spermatogonia in the Male Germline and Regulates the Self-Renewal of Spermatogonial Stem Cells in Mice . *Biology of Reproduction.* 2011;85(2):347-356.

O'Neil J, Shank J, Cusson N, Murre C, Kelliher M. TAL1/SCL induces leukemia by inhibiting the transcriptional activity of E47/HEB. *Cancer Cell* 2004;5: 587–596.

Orkin SH, Zon LI. Hematopoiesis: An Evolving Paradigm for Stem Cell Biology. *Cell*. 2008;132(4):631-644.

Osawa M, Hanada K, Hamada H, Nakauchi H. Long-term lymphohematopoietic reconstitution by a single CD34-low/negative hematopoietic stem cell. *Science*. 1996;273:242–245.

Ota S, Hisano Y, Muraki M, Hoshijima K, Dahlem TJ, Grunwald DJ, et al. Efficient identification of TALEN-mediated genome modifications using heteroduplex mobility assays. *Genes Cells*. 2013;18:450–8.

Ottersbach K, Dzierzak E. The murine placenta contains hematopoietic stem cells within the vascular labyrinth region. Developmental Cell. 2005

Paik EJ, Zon LI. Haematopoietic development in zebrafish. *Int J Dev Biol*. 2010; 54(6-7): 1127-1137.

Park HC, Kim CH, Bae YK, Yeo SY, Kim SH, Hong SK, et al. Analysis of upstream elements in the HuC promoter leads to the establishment of transgenic zebrafish with fluorescent neurons. Dev Biol.2000;227(2):279–293.

Park SJ, Kim RJ, Nam JS. Inhibitor of DNA-binding 4 contributes to the maintenance and expansion of cancer stem cells in 4T1 mouse mammary cancer cell line. *Laboratory Animal Research*. 2011;27(4):333-338. doi:10.5625/lar.2011.27.4.333.

Patterson LJ, Gering M, Patient R. Scl is required for dorsal aorta as well as blood formation in zebrafish embryos. Blood. 2005;105(9):3502–3511

Perk J, Iavarone A, Benezra R. Id family of helix-loop-helix proteins in cancer. *Nat Rev Cancer*.2005;5(8):603–614.

Pirot N, Deleuze V, El-Hajj R, Dohet C, Sablitzky F, et al. LYL1 activity is required for the maturation of newly formed blood vessels in adulthood. Blood. 2010;115:5270–5279.

Porcher C, Liao EC, Fujiwara Y, Zon LI, Orkin SH. Specification of hematopoietic and vascular development by the bHLH transcription factor *Scl* without direct DNA binding. *Development* 1999; 126:4603–4615.

Porcher C, Swat W, Rockwell K, Fujiwara Y, Alt F, Orkin S. The T cell leukemia oncoprotein SCL/tal-1 is essential for development of all hematopoietic lineages. *Cell*. 1996;86:47–57.

Pulford K, Lecointe N, Leroy VK, Jones M, Mathieu MD, et al. Expression of TAL-1 proteins in human tissues. *Blood*. 1995;85:675–684.

Rahme GJ, Israel MA. Id4 suppresses MMP2-mediated invasion of glioblastoma-derived cells by direct inactivation of Twist1 function. *Oncogene.* 2015;2(1): 53-62.

Ran FA, Hsu PD, Wright J, Agarwala V, Scott DA, Zhang F. Genome engineering using the CRISPR-Cas9 system. *Nature protocols*. 2013;8(11):2281-2308.

Rao M S. Multipotent and restricted precursors in the central nervous system. *Anat. Rec.* 1999;257, 137–148

Reyon D, Tsai SQ, Khayter C, Foden JA, Sander JD, Joung JK. FLASH assembly of TALENs for high-throughput genome editing. *Nat. Biotechnol*. 2012;30:460–465.

Riechmann V, Sablitzky F.Mutually exclusive expression of two dominant-negative helix-loop-helix (dnHLH) genes, Id4 and Id3, in the developing brain of the mouse suggests distinct regulatory roles of these dnHLH proteins during cellular proliferation and differentiation of the nervous system. *Cell Growth Differ* 1995; 6(7): 837-43.

Riechmann V, van Cruchten I, Sablitzky, F.The expression pattern of Id4, a novel dominant negative helix-loop-helix protein, is distinct from Id1, Id2 and Id3. *Nucleic Acids Res* 1994; 22(5): 749-55.

Rigolet M, Rich T, Gross-Morand MS, Molina-Gomes D, Viegas-Pequignot E, Junien C. cDNA cloning, tissue distribution and chromosomal localization of the human ID4 gene. DNA Res.1998;5:309–313.

Robb L, Lyons I, Li R, Hartley L, Kontgen F, Harvey RP, Metcalf D, Begley CG. Absence of yolk sac hematopoiesis from mice with a targeted disruption of the scl gene. *Proc Natl Acad Sci U S A.*1995;92:7075–7079.

Robu ME, Larson JD, Nasevicius A, Beiraghi S, Brenner C, Farber SA, Ekker SC. p53 activation by knockdown technologies. *PLoS Genet*. 2007;3, e78.

Roldan G, Delgado L, Muse IM. Tumoral expression of BRCA1, estrogen receptor alpha and ID4 protein in patients with sporadic breast cancer. *Cancer Biol Ther*. 2006;5:505–10.

Ross SE, Greenberg ME, Stiles CD. Basic Helix-Loop-Helix Factors in Cortical Development. *Neuron* 2003;39(1); 13-25

Rushlow C A, Hogan A, Pinchin S M, Howe K M, Lardelli M, Ish-Horowicz D. The Drosophila hairy protein acts in both segmentation and bristle patterning and shows homology to N-myc. *EMBO J.*1989;8:3095–3103.

Sablitzky F. Protein motifs: the Helix-Loop-Helix motif. Els 2005.

Sander, J.D., Dahlborg, E.J., Goodwin, M.J., Cade, L., Zhang, F., Cifuentes, D., Curtin, S.J., Blackburn, J.S., Thibodeau-Beganny, S., Qi, Y., et al. Selection-free zinc-finger-nuclease engineering by context-dependent assembly (CoDA). *Nat. Methods* 2011; 8, 67–69.

Sanjana NE, Cong L, Zhou Y, Cunniff MM, Feng G, Zhang F. A Transcription Activator-Like Effector (TALE) Toolbox for Genome Engineering. *Nature protocols*. 2012;7(1):171-192.

Sarkar D, Su Z-Z, Lebedeva IV, et al. *mda*-7 (IL-24) mediates selective apoptosis in human melanoma cells by inducing the coordinated overexpression of the GADD family of genes by means of p38 MAPK.*Proceedings of the National Academy of Sciences of the United States of America*. 2002;99(15):10054-10059.

Sasai Y, Kageyama R, Tagawa Y, Shigemoto R, Nakanishi S.Two mammalian helix-loop-helix factors structurally related to *Drosophila* hairy and Enhancer of split. *Genes Dev*., 1992; 6; 2620–2634.

Schlaeger TM, Schuh A, Flitter S, et al. Decoding Hematopoietic Specificity in the Helix-Loop-Helix Domain of the Transcription Factor SCL/Tal-1. *Molecular and Cellular Biology*. 2004;24(17):7491-7502. doi:10.1128/MCB.24.17.7491-7502.2004.

Schmidt EV. The role of c-myc in regulation of translation initiation. *Oncogene*. 2004;23:3217–3221.

Scholze H, Boch J (2010) TAL effector-DNA specificity. Virulence 1: 428–432.

Serwold T, Richie Ehrlich LI, Weissman IL. Reductive isolation from bone marrow and blood implicates common lymphoid progenitors as the major source of thymopoiesis. *Blood*. 2009;113(4):807-815.

Sharma P, Knowell AE, Chinaranagari S, Komaragiri S, Nagappan P, Patel D, Havrda MC, Chaudhary J. Id4 deficiency attenuates prostate development and promotes PIN-like lesions by regulating androgen receptor activity and expression of NKX3. 1 and PTEN. Mol Cancer. 2013;12(1):67.

Shestopalov IA, Sinha S, Chen JK. Light-controlled gene silencing in zebrafish embryos. *Nat. Chem. Biol.* 2007; 3, 650–651.

Shivdasani RA, Mayer EL, Orkin SH. Absence of blood formation in mice lacking the T-cell leukaemia oncoprotein tal-1/SCL. *Nature*. 1995;373:432–434.

Siekmann, A.F., Standley, C., Fogarty, K.E., Wolfe, S.A., and Lawson, N.D. Chemokine signaling guides regional patterning of the first embryonic artery. *Genes Dev*. 2009;23, 2272–2277.

Silver L, Palis ,J. Initiation of murine embryonic erythropoiesis: a spatial analysis. *Blood* 1997;89, 1154–1164.

Simanainen U, Allan CM, Lim P, McPherson S, Jimenez M, Zajac JD, Davey RA, Handelsman DJ. Disruption of prostate epithelial androgen receptor impedes prostate lobe-specific growth and function. *Endocrinology*. 2007;148:2264–2272.

Singh SK, Clarke ID, Terasaki M, Bonn VE, Hawkins C, Squire J, Dirks PB. Identification of a cancer stem cell in human brain tumors. *Cancer Res*. 2003;63:5821–5828.

Skromne I, Prince VE. Current perspectives in zebrafish reverse genetics: moving forward. *Dev Dyn.* 2008;237(4):861–882

Sood R and Liu P. Novel Insights into the Genetic Controls of Primitive and Definitive Hematopoiesis from Zebrafish Models. *Advances in Hematology*. 2012;2012:830703.

Souroullas GP, Salmon JM, Sablitzky F, Curtis DJ, Goodell MA. Adult Hematopoietic Stem and Progenitor Cells require either *Lyl1* or *Scl* for survival.*Cell stem cell*. 2009;4(2):180-186.

Srivastava D, Olson EN. Knowing in your heart what's right. Trends Cell Biol. 1997;7:447–453

Streisinger, G., Singer, F., Walker, C., Knauber, D., and Dower, N. (1986). Segregation analyses and gene-centromere distances in zebrafish. Genetics 112, 311–319.

Summerton J. Morpholino antisense oligomers: the case for an RNase H-independent structural type. Biochim Biophys Acta. 1999 Dec 10;1489(1):141-58.

Sun, Z., Amsterdam, A., Pazour, G.J., Cole, D.G., Miller, M.S., and Hopkins, N. A genetic screen in zebrafish identifies cilia genes as a principal cause of cystic kidney. *Development* 2004;131, 4085–4093.

Szilvassy SJ, Humphries RK, Lansdorp PM, Eaves AC and Eaves CJ..*Proc. Natl. Acad. Sci. USA*, 1990; 87, 8736–8740.

Tang T, Shi Y, Opalenik SR, Brantley-Sieders DM, Chen J, et al. Expression of the TAL1/SCL transcription factor in physiological and pathological vascular processes. *J Pathol*. 2006;210:121–129.

Taoudi S, Medvinsky A. Functional identification of the hematopoietic stem cell niche in the ventral domain of the embryonic dorsal aorta. *Proc Natl Acad Sci USA* 2007;104(22): 9399-403.

Temple, S. 2001. The development of neural stem cells. *Nature*. 2001;414; 112–117

Tesson L, Usal C, Menoret S, Leung E, Niles BJ, Remy S, Santiago Y, Vincent AI, Meng X, Zhang L, et al. Knockout rats generated by embryo microinjection of TALENs. *Nat. Biotechnol*. *2011*;29:695–696.

Thisse B, Pflumio S, Fürthauer M, Loppin B, Heyer V, Degrave A, Woehl R, Lux A, Steffan T, Charbonnier XQ and Thisse C. (2001) Expression of the zebrafish genome during embryogenesis (NIH R01 RR15402). ZFIN Direct Data Submission

Thisse, C., and Thisse, B.High-resolution in situ hybridization to wholemount zebrafish embryos. *Nat. Protoc*. 2008; 3, 59–69

Thompson MA, Ransom DG, Pratt SJ, MacLennan H, Kieran MW, Detrich HW, Vail B, Huber TL, Paw B, Brownlie AJ, et al. The cloche and spadetail genes differentially affect hematopoiesis and vasculogenesis. Dev Biol. 1998;197(2):248–269.

Till JE, McCulloch EA. A direct measurement of the radiation sensitivity of normal mouse bone marrow cells. *Radiation Res* 1961; 14: 213-222.

Tokuzawa Y, Yagi K, Yamashita Y, et al. Id4, a New Candidate Gene for Senile Osteoporosis, Acts as a Molecular Switch Promoting Osteoblast Differentiation. Barsh GS, ed. *PLoS Genetics*. 2010;6(7).

Tomita, K., Moriyoshi, K., Nakanishi, S., Guillemot, F., and Kageyama, R. Mammalian achaete-scute and atonal homologs regulate neuronal versus glial fate determination in the central nervous system. *EMBO J.* 2000;19; 5460–5472.

Toyama R, O'Connell ML, Wright CV, Kuehn MR, Dawid IB. Nodal induces ectopic goosecoid and lim1 expression and axis duplication in zebrafish. Development. 1995;121:383–391.

Traver D, Paw B H, Poss K D, Penberthy WT, Lin S, Zon LI. (2003). Transplantation and *in vivo* imaging of multilineage engraftment in zebrafish bloodless mutants. Nat. Immunol. 4, 1238–1246.

Trede NS, and Zon LI. Development of T-cells during fish embryogenesis. *Dev. Comp. Immunol*. 1998; 22:253–63

Umetani N, Mori T, Koyanagi K, Shinozaki M, Kim J, Giuliano AE, Hoon DS. Aberrant hypermethylation of ID4 gene promoter region increases risk of lymph node metastasis in T1 breast cancer.*Oncogene*. 2005;24(29):4721–4727.

Urnov FD, Rebar EJ, Holmes MC, Zhang HS, Gregory PD. Genome editing with engineered zinc finger nucleases. *Nat. Rev. Genet*. 2010;11, 636–646.

van Eekelen JA, Bradley CK, Gothert JR, Robb L, Elefanty AG, Begley CG, Harvey AR. Expression pattern of the stem cell leukaemia gene in the CNS of the embryonic and adult mouse. *Neuroscience* 2003;122; 421–436.

Vannucchi AM, Bianchi L, Cellai C, et al. Accentuated response to phenylhydrazine and erythropoietin in mice genetically impaired for their GATA-1 expression (GATA-1(low) mice). *Blood*. 2001;97:3040–3050.

Vescovi AL, Galli R, Reynolds BA. Brain tumour stem cells. *Nat Rev Cancer*. 2006;6(6):425–36.

Vetter M. A turn of the helix: preventing the glial fate. *Neurons.*2002; 29: 559-562.

Vincent A, Omura N, Hong SM, Jaffe A, Eshleman J, Goggins M. Genome-wide analysis of promoter methylation associated with gene expression profile in pancreatic adenocarcinoma. *Clin Cancer Res*.2011;17(13):4341–4354.

Visvader J, Begley CG, Adams JM. Differential expression of the LYL, *Scl* and E2A helix-loop-helix genes within the hemopoietic system. *Oncogene* 1991; 6:187–194.

Vogel G. Genomics: Sanger will sequence zebrafish genome. *Science* 2000; 290: 1671.

Wadman I, Li J, Bash RO, et al. Specific in vivo association between the bHLH and LIM proteins implicated in human T cell leukemia. *EMBO J* 1994; 13:4831–4839.

Walker, C., and Streisinger, G. (1983). Induction of mutations by gamma-rays in pregonial germ cells of zebrafish embryos. Genetics 103, 125–136.

Wang H, Yang H, Shivalila CS, Dawlaty MM, Cheng AW, Zhang F, Jaenisch R. One-step generation of mice carrying mutations in multiple genes by CRISPR/Cas-mediated genome engineering. *Cell*.2013;153:910–918.

Wang S, Sdrulla A, Johnson JE, Yokota Y, Barres BA. A role for the helix-loop-helix protein Id2 in the control of oligodendrocyte development. *Neuron* 2001; 29; 603–614

Wei W, Wen L, Huang P, Zhang Z, Chen Y, Xiao A, Huang H, Zhu Z, Zhang B, Lin S. Gfi1.1 regulates hematopoietic lineage differentiation during zebrafish embryogenesis. Cell Res.2008;18:677–685.

Weinstein BM, Schier AF, Abdelilah S *et al.* (1996). Hematopoietic mutations in the zebrafish. *Development123*:303–309.

Weintraub H, Dwarki V, Verma I, Davis R, Hollenberg S, Snider L, Lassar A, Tapscott S. Muscle-specific transcriptional activation by MyoD. *Genes Dev*. 1991;5:1377–1386.

Willett CE, Kawasaki H, Amemiya CT, Lin S, Steiner LA. Ikaros expression as a marker for lymphoid progenitors during zebrafish development. Dev Dyn. 2001;222:694–8.

Wilson SW, Rubenstein JL. Induction and dorsoventral patterning of the telencephalon. *Neuron* 2000;28; 641–651.

Wu G, Lyapina S, Das I, et al. SEL-10 Is an Inhibitor of Notch Signaling That Targets Notch for Ubiquitin-Mediated Protein Degradation. *Molecular and Cellular Biology*. 2001;21(21):7403-7415.

Wu Y, Liu Y, Levine EM, Rao MS. Hes1 but not Hes5 regulates an astrocyte versus oligodendrocyte fate choice in glial restricted precursors. *Dev. Dyn.* 2003;226; 675–689.

Yan W, Young AZ, Soares VC, Kelley R, Benezra R, Zhuang Y. High incidence of T-cell tumors in E2A-null mice and E2A/Id1 double-knockout mice. *Mol Cell Biol* 1997;17: 7317–7327.

Yehia G, Schlotter F, Razavi R, Alessandrini A, Molina CA. Mitogen-Activated Protein Kinase phosphorylates and targets inducible cAMP early repressor to ubiquitin-mediated destruction. *J Biol Chem* 2001; **276**:35272–9.

Yilmaz OH, Kiel MJ, Morrison SJ. SLAM family markers are conserved among hematopoietic stem cells from old and reconstituted mice and markedly increase their purity. *Blood*. 2006;107:924–930.

Yokota Y,Mori S, Nishikawa S, Mansouri A, Gruss P, Kusunoki T,Katakai T,. Shimizu A. The helix-loop-helix inhibitor Id2 and cell differentiation control. *Curr Top Microbiol Immunol*. 2000; 251: 35–41.

Yu C, Zhang Y, Yao S, Wei Y. A PCR Based Protocol for Detecting Indel Mutations Induced by TALENs and CRISPR/Cas9 in Zebrafish. Jennings B, ed. *PLoS ONE*. 2014;9(6):e98282.

Yu L, Liu C, Vandeusen J, Becknell B, Dai Z, Wu YZ, Raval A, Liu TH, Ding W, Mao C, Liu S, Smith LT, Lee S, Rassenti L, Marcucci G, Byrd J, et al. Global assessment of promoter methylation in a mouse model of cancer identifies ID4 as a putative tumor-suppressor gene in human leukemia. *Nat Genet*.2005;37(3):265–274.

Yun K, Mantani A, Garel S, Rubenstein J, Israel MA. Id4 regulates neural progenitor proliferation and differentiation *in vivo*. *Development*. 2004;131:5441–5448.

Zeng H, Yucel R, Kosan C, et al. Transcription factor Gfi1 regulates self-renewal and engraftment of hematopoietic stem cells. EMBO J 2004; 23:4116-4125.

Zhang Y, Zhang F, Li X, Baller JA, Qi Y, Starker CG, Bogdanove AJ, Voytas DF. Transcription activator-like effector nucleases enable efficient plant genome engineering. *Plant Physiol.* 2013;161:20–27.

Zhao Q, Zhou X, Mattei M. TFEC, a basic helix-loop-helix protein, forms heterodimers with TFE3 and inhibits TFE3-dependent transcription activation. *Mol Cell Biol.* 1993;13:4505–4512.

Zhong Y, et al. Overexpression of a transcription factor LYL1 induces T- and B-cell lymphoma in mice.Oncogene. 2007;26(48):6937–6947.

Zhou Q, Anderson DJ. The bHLH transcription factors OLIG2 and OLIG1 couple neuronal and glial subtype specification. *Cell* 2002; 109, 61–73.

Zhu W, Dahmen J, Bulfone A, Rigolet M, Hernandez MC, Kuo WL, Puelles L, Rubenstein JL, Israel MA. d gene expression during development and molecular cloning of the human Id-1 gene

Zohren F, Souroullas GP, Luo M, et al. Lyl1 regulates lymphoid specification and maintenance of early T lineage progenitors. *Nature immunology*. 2012;13(8):761-769.

Zon, L. I. 1995. Developmental biology of haematopoiesis. *Blood* 86:2876–91.

Appendix I

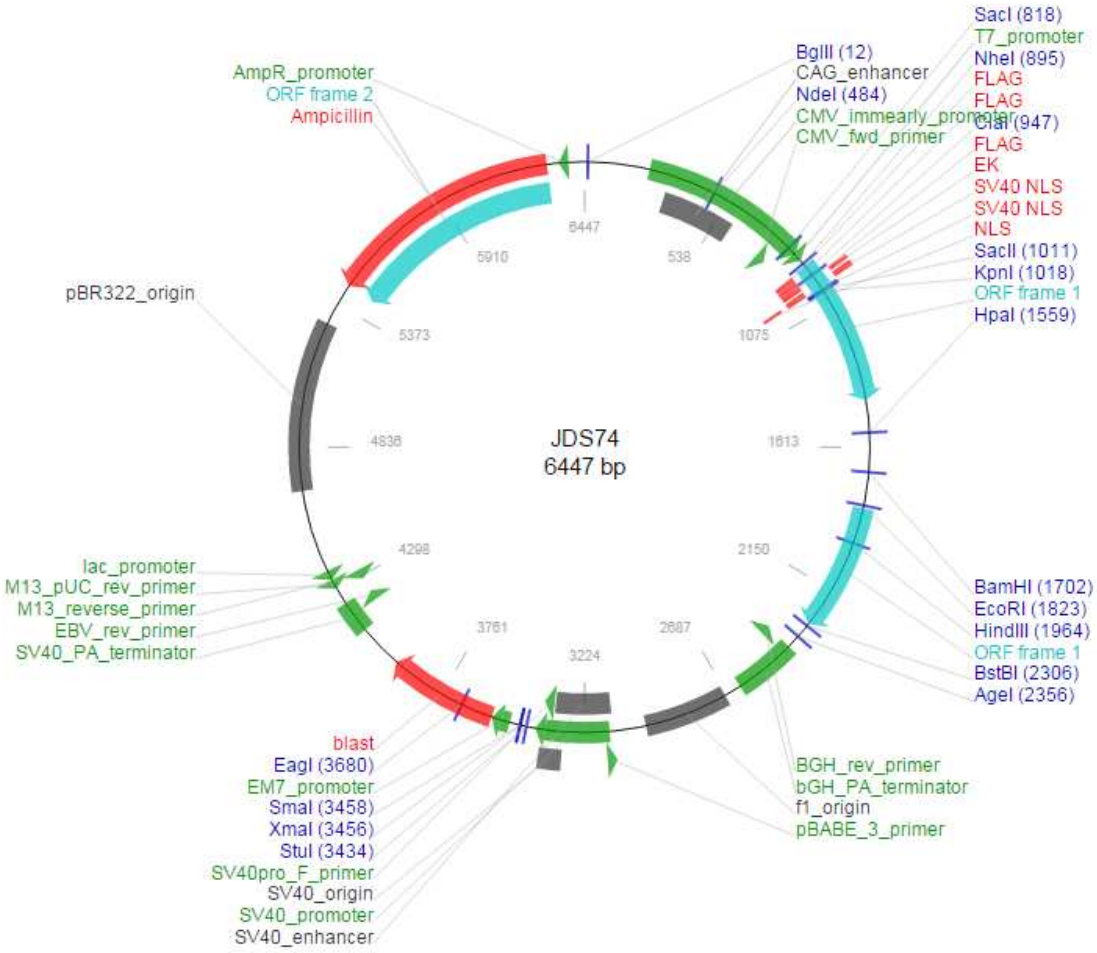

All TALEN plasmids were cloned on JDS74 deposited by Keith Joung lab. All TALEN insert were cloned into between Sac*I* and Hind*III*. (For TALEN target site refer section 3.1)

Appendix II

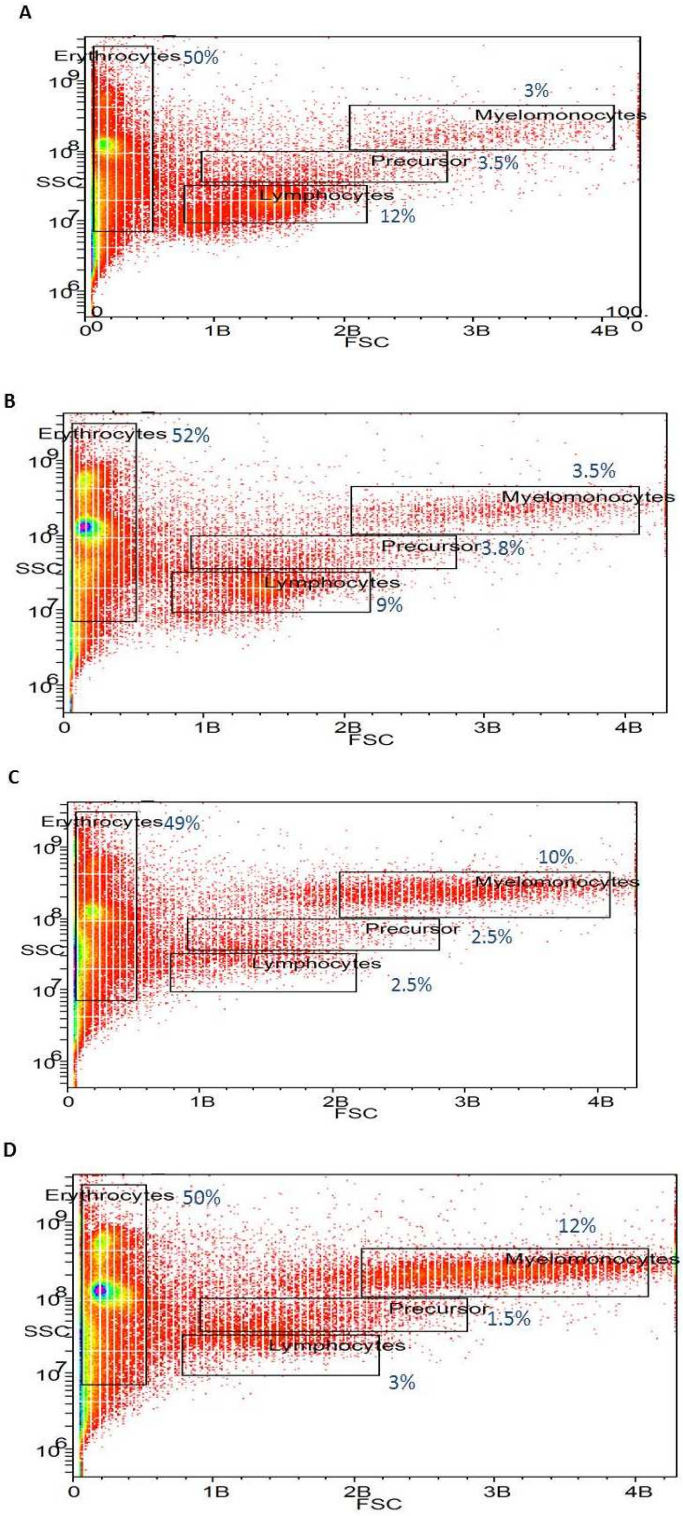

Separation of kidney marrow cells based on forward and side scatter (A,B) Wild type **(C, D)** *lyl1*$^{qmc801/qmc801}$